

ON THE ANALYSIS and DESIGN of A NEW TYPE of PARTIALLY
COMPLIANT MECHANISM

A THESIS SUBMITTED TO
THE GRADUATE SCHOOL OF NATURAL AND APPLIED SCIENCES
OF
MIDDLE EAST TECHNICAL UNIVERSITY

BY

ENGİN TANIK

IN PARTIAL FULFILLMENT OF THE REQUIREMENTS
FOR
THE DEGREE OF DOCTOR OF PHILOSOPHY
IN
MECHANICAL ENGINEERING

MAY 2007

Approval of this thesis:

**“ON THE ANALYSIS and DESIGN of A NEW TYPE of PARTIALLY
COMPLIANT MECHANISM”**

submitted by **ENGİN TANIK** in partial fulfillment of the requirements for the
degree of **Doctor of Philosophy in Mechanical Engineering** by,

Prof. Dr. Canan Özgen
Dean, Graduate School of **Natural and Applied Sciences**

Prof. Dr. Kemal İder
Head of Department , **Mechanical Engineering**

Prof. Dr. Eres Söylemez
Supervisor, **Mechanical Engineering, METU**

Examining Committee Members:

Prof. Dr. S. Kemal İder
Mechanical Engineering, METU

Prof. Dr. Eres Söylemez
Mechanical Engineering, METU

Prof. Dr. Tuna Balkan
Mechanical Engineering, METU

Prof. Dr. Reşit Soylu
Mechanical Engineering, METU

Prof. Dr. Yaşar T. Hondur
Mechanical Engineering, Gazi Univ.

Date: _____

I hereby declare that all information in this document has been obtained and presented in accordance with academic rules and ethical conduct. I also declare that, as required by these rules and conduct, I have fully cited and referenced all material and results that are not original to this work.

Name, Last name: Engin Tanık

Signature :

ABSTRACT

ON THE ANALYSIS and DESIGN of A NEW TYPE of PARTIALLY COMPLIANT MECHANISM

Tanık, Engin

Ph.D., Department of Mechanical Engineering

Supervisor: Prof. Dr. Eres Söylemez

May 2007, 120 pages

In this study analysis and design procedures of partially compliant mechanisms using two degree of freedom mechanism model are developed. The flexible segments are modeled as revolute joints with torsional springs. While one freedom is controlled by the input to the mechanism, the motion of the parts are governed both by the kinematics and the force balance. The procedure developed for the analysis of such mechanisms is shown on two different mechanisms: a five link mechanism with crank input and slider output (five-bar mechanism); a five link mechanism with crank input and rocker output. Design charts are prepared according to output-link oscillation and dimensionless design parameters.

Keywords: Compliant Mechanisms, Unconstrained, Multi Degree-of-Freedom

ÖZ

YENİ BİR TİP KISMI ESNEK MEKANİZMANIN ANALİZİ VE TASARIMI

Tanık, Engin

Doktora, Makina Mühendisliği Bölümü

Tez Yöneticisi: Prof. Dr. Eres Söylemez

Mayıs 2007, 120 Sayfa

Bu çalışmada yeni bir tip kısmi-esnek mekanizma için analiz ve dizayn prosedürü geliştirilmiştir. Esnek kısımlar döner masfalla ve burulma yayı ile modellenmiştir. Bir serbestlik giriş uzvu ile kontrol edilirken, uzuvların hareketi kinematik ve kuvvet dengesi ile sağlanmaktadır. Bu tip mekanizmaların analizi için geliştirilen prosedür iki farklı mekanizma ile gösterilmiştir: krank girişli kızak çıkışlı beş uzuvlu bir mekanizma; krank girişli sarkaç çıkışlı beş uzuvlu bir mekanizma. Çıkış uzvu salınımlarına göre boyutsuz tasarım parametleri ile tasarım abakları hazırlanmıştır

Anahtar Kelimeler: Esnek Mekanizmalar, Kısıtsız, Çok Serbestlik Derecesi

To My Parents

ACKNOWLEDGMENTS

The author wishes to express his deepest gratitude to his supervisor Prof. Dr. Eres Söylemez for his guidance, advice, criticism, encouragements and insight throughout the research.

The technical assistance of Mr. Volkan Parlaktaş are gratefully acknowledged.

TABLE OF CONTENTS

ABSTRACT.....	iv
ÖZ	v
ACKNOWLEDGMENTS	vii
TABLE OF CONTENTS.....	x
LIST of FIGURES	vi
LIST of SYMBOLS	xiv
CHAPTER	
1. INTRODUCTION.....	1
2. SURVEY of the RELATED LITERATURE.....	5
2.1 Pseudo-Rigid-Body Model	7
2.2 Unconstrained Mechanisms	13
3. UNCONSTRAINED MULTI DEGREE-OF-FREEDOM MECHANISMS..	18
3.1 Introduction.....	18
3.2 Analysis of Unconstrained Multi Degree-of-Freedom Mechanisms	23
4. VARIABLE STROKE MECHANISM	25
4.1 Introduction.....	25
4.2 Analysis of the Variable Stroke Mechanism.....	27
4.3 An Intuitive Design Procedure for the Variable Stroke Mechanism	31
4.4 Example	32

4.5	Examples	35
4.6	Effects of Different Initial Spring Position Constants on the Output Stroke	44
4.7	Examples	45
4.8	Generalization of the Variable Stroke Mechanism	47
4.9	Example(Design Charts for the Variable Stroke Mechanism).....	50
4.10	Example(Design Charts for the Variable Stroke Mechanism).....	54
4.11	Example	58
4.12	Example	58
5.	FIVE-BAR MECHANISM.....	59
5.1	Introduction	59
5.2	Analysis of the Five-Bar Mechanism.....	61
5.3	Definition of the Output-Link's Torque Function with Differential Method	65
5.4	Example	66
5.5	Example	69
5.6	An Approximate Estimation Technique for Dead Centers of the Five-Bar Mechanism.....	72
5.7	Examples	74
5.8	Generalization of the Five-Bar Mechanism	87
5.9	Examples (Design Charts for the Five Bar Mechanism)	93
6.	CONCLUSIONS and RECOMMENDATIONS	102
	REFERENCES.....	108

APPENDICES

A. Function of the Variable Stroke Mechanism	110
B. Code for the Analysis of the Variable Stroke Mechanism.....	111
C. Code for the Design Chart of the Variable Stroke Mechanism	113
D. Function of the Five-Bar Mechanism	115
E. Code for the Analysis of the Five-Bar Mechanism.....	116
F. Code for the Design Chart of the Five-Bar Mechanism	118
CIRRICULUM VITAE.....	120

LIST OF FIGURES

Figure 1.1 Compliant Crimping Mechanism and its Rigid-Body Counterpart.....	2
Figure 1.2 Partially Compliant Variable Stroke Mechanism	3
Figure 1.3 Partially Compliant Five-Bar Mechanism.....	3
Figure 1.4 A Flexible Segment and its Pseudo-Rigid Body Model.....	4
Figure 2.1 Flexible Segment and its Pseudo-Rigid-Body Model	8
Figure 2.2 A Compliant Slider-Crank Mechanism and its Pseudo-Rigid-Body Model	9
Figure 2.3 A Cantilever Beam (a) and its Pseudo-Rigid Body Model (b).....	10
Figure 2.4 The Differential	13
Figure 2.5 Examples of Under-Actuated Two Degree-of-Freedom Mechanisms	14
Figure 2.6 Multi-Port Lever	15
Figure 2.7 Strap Tightening and Cutting Tool	15
Figure 2.8 A Seven-Link Variable Structure Mechanism for 50^0 and 25^0 Swing Angles	16
Figure 2.9 Model of Underactuated n-DOF Finger	17
Figure 2.10 A Variable Oscillation Mechanism with a Translational Adjustment.....	17
Figure 3.1 Six-link Multi DOF Compliant Mechanism and its Pseudo-Rigid-Body Model	18
Figure 3.2 First Situation for the Six-Link Mechanism.....	21
Figure 3.3 Second Situation for the Six-Link Mechanism.....	21

Figure 3.4 Third Situation for the Six-Link Mechanism.....	22
Figure 4.1 Variable Stroke Mechanism	26
Figure 4.2 The Variable Stroke Mechanism with Spring Forces shown Active.....	27
Figure 4.3 Output-Load Function	32
Figure 4.4 The Variable Stroke Mechanism without and with the Output-Force.....	33
Figure 4.5 Output-Load Function	35
Figure 4.6 The Position Variables for Example 4.5.1.....	35-36
Figure 4.7 The Input Torque vs. Crank Angle for Example 4.5.1	36
Figure 4.8 The Variable Stroke Mechanism in Different Positions.....	37-38
Figure 4.9 The Position Variables for Example 4.5.2.....	39-40
Figure 4.10 The Input Torque vs. Crank Angle for Example 4.5.2	40
Figure 4.11 The Position Variables for Example 4.5.3.....	41-42
Figure 4.12 The Input Torque vs. Crank Angle for Example 4.5.3	42
Figure 4.13 Position of the Five-Bar Mechanism When the Springs are Unloaded ...	44
Figure 4.14 The Output-Link Stroke Variations for Different Values of c_{45}	45
Figure 4.15 The Output-Link Stroke Variations for Different Values of c_{34}	46
Figure 4.16 Output-Load Function	48
Figure 4.17 The Design Chart and the corresponding Spring Deflection of the Variable Stroke Mechanism for $k_{45}/k_{34} = 0.7, 1, 1.3$ and $a_3/a_2 = 2.5$..	51-53
Figure 4.18 The Design Chart and the corresponding Spring Deflection of the Variable Stroke Mechanism for $k_{45}/k_{34} = 0.7, 1, 1.3$ and $a_3/a_2 = 4$	55-57
Figure 5.1 Five-Bar Variable Structure Mechanism	59
Figure 5.2 The Five-Bar Mechanism with the Spring Forces shown Active.....	60
Figure 5.3 $\theta_{13}, \theta_{14}, \theta_{15}$ vs. θ_{12} for Example 5.4	67

Figure 5.4 T_{15} vs. θ_{12} for Example 5.4	67
Figure 5.5 $\theta_{13}, \theta_{14}, \theta_{15}$ vs. θ_{12} for Example 5.5	70
Figure 5.6 Oscillatory Regions for the Output-Link for Example 5.5	70
Figure 5.7 The Imaginary Coupler-Link for the Five-Bar Mechanism	72
Figure 5.8 The Position Variables for Example 5.7.1	74
Figure 5.9 The Position Variables and the Input torque for Example 5.7.2	76
Figure 5.10 The Position Variables for Example 5.7.3	77
Figure 5.11 Sketch of a Five-Bar Mechanism	79-83
Figure 5.12 T_{12}, T_{15} vs. θ_{12} for Example 5.7.5 for $k_{34} = k_{45} = 3$ N.unit/rad	84
Figure 5.13 T_{12}, T_{15} vs. θ_{12} for Example 5.7.5 for $k_{34} = k_{45} = 5$ N.unit/rad	85
Figure 5.14 T_{12}, T_{15} vs. θ_{12} for Example 5.7.5 for $k_{34} = k_{45} = 3$ N.unit/rad and $c_{34} = 1.5$ and $c_{45} = -0.5$	85
Figure 5.16 The Design Chart and the corresponding Spring Deflection of the Five-Bar Mechanism for $k_{45}/k_{34} = 0.7, 1, 1.3$ and $a_3/a_1 = a_4/a_1 = 0.7$..	94-95
Figure 5.17 The Design Chart and the corresponding Spring Deflection of the Five- Bar Mechanism for $k_{45}/k_{34} = 0.7, 1, 1.3$ and $a_3/a_1 = a_4/a_1 = 1.2$	98-100
Figure 6.1 Compliant Slider-Crank Mechanism in a Deflected Position and its single and two degree-of-freedom Pseudo-Rigid-Body Model	106

LIST OF SYMBOLS

a_i	Length of the i^{th} link
θ_{ij}	Angle between i^{th} and j^{th} links
s_{ij}	Position of j^{th} slider
Δs_{ij}	Stroke of the j^{th} slider
k_{ij}	Linear spring stiffness for i^{th} and j^{th} links
c_{ij}	Spring initial position constant between i^{th} and j^{th} links
T_{ij}	Torque applied from i^{th} to j^{th} link
F_{ij}	Force applied from i^{th} to j^{th} link
T	Maximum output-link torque value during work stroke
F	Maximum output-link force value during work stroke
Q_i	Generalized force
q_i	Virtual displacement
δx_{ij}	Infinitesimal displacement for j^{th} link
δW_i	Virtual work of active forces
ϕ_{16}	Angle of the Imaginary Coupler-Link of the Five-Bar Mechanism

CHAPTER I

INTRODUCTION

The main disadvantage of single degree-of-freedom mechanisms containing rigid links and rigid joints is that they are inherently inflexible. They cannot be adjusted or controlled readily for varying load conditions and requirements. Multi degree-of-freedom mechanisms with several inputs (as used in robots) are one possible solution to introduce flexibility. However, such mechanisms are expensive and slow in operation when compared with the classical mechanisms. In order to obtain some flexibility while keeping the advantages of classical mechanisms a multi-degree-of-freedom mechanism structure can be made to operate under the action of a single input. Such an application can be seen in car differentials in which a two degree-of-freedom mechanism operates in two different modes depending on the torque applied at the output wheels. This can be generalized to any multi degree-of-freedom unconstrained mechanism in which there are springs to store and release energy at the joints where we have an oscillating motion. A revolute joint with a spring can be realized by a flexible element in between the two rigid links. Such a system is known as “pseudo compliant joint”. Compliant mechanisms and pseudo-compliant (Figure 1.1) modeling of these mechanisms are being investigated by several researchers because such mechanisms are flexible, cheaper, lighter and easy to manufacture. However, the main disadvantage of the compliant mechanisms is the difficulty of analyzing and designing them. To simplify the analysis of the compliant mechanisms, single degree-of-freedom “pseudo-rigid-body” modeling technique is used in the literature. This technique is also used for analysis of the compliant mechanism with small-flexural pivots.

However, in the literature, analysis of the compliant mechanisms using “multi” degree-of-freedom pseudo-rigid-body modeling is not available. This approach makes a mechanism unconstrained (the number of inputs of the system is less than the degree-of-freedom of a system). Therefore, in this study an attempt for analysis and design of the unconstrained multi degree-of-freedom mechanisms is presented.

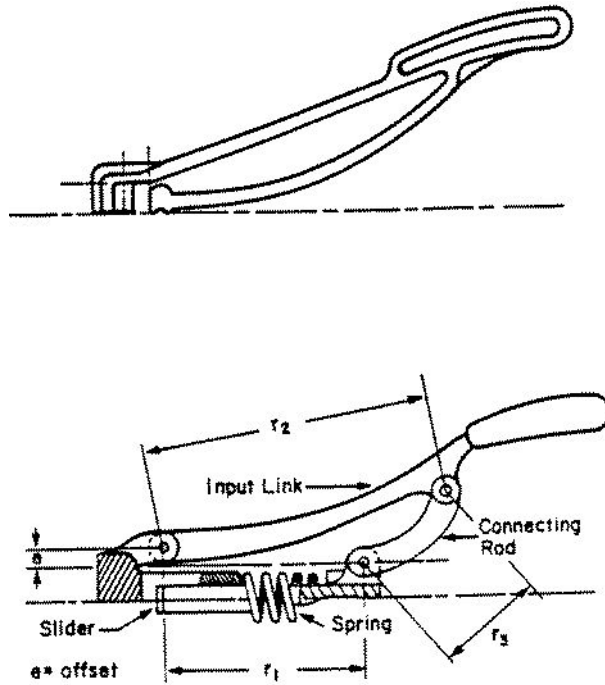


Figure 1.1 Compliant Crimping Mechanism and its Rigid-Body Counterpart [1]

To investigate the behavior of a multi degree-of-freedom unconstrained mechanism, two different mechanisms are considered. Firstly, a five-link in-line slider-crank mechanism (Figure 1.2) (called variable stroke mechanism in this study) is taken into consideration (Chapter 4). This mechanism is a two degree-of-freedom mechanism with one input at the crank. An analysis technique which considers both kinematics and forces simultaneously is introduced. After performing the kinematic and force analysis of the mechanism, a two-dimensional design chart according to the output-link oscillations using dimensionless parameters is produced.

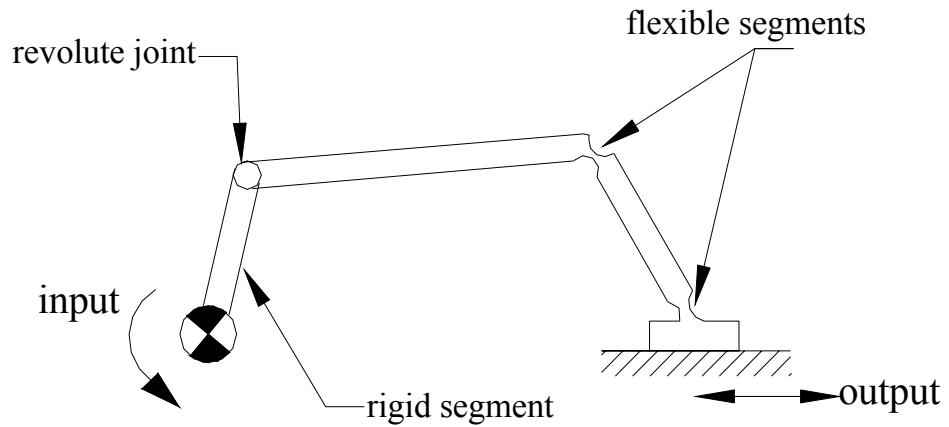


Figure 1.2 Partially Compliant Variable Stroke Mechanism

In the second part of the study, another multi degree-of-freedom mechanism, a “five-bar mechanism” (Figure 1.3) is investigated (Chapter 5). This is also a two degree-of-freedom mechanism with one input. An analysis technique similar to the one applied for the variable stroke mechanism is used. Similarly, using dimensionless parameters, three-dimensional design charts are developed for the five-bar mechanism which relates output-link oscillation, link proportions and spring parameters.

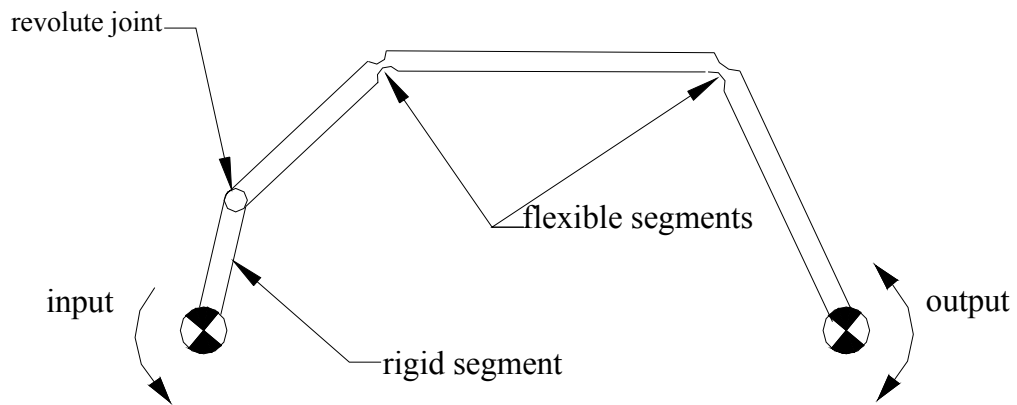


Figure 1.3 Partially Compliant Five-Bar Mechanism

Kinematics of the unconstrained mechanisms is also related to their loading conditions. Generally, before applying load and performing analysis, defining exact direction change position of the output-link is not possible. Therefore, a method which estimates direction change of output-link (dead centers) is required to obtain a function which can change output-load's direction according to work or return stroke. A method is presented in Chapter 5 Section 6 for the estimation of approximate dead centers of the five bar mechanism. This approach may also be useful for analysis of different types of such unconstrained mechanisms.

Analysis of unconstrained multi degree-of-freedom mechanisms is not as simple as that of single degree-of-freedom mechanisms. For such mechanisms, kinematic analysis must be performed together with force analysis. For simplicity, low-speed analysis is taken into consideration. Therefore, static equilibrium is assumed for the analyses.

The maximum value of the output-load during the work stroke is assumed to be five times of the return stroke's maximum value, for all of the following analyses and the design charts. The direction of these loads is assumed to be always resistive to the motion of the output-link.

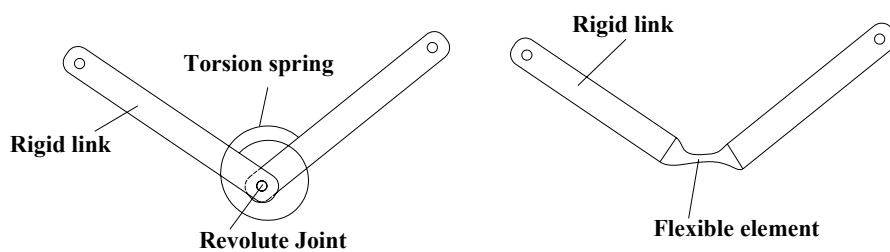


Figure 1.4 A Flexible Segment and its Pseudo-Rigid Body Model [1]

CHAPTER II

SURVEY of the RELATED LITERATURE

In this study, partially compliant unconstrained multi degree-of-freedom mechanisms are taken into consideration. Therefore, this chapter presents a survey of the related literature for compliant and unconstrained mechanisms.

Compliant mechanisms are flexible mechanisms, which gain some or all of their motion through the deflection of flexible members. These mechanisms can be fully compliant and partially compliant. A fully compliant mechanism such as in Figure 1.1 is one that has no rigid body joints. A partially compliant mechanism such as in Figure 1.2 is one that has some compliant members and some non-compliant joints.

An advantage of compliant mechanisms is the reduction in the total number of parts required to accomplish a certain task. This reduces manufacturing and assembly time and cost. Some mechanisms may even be constructed of one piece. This kind of design has been given a new name recently, “Design for no assembly”.

Generally compliant mechanisms are lighter than rigid link mechanisms synthesized for the same purpose. Another advantage of compliant mechanisms is the ease with which they are miniaturized. Compliant mechanisms also have a smaller number of movable joints, such as pin (revolute) and sliding joints. This results in reduced wear and need for lubrication. These are desirable characteristics for applications where the mechanism is not easily accessible, or for operation in harsh environments that may adversely affect joints. The reduction of the number of joints can also increase mechanism precision since backlash may be reduced or eliminated. This fact has

often been used in the design of instrumentation. Vibration and noise caused by the turning and sliding joints of rigid-body mechanisms may also be reduced in some applications by using compliant mechanisms.

The main disadvantage of compliant mechanisms is the difficulty in their analyzes and design. It is necessary to understand the interactions between “mechanism theory” and “strength of materials”, in a complex situation.

Fatigue life is another issue. Some compliant segments are often critically loaded cyclically; those members must be designed to have sufficient fatigue life to perform their prescribed functions.

Energy storage of the flexible members can be (an advantage for some cases) disadvantage for some mechanisms. Because all of the input is not transmitted as output; some is stored in the mechanism.

The motion from the deflection of compliant links is also limited by the strength of the deflecting members. Furthermore, a compliant link can not produce a continuous rotational motion such as is possible with a pin joint. Compliant links that remain under stress for long periods of time or at high temperatures may experience stress relaxation or creep.

2.1 Pseudo-Rigid-Body Model

The pseudo-rigid-body model [1] is used to simplify the analysis and design of compliant mechanisms. It is used to unify compliant mechanism and rigid-body mechanism theory by providing a method of modeling the nonlinear deflection of flexible beams. This method of modeling allows well-known rigid-body analysis methods to be used in the analysis of compliant mechanisms.

Salamon [2] introduced a methodology for compliant mechanism design that used a pseudo-rigid-body model of the compliant mechanism with compliance modeled as torsional and linear springs. These models are much easier to analyze than idealized models which require finite element or elliptic integral solutions. The most important attribute of the pseudo-rigid-body model is that it significantly simplifies the design process.

Howell and Midha [3], [4] used closed-form elliptic-integral solutions to develop deflection approximations for an initially straight, flexible segment with linear material properties. Figure 2.1 shows such a member and its pseudo-rigid-body model. The model consists of two rigid links, connected by a "characteristic pivot" to represent the displacement, and a torsional spring to model the beam stiffness or resistance to the applied force. This model predicts the deflection path of the beam end for a given end load, to within 0.5% of the closed-form elliptic integral solutions for quite large deflections. The location of the characteristic pivot is expressed in terms of the "characteristic radius factor", γ , which represents the fraction of the beam length at which the pivot is located. Once γ is determined, the deflection path may be parameterized in terms of θ , the "pseudo-rigid-body angle."

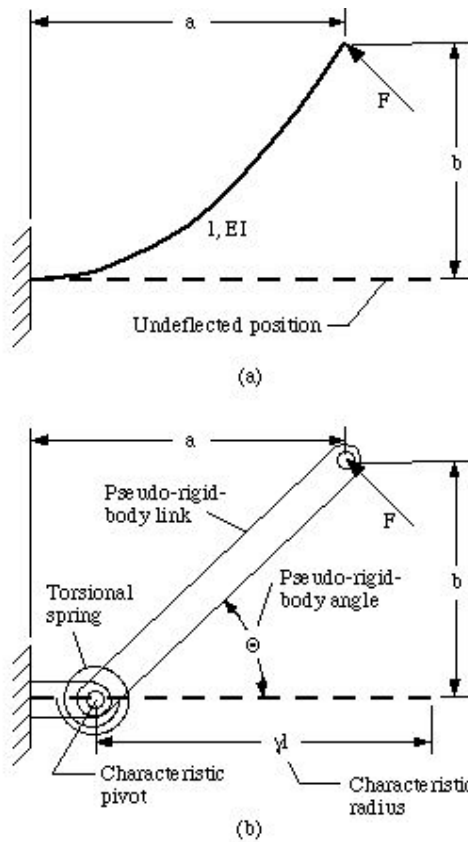


Figure 2.1 A Flexible Segment and its Pseudo-Rigid-Body Model [1]

Pseudo-rigid-body models for individual flexible segments offer a simplified method of determining the deflections of large-deflection members. The availability of such a method for individual segments suggests its use to model more complex systems which include flexible segments. This pseudo-rigid-body model concept proves to be very useful in simplifying the analysis and synthesis of compliant mechanisms. Its advantage lies in its ability to develop a pseudo-rigid-body model of a compliant mechanism, and then use the large body of knowledge available in the field of rigid-body mechanism analysis and design. In this way, the pseudo-rigid-body model concept acts to unify compliant and rigid-body mechanism theories. Figure 2.2 shows another example of a compliant mechanism and its pseudo-rigid-body model.

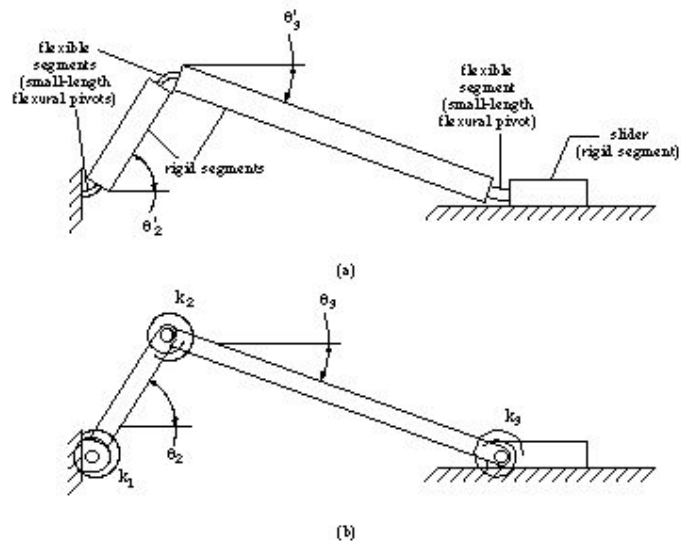


Figure 2.2 A Compliant Slider-Crank Mechanism and Pseudo-Rigid-Body Model [1]

Howell and Midha [3], [5] analyzed compliant mechanisms with small-length flexural pivots. Since the lengths of the flexural members are small relative to the lengths of the rigid segments, the flexural pivots are modeled as kinematic joints at the center of the flexible segment. Torsional springs are used to represent the member stiffness. The accuracy of this method decreases as the relative length of the flexural member increases, and a different approach is required for compliant mechanisms containing longer flexural pivots. This model will be taken into consideration in next part of this study.

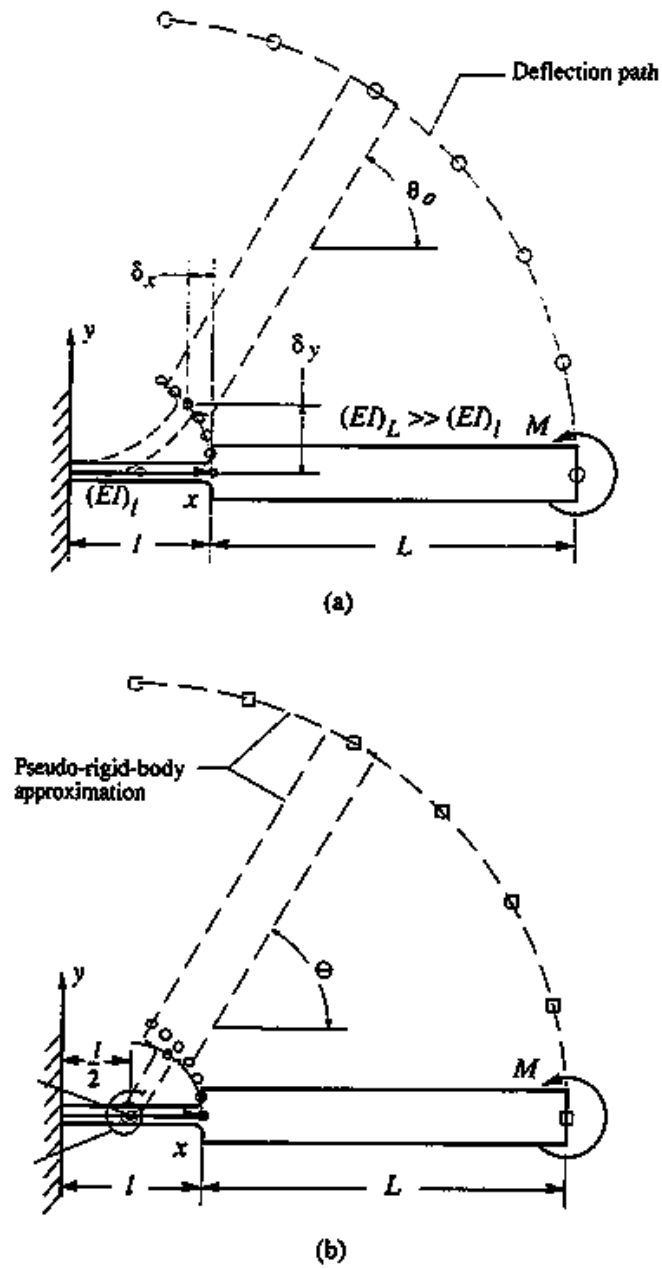


Figure 2.3 A Cantilever Beam (a) and its Pseudo-Rigid Body Model (b) [3]

In Figure 2.3, the cantilever beam has two segments, one is short and flexible and the other is longer and rigid. If the smaller segment is significantly shorter and more flexible than the longer segment, that is $L \gg l$ and $(EI)_L \gg (EI)_l$.

The short segment is called a small-length flexural pivot. (Figure 2.3 shows l with an exaggerated length. Usually L is 10 or more times longer than l .)

Since the flexible section is much shorter than the rigid section, the motion of the system may be modeled as consisting of two rigid sections; the motion of the system may be modeled as two rigid links joined at a pin joint, called characteristic pivot. The characteristic pivot is assumed to be located at the center of the flexural pivot, as shown in Figure 2.3(b). This is an accurate assumption because the deflection occurs at the flexible segment and it is small compared to the length of the rigid segment. For small-length flexural pivots, the pseudo-rigid-body angle is equal to the beam end angle. ($\theta = \theta_0$)

The beam's resistance to deflection is modeled using a torsional spring with spring constant K . The torque required to deflect the torsional spring through an angle of θ is given in Eq. 2.1

$$T = K \theta \quad (2.1)$$

The spring constant, K , may be found from elementary beam theory. The end angle for a beam with a moment is given in Eq. 2.2 as

$$\theta_0 = ML/(EI)_l \quad (2.2)$$

Since $M = T$ and $\theta_0 = \theta$, the spring constant can be found as

$$K = (EI)_l/l \quad (2.3)$$

This model is accurate if bending is the dominant loading in the flexural pivot. If transverse and axial loads are significantly high, a greater error will be introduced into the model.

The nature of small-length flexural pivots ensures that the assumption that bending is the predominant loading is accurate in most applications.

In analysis, the kinematic motion, input requirements, and the component stresses may be determined quickly and efficiently by means of the pseudo-rigid-body model. The greatest benefit of the pseudo-rigid-body model concept is realized in compliant mechanism design. In the early design stages, the pseudo-rigid-body model may serve as a fast and efficient method of evaluating many different trial designs to meet the specific design objectives. It also allows the design of systems to perform more complex tasks than would otherwise be possible. If a designer relies solely on prototyping or full numerical analysis, an initial design must be obtained before it can be modeled or built. The pseudo-rigid-body model, on the other hand, may be used to obtain a preliminary design which may then be optimized. Once a design which meets the specified design objectives is obtained, it may be further refined using methods such as nonlinear finite element analysis, and it may then be prototyped and tested.

Brian P. Trease [6] investigated the drawbacks of typical flexure connectors and presented several new designs for highly effective, kinematically well-behaved compliant joints.

2.2 Unconstrained Mechanisms

The mechanisms that are investigated in the next sections are unconstrained. Their degree-of-freedom is at least two. The number of the inputs is one.

Conventional differential of a car is a common example for an unconstrained mechanism. It is a two degree-of-freedom mechanism with one input. For static equilibrium, torque on the output shafts must be exactly the same due to the idler gear in its construction. In Figure 2.4, the tangential forces acting on gears of a differential are shown. Since there is no torque on the shaft of the idler gear, the tangential forces on both sides of the idler gear must be the same. Consequently, the tangential forces and the torques on the output shaft gears must also be the same for static equilibrium.

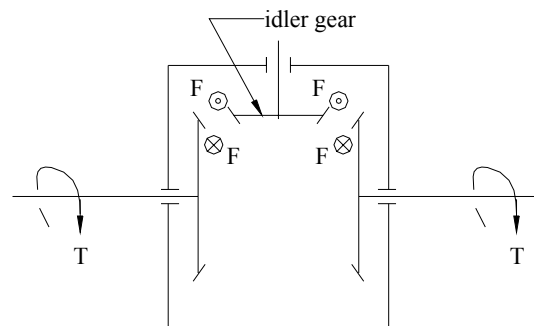


Figure 2.4 The Differential

The output shafts can rotate with different angular velocities according to curvature of the road. As an extreme case, when one side of a road is ice covered, the wheel on the slippery side of the road spins and other wheel stalls.

Assuming that a car has enough power to cause a spin at either a wheel or the car is obstructed to move. If the two traction wheels are on surfaces with different coefficient of friction, only one wheel spins and the other one will be motionless. This is the general characteristic of unconstrained mechanisms.

Thierry Laliberte and Clement M. Gosselin [7] carried out a study on simulation and design of under actuated mechanical hands. The taxonomy of the grasps is first reviewed in their study. Then, the principle of under actuation which leads to shape adaptation of the hand is introduced and a review of the existing under actuated mechanical hands is provided. Architectures of two-degree-of-freedom under actuated fingers are then proposed and a simulation tool is designed to analyze their behavior. It is shown that under actuation is a very promising avenue when only grasping is required (no manipulation). An under actuated finger is selected and this finger is used in the design of a three fingered hand. Grasps-chosen from the taxonomy which can be performed with this hand are then illustrated [7].

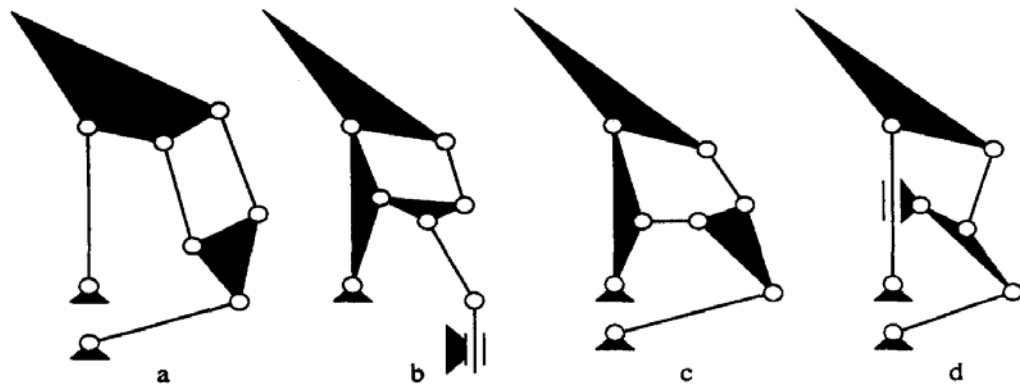


Figure 2.5 Examples of Under-Actuated Two Degree-of-Freedom Mechanisms [7]

A mechanical logic element, multi-port lever, investigated by Söylemez and Freudenstein [8] is shown in Figure 2.6. This is a multi degree-of-freedom multi-port-lever configuration involves a link, the planar displacement of which is a rotation about one of several parallel axes or ports. Connecting rods connect the ports to sliders on both sides of each port and the sliders are loaded by compression springs. At point O the lever is actuated by an initially horizontal force, P , called control force.

If the magnitude of the control force increases slowly from zero, a force level will be reached at which the lever will just begin to move. The motion of the lever will be rotation about one of the ports, which is a function the force exerted by the springs.

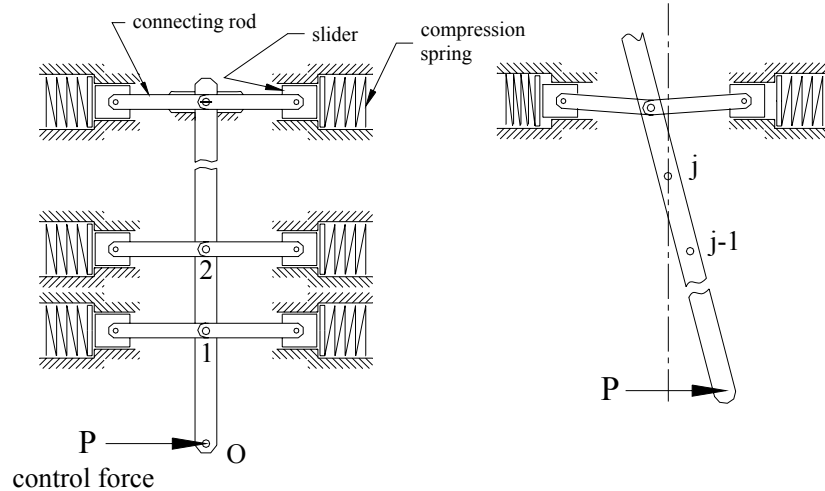


Figure 2.6 Multi-Port Lever [8]

Strap tool (Figure 2.7) is an application of two-port lever which tightens and automatically cuts off a plastic strap about a bundle of wires

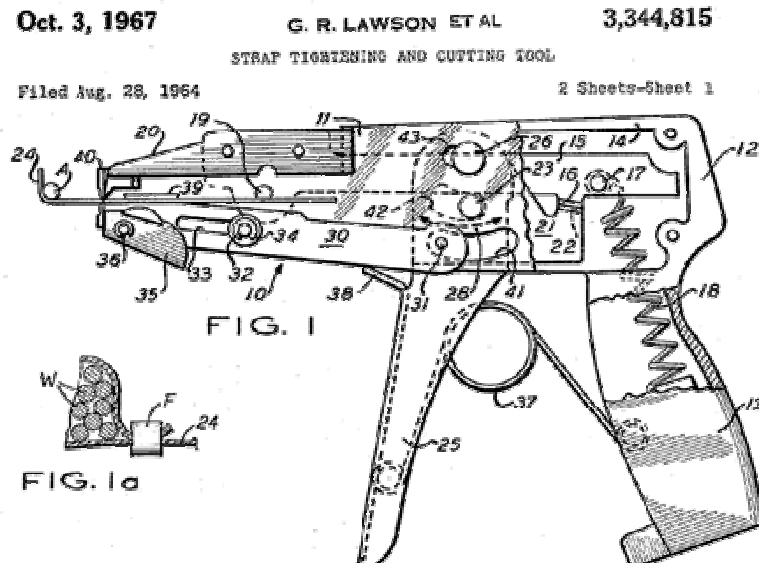


Figure 2.7 Strap Tightening and Cutting Tool [8]

E. Tanık and E. Söylemez [9] derived a synthesis procedure for a variable structure using two different types of seven-link unconstrained mechanisms. These mechanisms run as six-link mechanisms for different positions of the control-link to achieve different (but specified) output link oscillation. The change in the structure occurs when the output load condition exceeds a certain threshold value. One of the mechanisms synthesized (Figure 2.8) is analyzed in detail considering the static forces which also includes the motion during the switching. The switching action is limited to certain crank positions during the motion. Such variable structure applications provide a cheap and reliable mechanical logic system which can be used for different applications

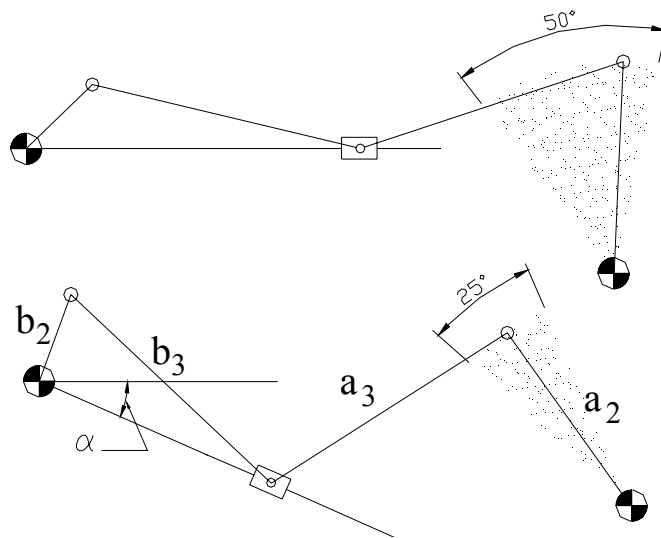


Figure 2.8 A Seven-Link Variable Structure Mechanism for 50° and 25° Swing Angles [9]

Lionel Birglen and Clément M. Gosselin [10] established a fundamental basis for the analysis of underactuated fingers with a general approach. A new method to obtain the force capabilities of any underactuated fingers is presented [10]. Force capability is defined as the ability to generate an external wrench onto a fixed object with a given set of phalanges. A general -DOF, 1-degree-of-actuation (DOA) finger with four-bar linkages is considered for analysis Figure 2.9.

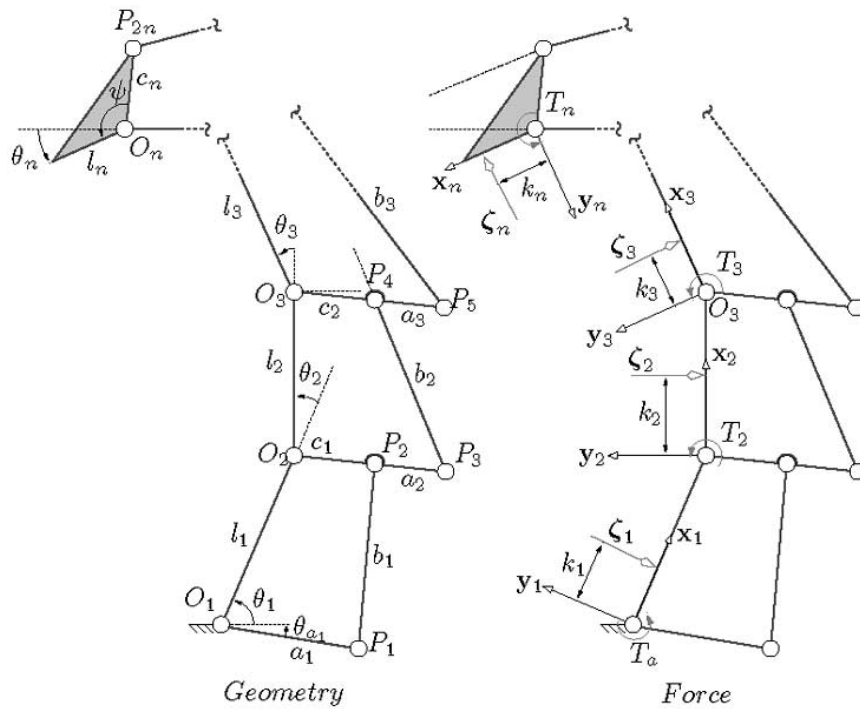


Figure 2.9 Model of Underactuated n-DOF Finger [10]

Kireççi, Dülger and Gültekin [11] used a seven-link, two degree-of-freedom mechanism (This is an example of variable structure, however it is a constrained mechanism), (Figure 2.10) for variable oscillation at its output. The input is at link 2 and the translational adjustment at link 5 provides the variable oscillation. However, since the adjustment control system is mounted on link 4, which is driven by a servomotor, the inertia of link 4 increases. Consequently, at high-speed operations the forces become larger.

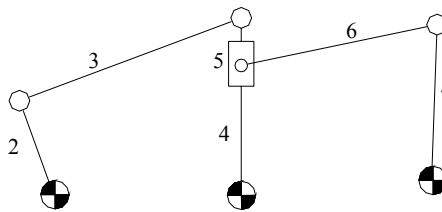


Figure 2.10 A Variable Oscillation Mechanism with a Translational Adjustment [11]

CHAPTER III

UNCONSTRAINED MULTI-DEGREE-OF-FREEDOM MECHANISMS

3.1 Introduction

In this chapter, general characteristics of unconstrained (underactuated) compliant multi-degree-of-freedom mechanisms with small-length flexural pivots are considered. The motion characteristics of such mechanisms are very similar to the conventional differential mechanism (Section 2.2) in which the two degree-of-freedom motion is constrained by the kinematics and the force equilibrium conditions.

An example of a compliant multi-degree of freedom mechanism and its pseudo-rigid-body model are shown in Figure 3.1. Basically, this mechanism is formed by three members; the fixed link, link 2 (crank) and links 3, 4, 5, 6 (Links 3, 4, 5, 6 are the parts of a simple link having some thin segments). Link 2 is connected to link 3 by a revolute joint.

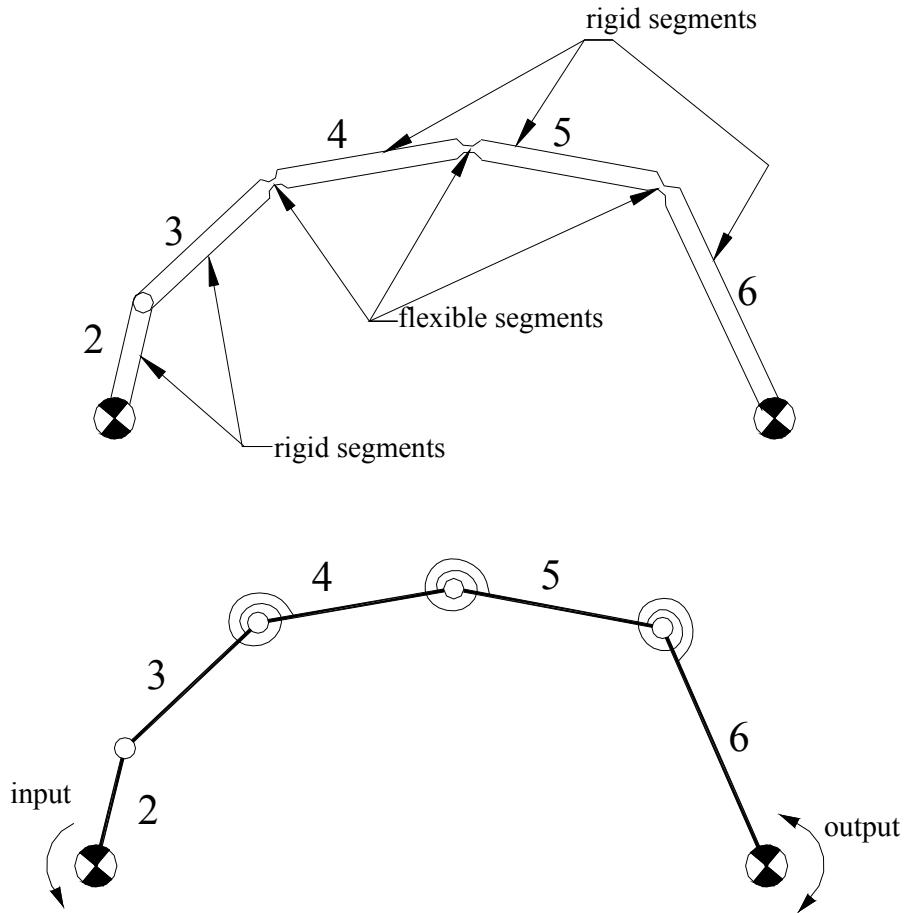


Figure 3.1 (a) Six-link Multi DOF Compliant Mechanism and (b) its Pseudo-Rigid-Body Model

There are small-length flexural pivots between links 3 and 4, links 4 and 5, and links 5 and 6. Since the lengths of the flexural members are assumed to be small in comparison with the length of the rigid segments, the flexural pivots are modeled as revolute joints at the center of the flexible segment (Figure 3.1b). The torsional springs are used to represent the member stiffness. So this technique is called pseudo-rigid-body model [2]. This concept proves to be very useful in simplifying analysis and synthesis of the compliant mechanisms as explained in detail Chapter II. In the following sections of the study, “pseudo-rigid-body model” is used a base for the study.

Consequently, from now on, kinematics of the mechanism will be investigated with the help of the pseudo-rigid-model shown in Figure 3.1b.

Assuming that the links are dimensioned properly, the crank (link 2) can make a complete rotation. Link 2 is the input; link 6 is the output of this three-degree-of-freedom mechanism (Fig. 3.2b). Therefore, with one input and three degree-of-freedom the mechanism is unconstrained.

Kinematics of this mechanism depends on the spring constants, the initial tensions, positions and input-output forces. When the static force equilibrium is considered, the relative motion of the links occurs in a sequence similar to that of the car differential example given in Section 2.2. Therefore, the mechanism will behave as if it is a single degree-of-freedom mechanism. Furthermore, if the output-link load changes, different configurations can be encountered within the same cycle. Appropriate spring rates and initial positions may change force characteristics and the stroke of the mechanism for various tasks.

In order to visualize how such mechanism behaves, the following modeling approach can be helpful. For a multi-degree of freedom unconstrained mechanism, the possible different structures that may occur in a cycle are shown in Figures 3.2, 3.3 and 3.4.

If the relative motion starts between links 3 and 4 at the position shown, the structure will behave as a four-bar mechanism as shown in Figure 3.2. And at this position there is no relative motion between links 4, 5 and links 5, 6.

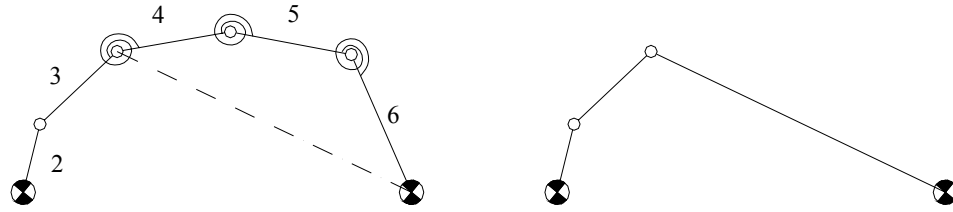


Figure 3.2 First Situation for the Six-Link Mechanism

If the relative motion starts between links 4 and 5 at the position shown, the structure will behave as a four-bar mechanism as shown in Figure 3.3. And at the position there is no relative motion between links 3, 4 and links 5, 6.

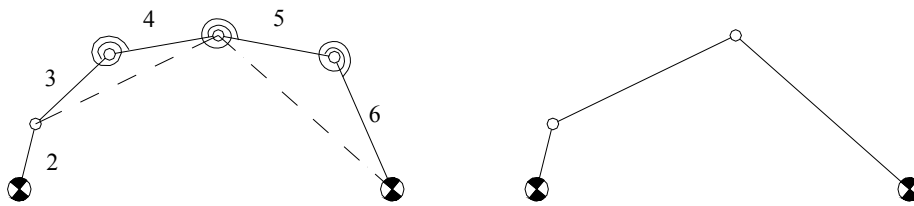


Figure 3.3 Second Situation for the Six-Link Mechanism

If the relative motion starts between links 5 and 6 at the position shown, the structure will behave as a four-bar mechanism as shown in Figure 3.4. And at the position there is no relative motion between links 3, 4 and links 4, 5.

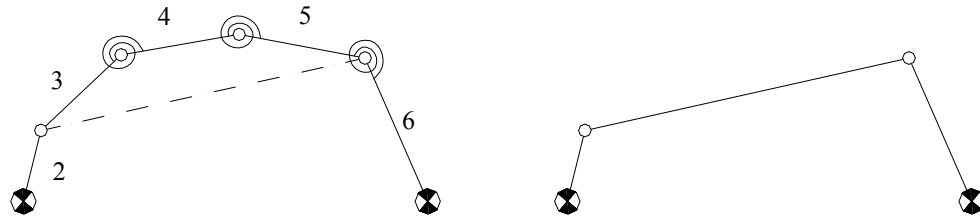


Figure 3.4 Third Situation for the Six-Link Mechanism

The three different possible structures which can be formed by the six-link mechanism are shown in the above figures. But the proportions of the structure may differ according to the position at which these structural changes occur. Shifting position from one structure to another may be during a small or a large rotation of the crank. Variation in the output-link load may change the structure considerably. Also the stiffness and the initial positions of the spring can affect the characteristics of the mechanism.

To the best of our knowledge, investigations on multi degree-of-freedom mechanisms with small-length flexural pivots are not available in literature. Therefore, this study is unique from that side of view. In the following sections, some analysis and design techniques for two multi-degree-of-freedom mechanisms are introduced.

3.2 Analysis of Unconstrained Multi Degree-of-Freedom Mechanisms

Analysis of multi degree-of-freedom mechanisms is not as simple as single degree-of-freedom mechanisms. For such mechanisms, kinematic relations must be treated together with force analysis.

For the analysis of the mechanisms the method of virtual work is used. This method has great advantage to formulate the required equations of static equilibrium without having to consider the mutual reactions exerted upon one another by the bodies of the system.

The principle [12] is simply stated, however each word in the statement must be clearly explained:

- *Virtual displacements*: A set of infinitesimal displacements which are consistent with the constraints
- *Virtual work*: Work done by specified forces on virtual displacements
- *Active(External) forces*: All forces which do non-zero virtual work
- *Ideal mechanical system*: System where constraints do no work
- *Generalized forces*: Terms which multiply the virtual generalized displacements in the expression for virtual work of active forces.
- *Equilibrium*: A state where the resultant force on each particle of the system vanishes
- *Generalized Equilibrium*: A state where all the generalized forces of a system vanish; equivalent to equilibrium for systems “at rest”

With the above definitions, the principle of virtual work may be formulated in the following two-part statement:

1- If an ideal mechanical system is in equilibrium, the net virtual work of all the active forces vanishes for every set of virtual displacements.

2- If the net virtual work of all the active forces vanishes, for every set of virtual displacements, an ideal mechanical system is in a state of generalized equilibrium.

The virtual work for a system with F degree-of-freedom [12] can be expressed in generalized coordinates as;

$$\delta W = Q_1 \delta q_1 + Q_2 \delta q_2 + \dots + Q_F \delta q_F \quad (3.1)$$

Where Q_i represents generalized forces and q_i represents virtual displacements.

Hence, the principle of virtual work states that a necessary and sufficient condition for generalized equilibrium is that each of the generalized forces Q_i must vanish.

$$Q_1 = 0, \quad Q_2 = 0, \dots, \quad Q_F = 0 \quad (3.2)$$

Generalized equilibrium is assumed for the mechanisms analyzed for all positions of the given crank angle as the input of the mechanisms.

For all the mechanisms analyzed, low-speed operation is assumed. Masses of links are assumed to be negligible in comparison with the applied loads. Therefore, all inertia and gravity forces of the links are neglected.

CHAPTER IV

VARIABLE STROKE MECHANISM

4.1 Introduction

Initially, for simplicity of the equations a two degree-of-freedom unconstrained mechanism is analyzed. This mechanism is shown Figure 4.1

It is a two degree-of-freedom in-line slider-crank. Two torsional springs (k_{34} , k_{45}) are mounted in between links 3 and 4, link 4 and the slider. The input is at the crank (link 2) and the output is at the slider.

Since the output-link stroke of the mechanism may change with the variation of the output load, this mechanism is called as variable stroke mechanism in this study.

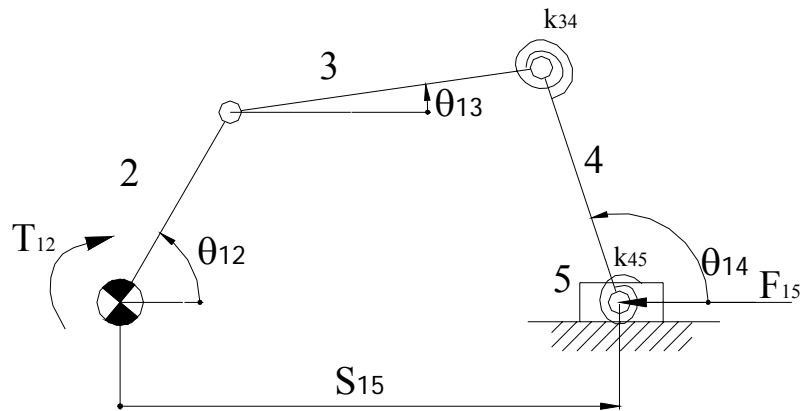


Figure 4.1 Variable Stroke Mechanism

This mechanism is one of the simplest multi degree-of-freedom mechanisms because one parameter (eccentricity) is eliminated in the analysis and design procedures. The absence of the eccentricity has one more benefit for the easiness of the analysis and design (It is mentioned at the end of Section 3 in detail)

The variable stroke mechanism is analyzed in detail in Section 4.2 by the method of virtual work mentioned in Section 3.2.

The link proportions are selected such that the crank can make full-rotation. The output-load is assumed to be resistive to the motion of the output link, the direction of rotation of the crank is assumed to be counter clock-wise.

A generalization procedure is introduced in Section 4.8 to obtain design charts relating the output force and spring constants to the output stroke. The design charts are given in Example 4.9.

4.2 Analysis of the Variable Stroke Mechanism

In this section, analysis of the mechanism is done according to the method and the assumptions mentioned in Section 3.2

The virtual work of the active loads is;

$$\delta W_1 = -T_{12} \delta \theta_{12}, \quad \delta W_2 = -F_{15} \delta s \quad (4.1)$$

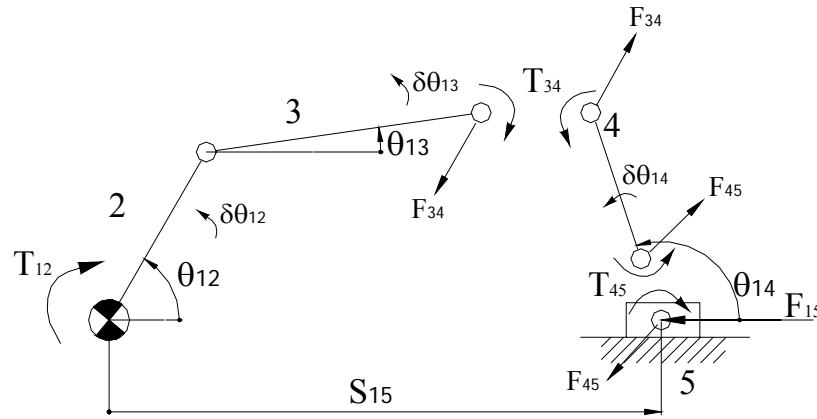


Figure 4.2 The Variable Stroke Mechanism with Spring Forces shown Active

Springs may always be removed from a system provided that equal, opposite forces (torques) which they exert upon their points of attachments are taken into consideration.

Therefore, the virtual works of the springs are (Figure 4.2);

$$\delta W_3 = -T_{34} \delta \theta_{13} + T_{34} \delta \theta_{14}, \quad \delta W_4 = T_{45} \delta \theta_{14} \quad (4.2)$$

where,

$$T_{34} = k_{34} (\theta_{13} - \theta_{14} + c_{34}), \quad T_{45} = k_{45} (-\theta_{14} + c_{45}) \quad (4.3)$$

In the above equations, “ k_{ij} ” represents the linear spring stiffness and “ c_{ij} ” is the spring initial position constant between i^{th} and j^{th} links. a_i represents the length of the i^{th} link.

Then, the virtual work of all the active forces is

$$\delta W = \delta W_1 + \delta W_2 + \delta W_3 + \delta W_4 \quad (4.4)$$

Or,

$$\delta W = -T_{12}\delta\theta_{12} - F_{15}\delta s_{15} + T_{34}(-\delta\theta_{13} + \delta\theta_{14}) + T_{45}\delta\theta_{14} \quad (4.5)$$

In generalized coordinates, the virtual work of a system with two degree-of-freedom (The degree-of-freedom of the variable stroke mechanism is two) can be expressed as;

$$\delta W = Q_1\delta q_1 + Q_2\delta q_2 \quad (4.6)$$

Where Q_i represents generalized forces and q_i represents virtual displacements.

Therefore, the four infinitesimal displacements in Equation 4.5 must be reduced to two virtual displacements.

The loop closure equations of the mechanism are

$$a_2 \cos \theta_{12} + a_3 \cos \theta_{13} - a_4 \cos \theta_{14} = s_{15} \quad (4.7)$$

$$a_2 \sin \theta_{12} + a_3 \sin \theta_{13} - a_4 \sin \theta_{14} = 0 \quad (4.8)$$

By taking differentials across of Equations 4.7 and 4.8 yields

$$-a_2 \sin \theta_{12} \delta\theta_{12} - a_3 \sin \theta_{13} \delta\theta_{13} + a_4 \sin \theta_{14} \delta\theta_{14} = \delta s_{15} \quad (4.9)$$

$$a_2 \cos \theta_{12} \delta\theta_{12} + a_3 \cos \theta_{13} \delta\theta_{13} - a_4 \cos \theta_{14} \delta\theta_{14} = 0 \quad (4.10)$$

From Equations 4.9 and 4.10, $\delta\theta_{13}$ and $\delta\theta_{14}$ can be determined as

$$\delta\theta_{13} = \frac{a_2 \sin(\theta_{12} - \theta_{14}) \delta\theta_{12} + \cos(\theta_{14}) \delta s_{15}}{a_3 \sin(\theta_{14} - \theta_{13})} \quad (4.11)$$

$$\delta\theta_{14} = \frac{a_2 \sin(\theta_{12} - \theta_{13}) \delta\theta_{12} + \cos(\theta_{13}) \delta s_{15}}{a_4 \sin(\theta_{14} - \theta_{13})} \quad (4.12)$$

Substituting Equations 4.11 and 4.12 into Equation 4.5, yields the form below:

$$\delta W = \delta\theta_{12} \cdot Q_1 + \delta s_{15} \cdot Q_2 \quad (4.13)$$

The principle of virtual work tells that a necessary and sufficient condition for generalized equilibrium is that each of the generalized forces Q_i must vanish.

$$Q_1 = 0, \quad Q_2 = 0 \quad (4.14)$$

According to the above procedure, after performing necessary manipulations the two equilibrium equations can be obtained as:

$$k_{34}(\theta_{13} - \theta_{14} + c_{34}) \frac{a_2 \{\sin(\theta_{12} - \theta_{13}) - \sin(\theta_{12} - \theta_{14})\}}{a_3 \sin(\theta_{14} - \theta_{13})} +$$

$$k_{45}(-\theta_{14} + c_{45}) \frac{a_2 \sin(\theta_{12} - \theta_{13})}{a_4 \sin(\theta_{14} - \theta_{13})} = T_{12} \quad (4.15)$$

$$\begin{aligned}
& k_{34}(\theta_{13} - \theta_{14} + c_{34}) \frac{(\cos(\theta_{13}) - \cos(\theta_{14}))}{a_3 \sin(\theta_{14} - \theta_{13})} + \\
& k_{45}(-\theta_{14} + c_{45}) \frac{\cos(\theta_{13})}{a_4 \sin(\theta_{14} - \theta_{13})} = F_{15}
\end{aligned} \tag{4.16}$$

The kinematic and the force analysis of the mechanism can be performed by solving Equations 4.7, 4.8, 4.15, 4.16 simultaneously.

To obtain the appropriate link proportions, if four of the five position variables are known F_{15} and T_{12} can be determined in a closed-form. But generally this is not the required case. If the output force (F_{15}) and the crank angle (θ_{12}) are known (that is the most common case), Eqs 4.7, 4.8, 4.15, 4.16 become highly non-linear for the rest unknown parameters. These parameters are; θ_{13} , θ_{14} , stroke s_{15} and input torque T_{12} .

Analytical solution of these non-linear equations (Equations 4.7, 4.8, 4.15, 4.16) may not be possible. Therefore, these equations can be solved numerically to determine the required parameters.

Since, the kinematics of multi degree-of-freedom unconstrained mechanisms is uncertain before the loads are applied; generally working zone of output-link is also uncertain. Moreover, magnitude of the output load is a parameter that directly affects the output-link's oscillation interval. But the case is different for the variable stroke mechanism; from many examples it is observed that, for resistive output loads, when $\theta_{12} = 0$ or $\theta_{12} = \pi$ the mechanism is "approximately" at the dead centers. In other words, as in the conventional in-line slider-crank mechanism, the crank position is the major parameter that defines working and return strokes. Then, it can be assumed that the output-link load is simply a function of the crank's position for the "inline" variable stroke mechanism. In the case of extreme conditions (such as sudden change in the direction of motion of the output-force and exaggerated link proportions) this assumption may not be valid.

In this study, these non-linear equations are solved numerically via Matlab (by using the “fsolve” function which finds a root (zero) of a system of nonlinear equations). All the equations of the mechanisms investigated in following examples are solved for full-rotation of crank with one degree increments. Many trials show that feasible solutions of these non-linear equations require close initial guesses. For instance, a set of initial guess for zero degree of crank angle may not be appropriate for the same mechanism at 180^0 . Therefore, in order to obtain a proper solution quickly, the code used for the solution is modified so that initial guesses are obtained from the previous cycle’s set of solutions.

4.3 An Intuitive Design Procedure for the Variable Stroke Mechanism

The equations of motion of the variable stroke mechanism are obtained in Section 4.2. However, at this step, appropriate link proportions, spring constants and initial spring positions are not known. The highly-non linear equations (Equations 4.7, 4.8, 4.15, 4.16) are to be solved numerically for the complete cycle. Most probably, randomly selected set of parameters will not yield rational solutions. Therefore, as a starting point, a design approach is required to obtain feasible set of parameters. In the next example, an intuitive method is introduced to obtain appropriate link proportions and spring parameters. After the first design, with parametric optimization methods, better design can be achieved. In Example 4.4, an intuitive design procedure for a variable stroke mechanism is shown.

4.4 Example

In this example, a variable stroke mechanism for the following output load is designed. The output load is defined as a function of the position of the crank as explained on page 30.

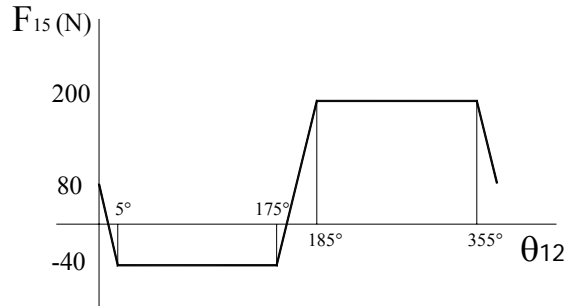


Figure 4.3 Output-Load Function

For the mechanism shown in Figure 4.1, initially, appropriate link lengths can be estimated. Generally, for the mechanisms whose crank can make full rotations, crank is the shortest link. Therefore, for full-rotation of the crank, a_2 can be selected one fourth of sum of the length of a_3 and a_4 .

In order to compare kinematic characteristics of the variable stroke mechanism with that of a conventional in-line slider-crank mechanism, a relatively short link length for link 4 can be chosen. Therefore, let $a_2 = a_4 = 1$ unit. So, a_3 will be 3-unit which makes the crank one-fourth of the sum of a_3 and a_4 .

Next, the spring constants and initial spring positions can be estimated. If the springs are too stiff with respect to the output force, high internal forces may occur. Also flexibility of the mechanism for variable output-load conditions will decrease. In contrary, if the springs are too soft, the mechanism may collapse suddenly when the output force is applied. The spring constants must be selected so that mechanism should behave in between these two cases.

An appropriate situation that may occur after loading the mechanism is shown in Figure 4.4. Referring to below condition (which seems to be a feasible mechanism intuitively), estimation for the spring constants can be done as follows:

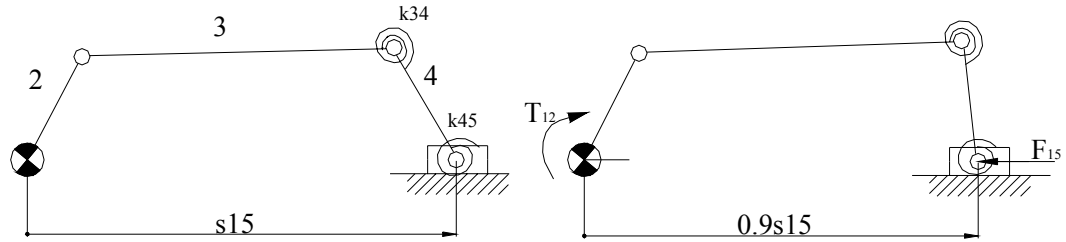


Figure 4.4 The Variable Stroke Mechanism without (left) and with the Output-Force

Before the output load is applied (as it is seen from the left figure), s_{15} is approximately 80% of the sum of the link lengths. So, let s_{15} be $0.8(1+4+1) = 4$. After the load is applied (Let F_{15} is increased from 0 to 200N gradually), assuming 10% reduction in s_{15} and 40° rotation for the torsional springs; spring constants can be estimated with the following work-energy equation:

$$2\left(\frac{1}{2}k\theta^2\right) = F_{avg}(0.1s) \quad (4.17)$$

Substituting the related data, spring constant k can be determined as;

$$k\left(40\frac{\pi}{180}\right)^2 = \left(\frac{0+200}{2}\right)(0.1 \cdot 4) \quad (4.18)$$

$$k = 82 \text{Nunit} / \text{rad}$$

So one can take each spring constant as $k_{34} = k_{45} = k = 100 \text{Nunit/rad}$. (The spring constants are assumed to be identical)

Finally, free position of the springs can be determined. From Figure 4.3, it is assumed that the springs are unstretched at the unloaded position. A spring is unloaded when the applied torque to the related link is zero:

$$T_{s34} = k_{34}(\theta_{13} - \theta_{14} + c_{34}) = 0, \quad T_{s45} = k_{45}(-\theta_{14} + c_{45}) = 0 \quad (4.19)$$

From Figure 4.3, it is observed that, approximate values of the link angles are $\theta_{13} = 10^\circ$, $\theta_{14} = 130^\circ$. Substituting these variables into above equations;

$$\begin{aligned} (10 - 130 + c_{34}) &= 0, \quad (-130 + c_{45}) = 0 \\ c_{34} &= 120^\circ, \quad c_{45} = 130^\circ \end{aligned} \quad (4.20)$$

Rounding the above data, one can select $c_{34} = c_{45} = 150^\circ$.

4.5 Examples

4.5.1 Example

For full-rotation of the crank, position analysis of the mechanism designed intuitively in Example 4.4 is required for the loading below:

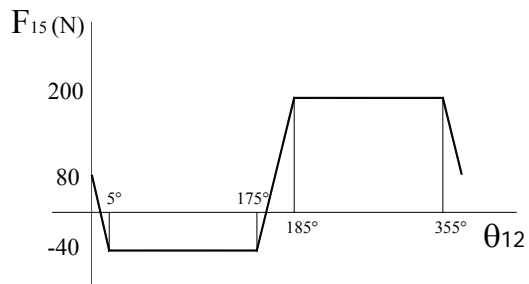


Figure 4.5 Output-Load Function

Link lengths: $a_2 = a_4 = 1$ unit and $a_3 = 3$ units.

Spring variables: $k_{34} = k_{45} = k = 100$ Nunit/rad and $c_{34} = c_{45} = 2.618$ rad

θ_{13} , θ_{14} and T_{12} can be determined by solving Non-linear Equations 4.7, 4.8, 4.15, 4.16 numerically (By using the codes given in Appendices A and B) for one degree crank angle increments,. In Figure 4.6a-b θ_{13} , θ_{14} and s_{15} vs. θ_{12} are shown.

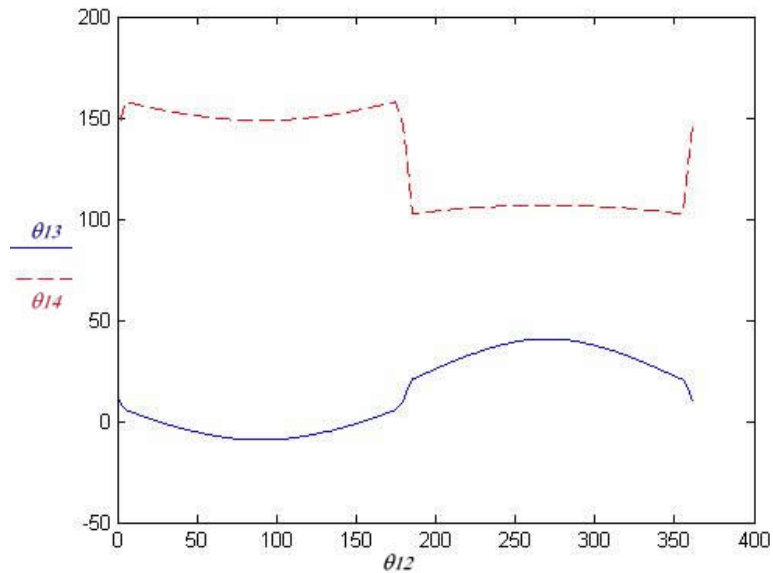


Figure 4.6a θ_{13} , θ_{14} vs. θ_{12} for $k_{34} = k_{45} = 100$ Nunit/rad

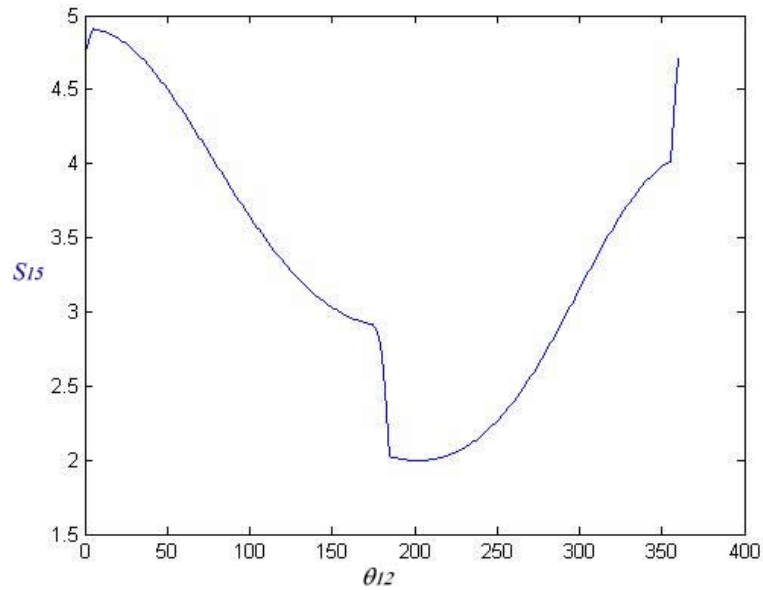


Figure 4.6b s_{15} vs. θ_{12} for $k_{34} = k_{45} = 100 \text{Nunit/rad}$

From Figure 4.6a it can be observed that link 4 remains approximately at the same angle during the reverse and forward strokes. During the work stroke $\theta_{14} = 115^\circ$ and is almost constant. After solving the equations, input torque T_{12} can also be determined. The below figure shows the variation of input torque with the crank angle.

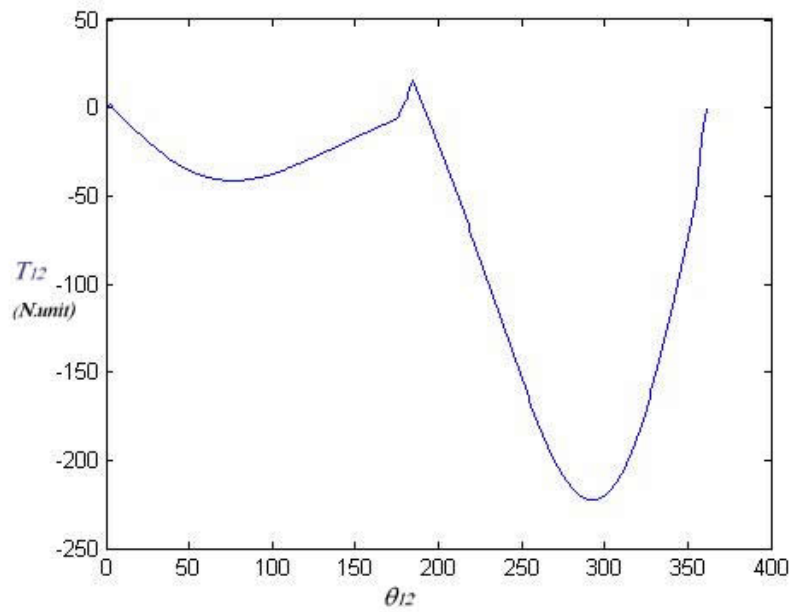


Figure 4.7 T_{12} vs. θ_{12} for $k_{34} = k_{45} = 100 \text{Nunit/rad}$

Magnitude of the input to the T_{12} increases for $180^0 < \theta_{12} < 360^0$ since this interval corresponds to the work-zone. Also negative sign of the input torque nearly for whole cycle is intuitively expected when the model is investigated (Equation 4.5 and Figure 4.1).

In order to visualize the motion of the variable stroke mechanism, the animation of the structure for every 45^0 crank angles is shown in Figure 4.8.

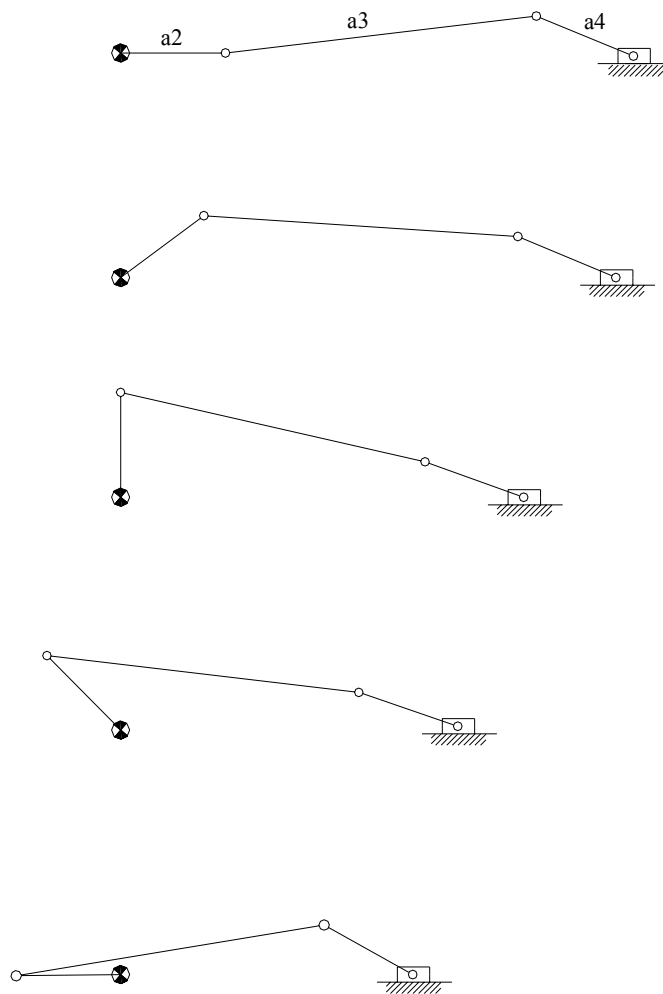


Figure 4.8a The Variable Stroke Mechanism in Different Positions

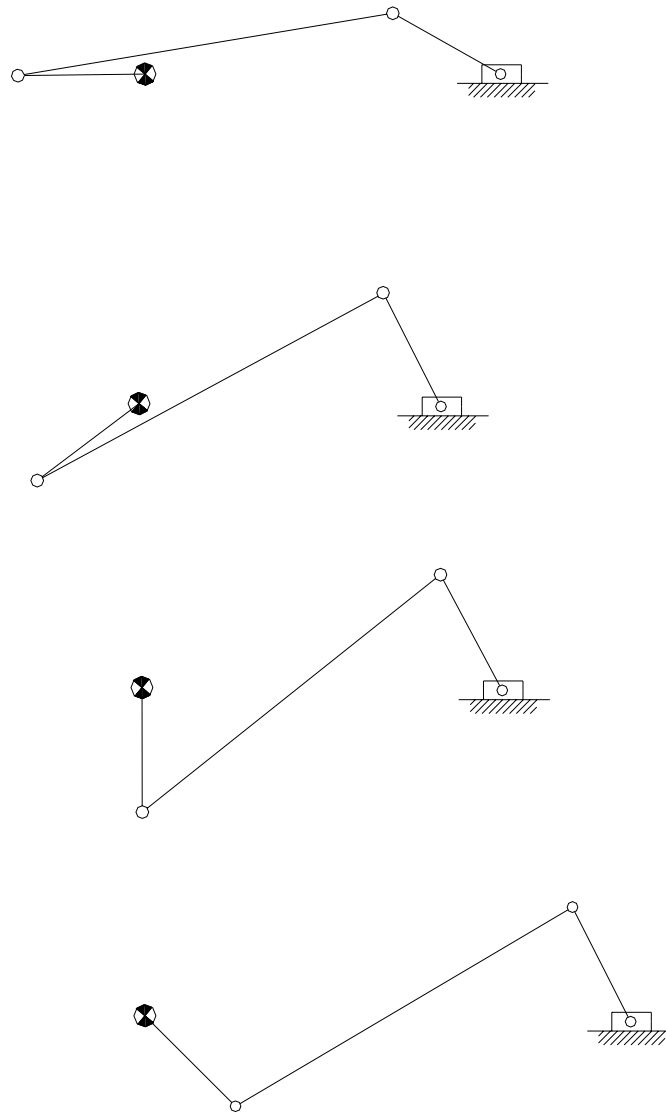


Figure 4.8b The Variable Stroke Mechanism in Different Positions

As it is mentioned in the last paragraph of Section 4.2, the set of non-linear equations is solved via Matlab. The results of the solution at each step are used as the initial guess for the next step. Rational solutions may be obtained in this manner. If the guesses are radically different, appropriate solutions can not be obtained.

4.5.2 Example

Perform the analysis of the five-bar in Example 4.5.1 with same data except a different spring constants; $k_{34} = k_{45} = 50 \text{ N.unit/rad}$

Link lengths: $a_2 = a_4 = 1 \text{ unit}$ and $a_3 = 3 \text{ units}$.

Spring variables: $c_{34} = c_{45} = 2.618$

θ_{13} , θ_{14} and input torque can be determined by solving Non-linear Equations 4.7, 4.8, 4.15, 4.16 numerically (By using the codes given in Appendices A and B) for one degree crank angle increments. In Figure 4.9a-b θ_{13} , θ_{14} and s_{15} vs. θ_{12} are shown:

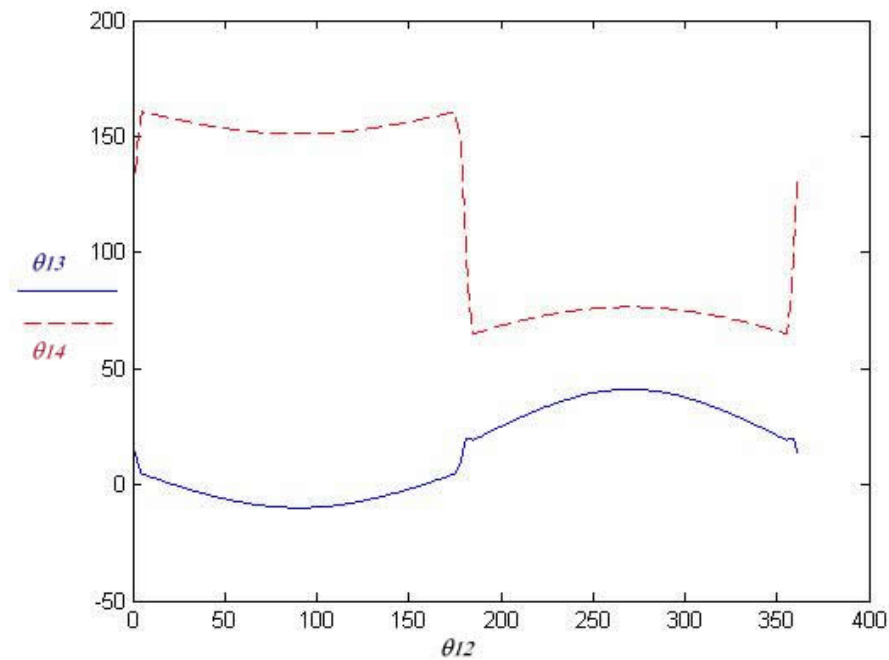


Figure 4.9a θ_{13} , θ_{14} vs. θ_{12} for $k_{34} = k_{45} = 50 \text{ N.unit/rad}$

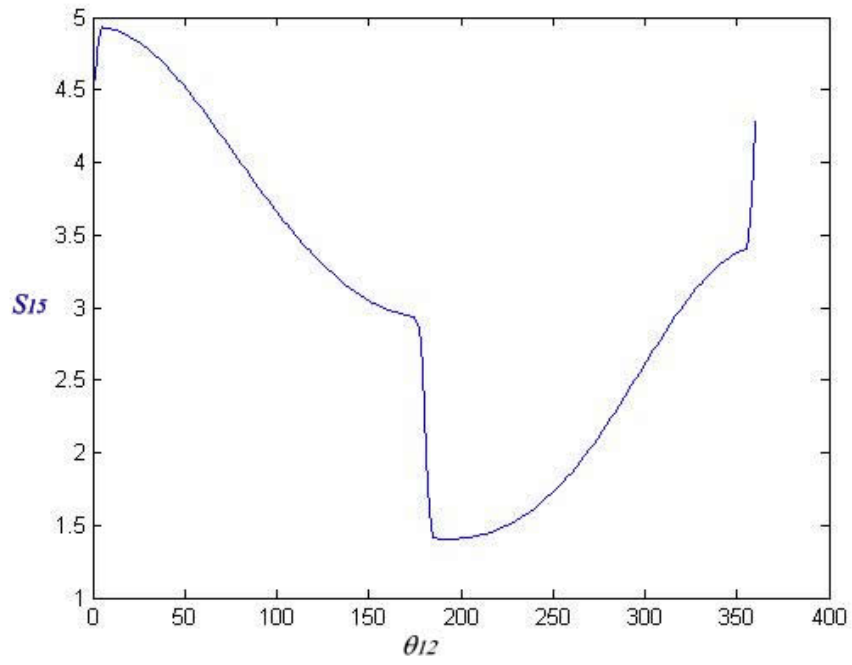


Figure 4.9b s_{15} vs. θ_{12} for $k_{34} = k_{45} = 50$ N.unit/rad

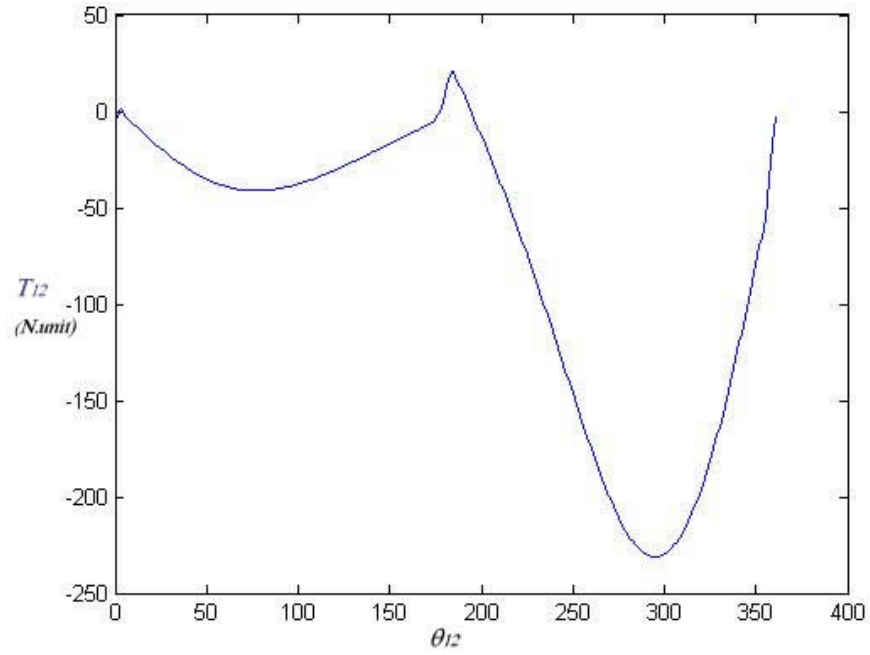


Figure 4.10 T_{12} vs. θ_{12} for $k_{34} = k_{45} = 50$ N.unit/rad

4.5.3 Example

Perform the analysis of the five-bar in Example 4.5.1 with same data except a different initial spring constants; $c_{34} = c_{45} = 1.5$.

θ_{13} , θ_{14} and input torque can be determined by solving Non-linear Equations 4.7, 4.8, 4.15, 4.16 numerically (By using the codes given in Appendices A and B) for one degree crank angle increment. In Figure 4.11a-b θ_{13} , θ_{14} and s_{15} vs. θ_{12} are shown:

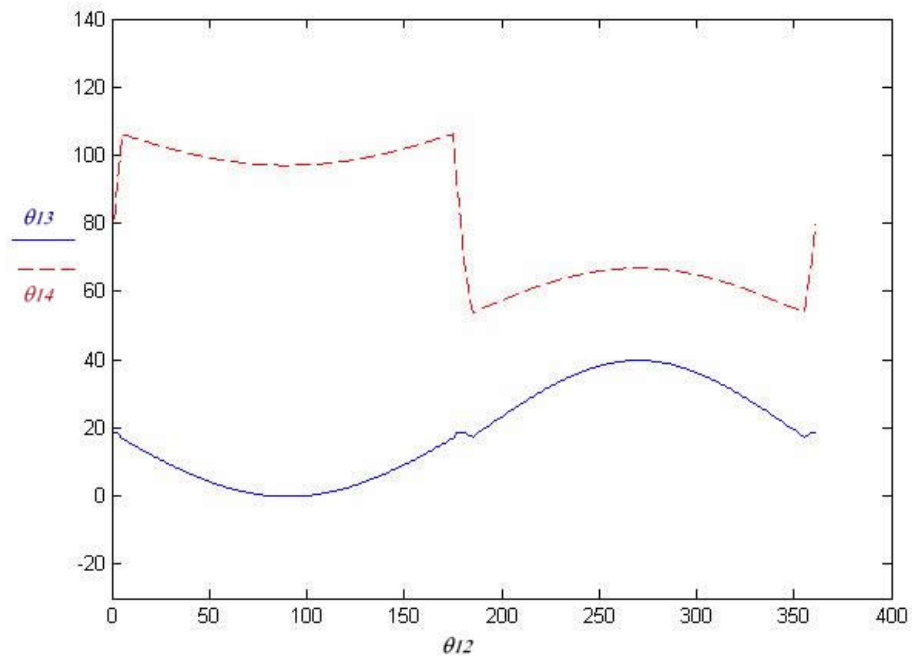


Figure 4.11a θ_{13} , θ_{14} vs. θ_{12} for $c_{34} = c_{45} = 1.5$

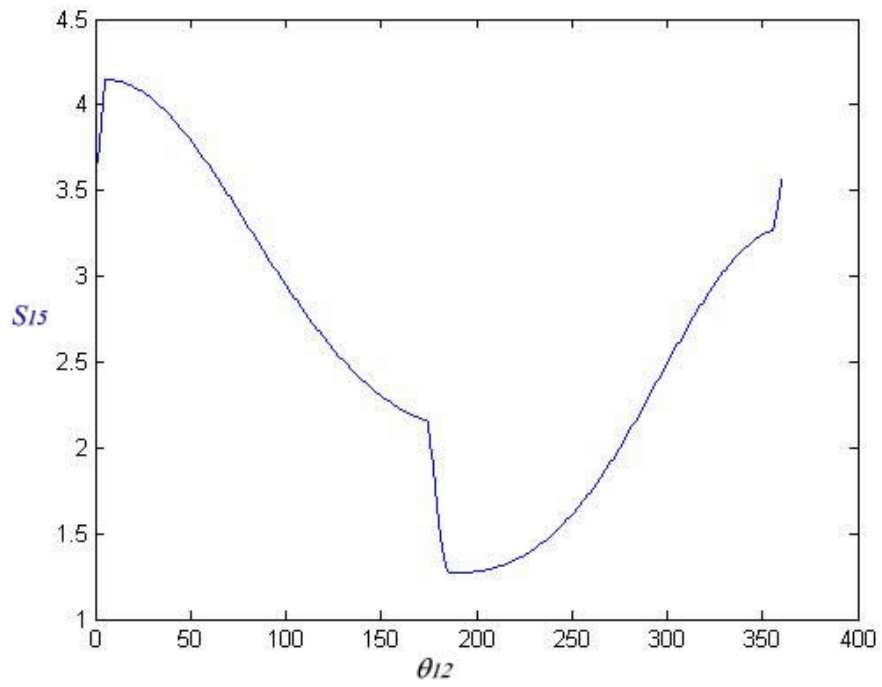


Figure 4.11b S_{15} vs. θ_{12} for $c_{34} = c_{45} = 1.5$

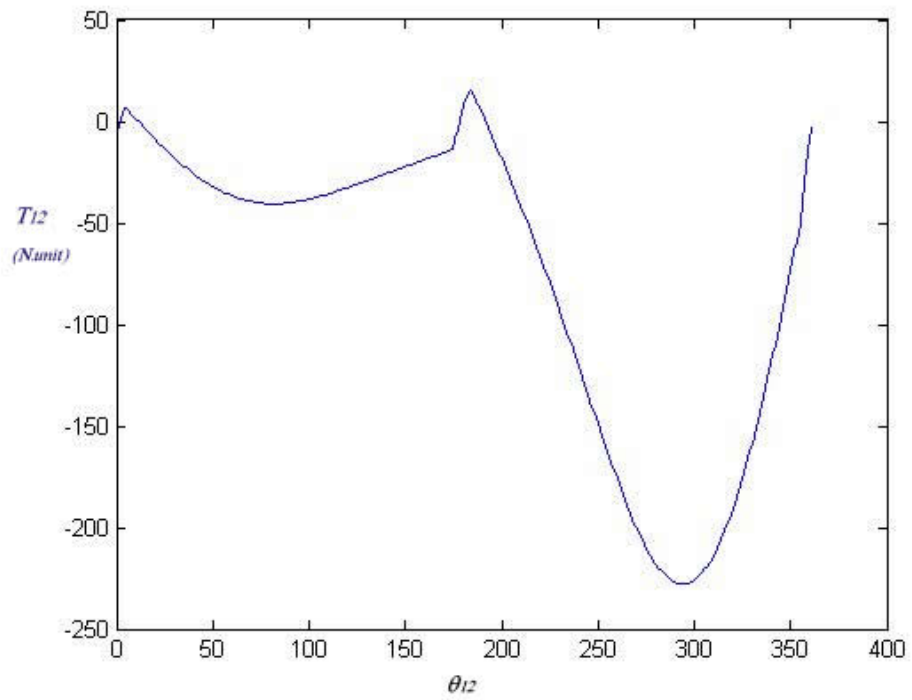


Figure 4.12 T_{12} vs. θ_{12} for $c_{34} = c_{45} = 1.5$

In examples 4.5.1- 2 and 3, for all the three cases the input torque is almost the same. But the kinematics of the mechanisms varies with spring parameters. Therefore, effect of various spring parameters can be investigated to obtain flexibility. Also it can be seen from Examples 4.5-1-2-3 (Figures 4.6a, 4.9b, 4.11b) that the direction changes of the output-link (dead centers) occur approximately around $\theta_{12} = 0$ or $\theta_{12} = \pi$ according to the loading given in Figure 4.5 (Note that these examples do not guarantee that the dead centers always occur when $\theta_{12} = 0$ or $\theta_{12} = \pi$, for all type of loading conditions) In the next section, effects of different initial spring positions are investigated

4.6 Effects of Different Initial Spring Position Constants on the Output Stroke

In this study, compliant multi-degree-of-freedom mechanisms are taken into consideration by using their pseudo rigid body model. This method is mentioned in Section 3.1. As an exception in the following examples (4.7), it is assumed that there is a “real” mechanism formed by torsional springs and rigid links as in Figure 3.1b. By using the same structure, output-link stroke variations can be analyzed with only changing the initial positions of the springs. For the following example, the code in Matlab is modified to determine maximum and minimum values of the s_{15} for a complete rotation of the crank. Before analyzing the effects of initial spring positions, it will be useful to sketch physical meaning of c_{ij} (spring initial position constant). In Figure 4.11 assuming that the springs are unstretched at the position. The springs are unloaded when the applied torque to the related links is zero:

$$T_{s34} = k_{34}(\theta_{13} - \theta_{14} + c_{34}) = 0, \quad T_{s45} = k_{45}(-\theta_{14} + c_{45}) = 0 \quad (4.21)$$

And,

$$c_{34} = -\theta_{13} + \theta_{14} \quad c_{45} = \theta_{14} \quad (4.22)$$

Then the initial spring positions can be illustrated as angles shown as shown in Figure 4.13.

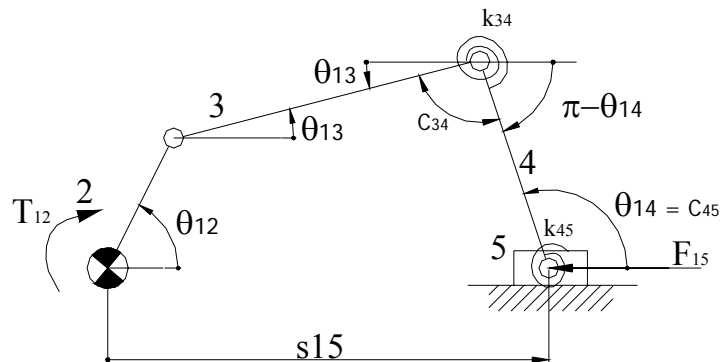


Figure 4.13 Position of the Five-Bar Mechanism When the Springs are Unloaded

4.7 Examples

4.7.1-Example

By changing the initial position of the second spring (c_{45}), determine stroke variations for the same loading for the mechanism analyzed in the Example 4.5.1. Assume c_{45} varies between -10^0 and 150^0 .

Similarly by solving non-linear Equations 4.7, 4.8, 4.15, 4.16 numerically (By using the codes given in Appendices A and B), the stroke of the mechanism is obtained as follows (Figure 4.14):

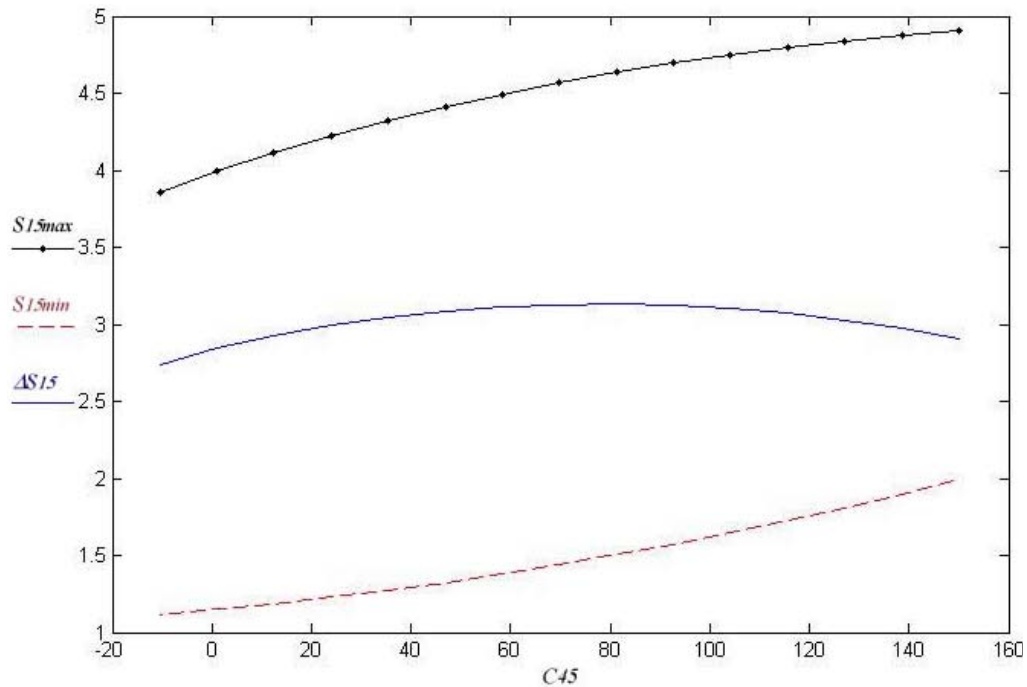


Figure 4.14 The Output-Link Stroke Variations for Different Values of c_{45}

In Figure 4.14, s_{15max} indicates the maximum value of s_{15} , s_{15min} indicates the minimum value of s_{15} in a cycle. Δs_{15} indicates the difference of these two functions which is the stroke of the mechanism. From the graph it can be clearly seen that, as c_{45} is changed working region of the output-link changes significantly, but the change in the total stroke is slight.

4.7.2 Example

By changing the initial position of the first spring, determine the stroke variations for the same loading for the mechanism analyzed in the Example 4.5.1. Assume c_{34} varies between -10^0 and 150^0 .

By solving non-linear Equations 4.7, 4.8, 4.15, 4.16 numerically (By using the codes given in Appendices A and B), the stroke of the mechanism is obtained as follows (Figure 4.15).

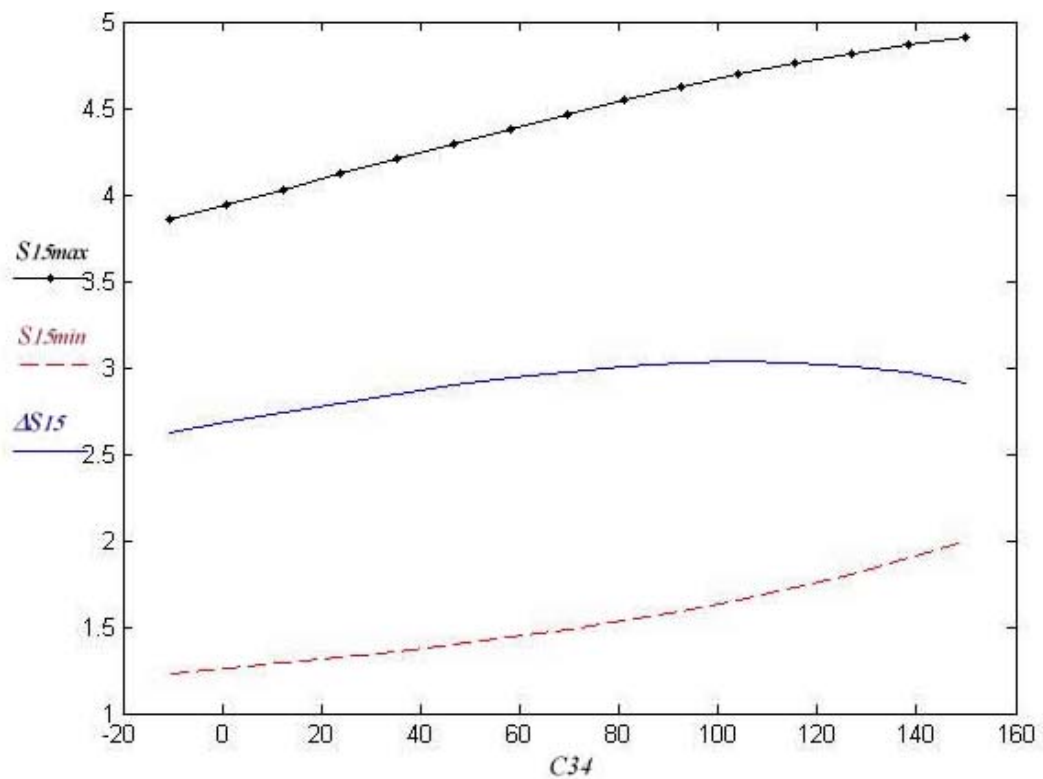


Figure 4.15 The Output-Link Stroke Variations for Different Values of c_{34}

In this example, as c_{34} is changed, working zone of the output-link also shifts. However, change in the stroke is larger when compared with the effect of c_{45} .

4.8 Generalization of the Variable Stroke Mechanism

Synthesis of this type of multi degree-of-freedom mechanisms with springs mounted between some links is uncertain. But at least, a chart relating the output force and spring constants and stroke of the mechanism is essential.

In Equations 4.7, 4.8, 4.15, 4.16 there are seven free design parameters (a_2 a_3 a_4 k_{34} k_{45} c_{34} c_{45}) for the structure. For every combination of these parameters a different output-stroke (Δs_{15}) may be obtained. Also output-force “ F_{15} ” is a free parameter. Since this is an unconstrained mechanism, all these eight parameters are functions of the kinematics of the mechanism. To obtain a simple-two dimensional chart, these parameters must be manipulated.

Firstly, all the related equations (4.7, 4.8, 4.15, 4.16) can be divided or multiplied with a_2 . So link proportions can be considered as a_3/a_2 , a_4/a_2 and s_{15}/a_2 .

Successive trials showed that, the spring initial position constants “ c_{ij} ” don’t have a major effect on the stroke of the mechanism. At this moment, this parameter can be kept constant with a suitable value. As found in Section 4.3, $c_{34} = c_{45} = c$ can be taken as 2.75 rad. Several trials showed that this intuitive approach for the initial spring position constants is appropriate.

Next, force and spring constants can be simplified; in Equations 4.15, 4.16 it is seen that input torque T_{12} and output force F_{15} are linearly proportional with the spring constant k . Therefore, increasing or decreasing both spring constants and output force magnitude linearly yields exactly the same kinematics. Then spring constant and output force can be considered as a single design parameter. Therefore dividing the equations by k_{34} , a more useful $F_{15} a_2/k_{34}$ ratio is introduced.

Let the maximum value of output-force F_{15} be F in the work stroke ($180^\circ < \theta_{12} < 360^\circ$) and one-fifth of this value in the return stroke ($F_{15} = -F/5$) (both are resistive forces to the motion of the slider). In this design procedure, trapezoidal output-force is assumed. The output-link force is given below as a function of the crank angle in graphical form (The criteria to form such kind of loading is mentioned in detail in Section 4.2, Page 30)

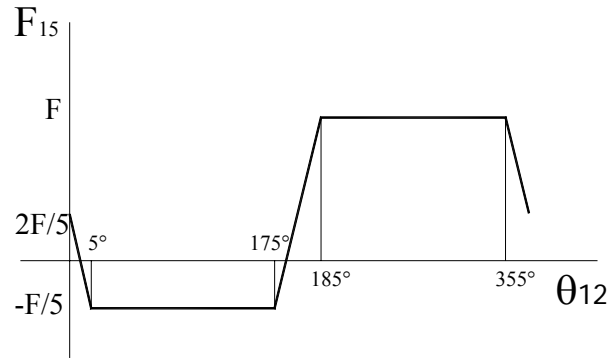


Figure 4.16 Output-Load Function

The kinematic and force equations are rearranged according to above procedure as follows:

Dividing Equation 4.7 by a_2 , 4.23 can be obtained.

$$\cos \theta_{12} + \frac{a_3}{a_2} \cos \theta_{13} - \frac{a_4}{a_2} \cos \theta_{14} = \frac{s_{15}}{a_2} \quad (4.23)$$

Dividing Equation 4.8 by a_2 , 4.24 can be obtained:

$$\sin \theta_{12} + \frac{a_3}{a_2} \sin \theta_{13} - \frac{a_4}{a_2} \sin \theta_{14} = 0 \quad (4.24)$$

Dividing Equation 4.15 by k_{34} , Equation 4.25 can be obtained:

$$\begin{aligned}
& (\theta_{13} - \theta_{14} + c) \frac{\{\sin(\theta_{12} - \theta_{13}) - \sin(\theta_{12} - \theta_{14})\}}{\frac{a_3}{a_2} \sin(\theta_{14} - \theta_{13})} + \\
& \frac{k_{45}}{k_{34}} (-\theta_{14} + c) \frac{\sin(\theta_{12} - \theta_{13})}{\frac{a_4}{a_2} \sin(\theta_{14} - \theta_{13})} = \frac{T_{12}}{k_{34}}
\end{aligned} \tag{4.25}$$

Multiplying Equation 4.16 by a_2/k_{34} , 4.26 can be obtained:

$$\begin{aligned}
& (\theta_{13} - \theta_{14} + c) \frac{(\cos(\theta_{13}) - \cos(\theta_{14}))}{\frac{a_3}{a_2} \sin(\theta_{14} - \theta_{13})} + \\
& \frac{k_{45}}{k_{34}} (-\theta_{14} + c) \frac{\cos(\theta_{13})}{\frac{a_4}{a_2} \sin(\theta_{14} - \theta_{13})} = \frac{F_{15} a_2}{k_{34}}
\end{aligned} \tag{4.26}$$

Now, in equations 4.23-24-25-26, there are four free parameters: three design parameters (a_3/a_2 , a_4/a_2 , k_{45}/k_{34}) and a force-spring ratio Fa_2/k_{34} . For all combination of these parameters, different output strokes can be achieved. In order to generalize the approach, unit length can be taken into consideration. Therefore, the unit of spring constants becomes *Nunit/rad*.

By using Matlab, for a constant a_3/a_2 and k_{45}/k_{34} ratio, increasing a_4/a_2 with small increments for a set of different values of Fa_2/k_{34} , equations 4.23-24-25-26 can be solved numerically for whole crank rotation. After full-rotation of the crank, maximum and minimum value of the s_{15}/a_2 (which yields to the stroke) can be determined. For the interval of the pre-determined design parameters, this procedure can be repeated. Finally, by interpolating results data, a design chart can be obtained.

4.9 Example

Determine design charts for $Fa_2/k_{34} = \{1, 1.5, 2, 3, 10\}$, $a_4/a_2 = \{0.1, 0.2, \dots, 0.9, 1\}$, $a_3/a_2 = \{5/2\}$ and $k_{45}/k_{34} = \{0.7, 1, 1.3\}$ according to the procedure mentioned in Section 4.8. Also check the maximum spring deflections from their corresponding un-deflected positions for each chart.

By solving equations 4.23, 4.24, 4.25 and 4.26 numerically (By using the codes given in Appendices A and C) and using “cubic spline interpolation” for the related data, the design charts below are obtained:

The maximum spring deflection chart indicates the absolute value of the greater deflection of the two springs from their un-deflected position that occurs after the full-rotation of the crank.

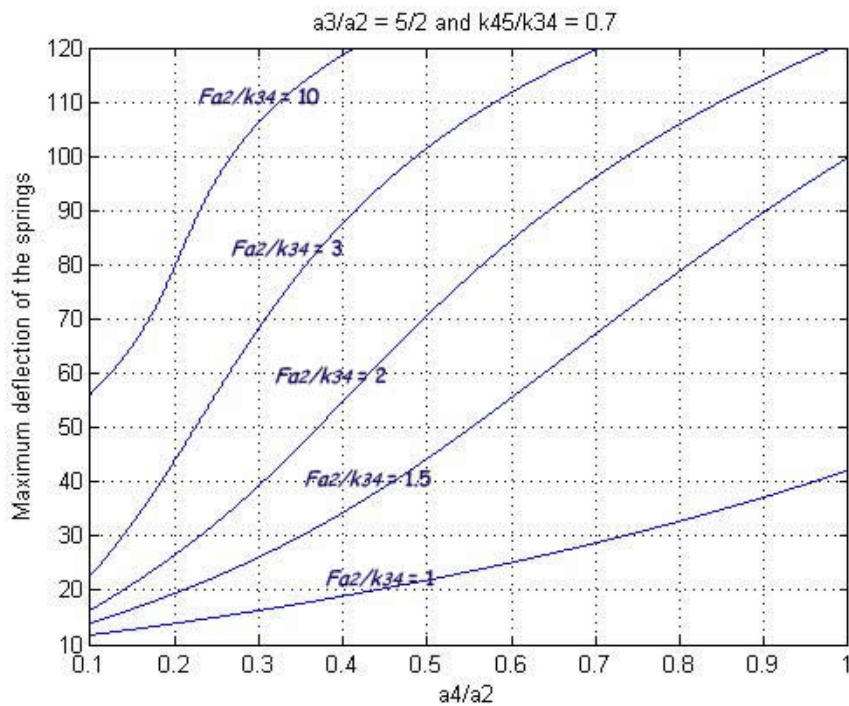
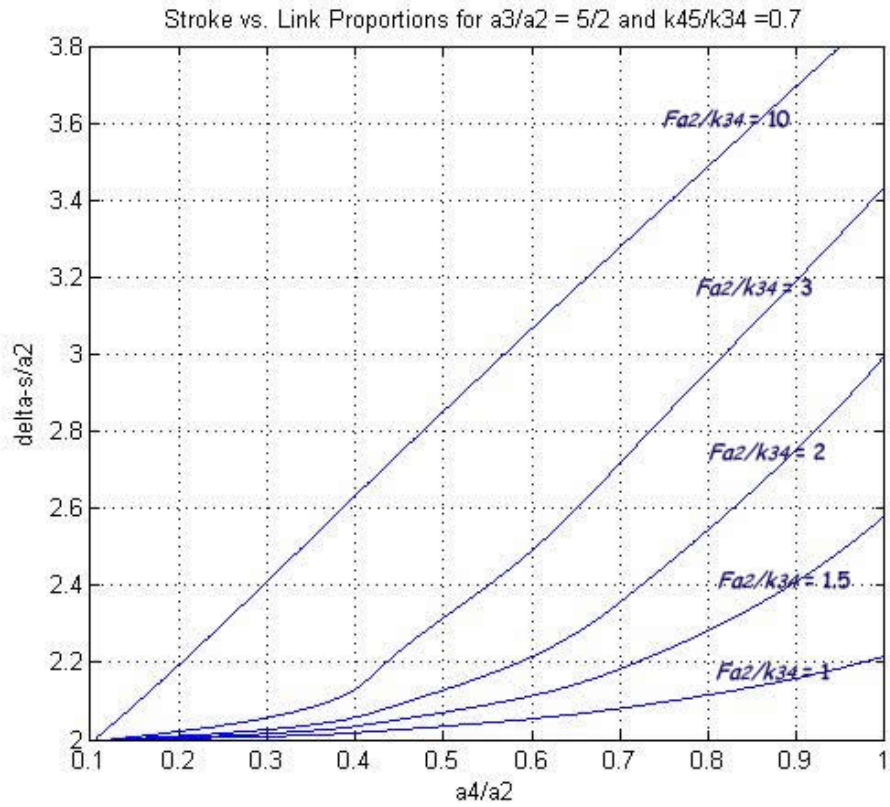


Figure 4.17a The Design Chart and the corresponding Spring Deflection of the Variable Stroke Mechanism for $k_{45}/k_{34} = 0.7$ and $a_3/a_2 = 2.5$

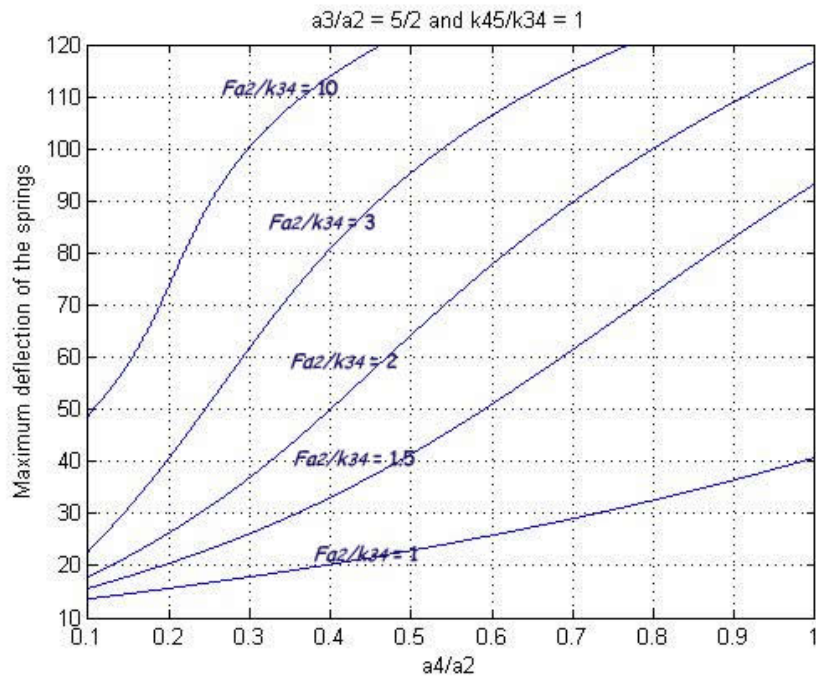
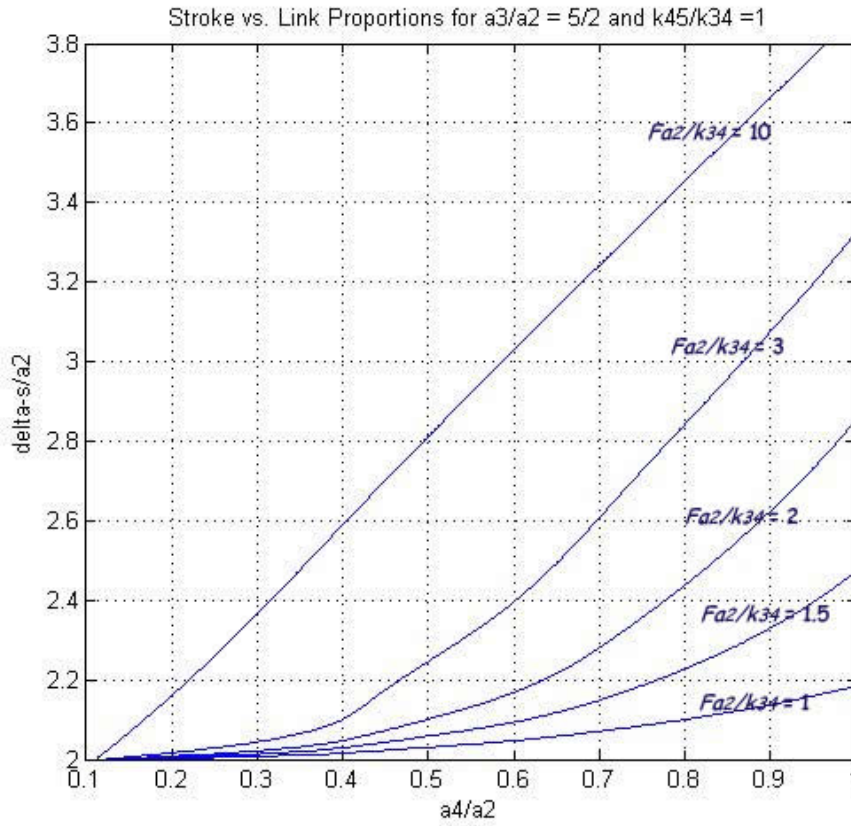


Figure 4.17b The Design Chart and the corresponding Spring Deflection of the Variable Stroke Mechanism for $k_{45}/k_{34} = 1$ and $a_3/a_2 = 2.5$

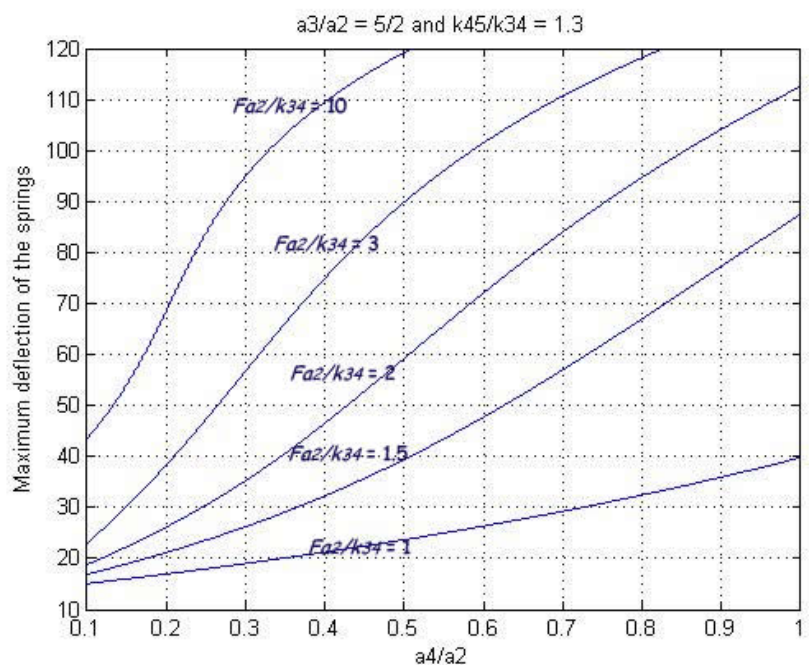
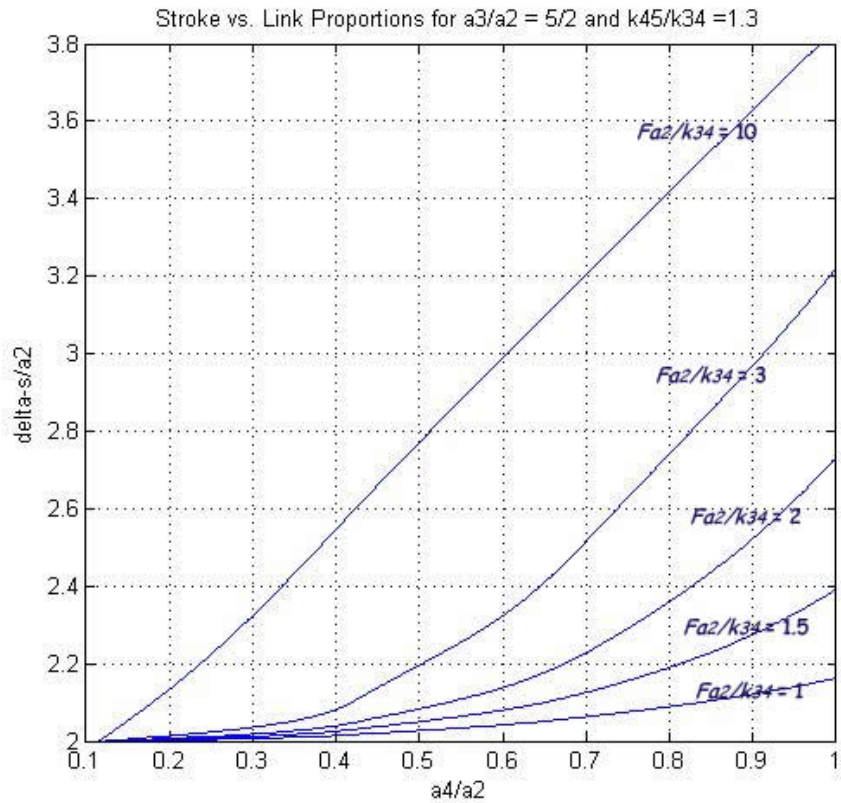


Figure 4.17c The Design Chart and the corresponding Spring Deflection of the Variable Stroke Mechanism for $k_{45}/k_{34} = 1.3$ and $a_3/a_2 = 2.5$

4.10 Example

Determine design charts for $Fa_2/k_{34} = \{1, 1.5, 2, 3, 10\}$, $a_4/a_2 = \{0.1, 0.2, \dots, 0.9, 1\}$, $a_3/a_2 = \{7/2\}$ and $k_{45}/k_{34} = \{0.7, 1, 1.3\}$ according to the procedure mentioned in Section 4.8. Also check the maximum spring deflections from their corresponding un-deflected positions for each chart.

By solving equations 4.23, 4.24, 4.25 and 4.26 numerically (By using the codes given in Appendices A and C) and using “cubic spline interpolation” for the related data, the design charts below are obtained:

The maximum spring deflection chart indicates the absolute value of the greater deflection of the two springs from their un-deflected position that occurs after the full-rotation of the crank.

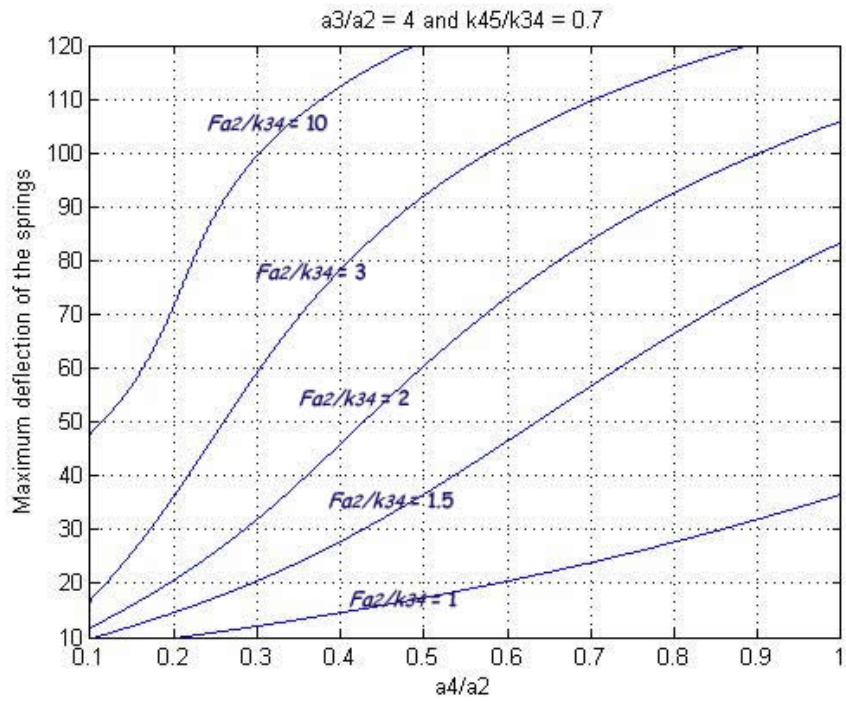
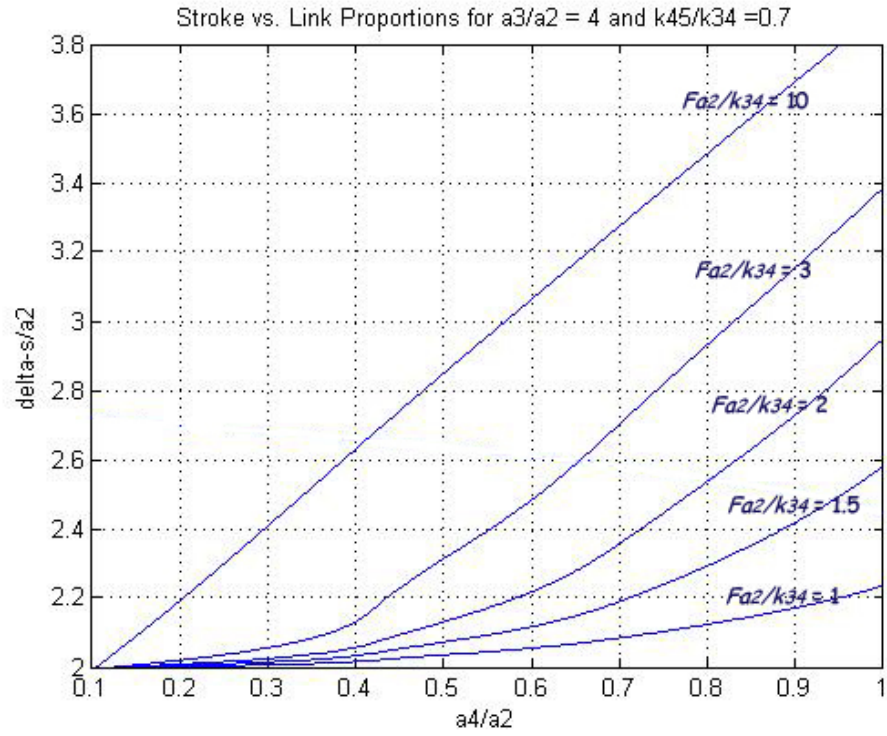


Figure 4.18a The Design Chart and the corresponding Spring Deflection of the Variable Stroke Mechanism for $k_{45}/k_{34} = 0.7$ and $a_3/a_2 = 4$

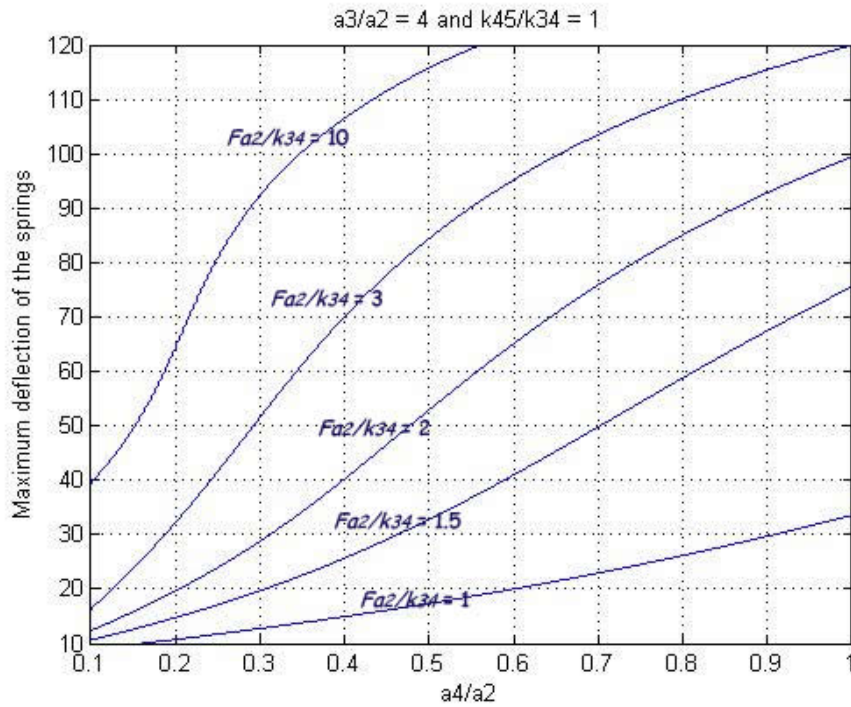
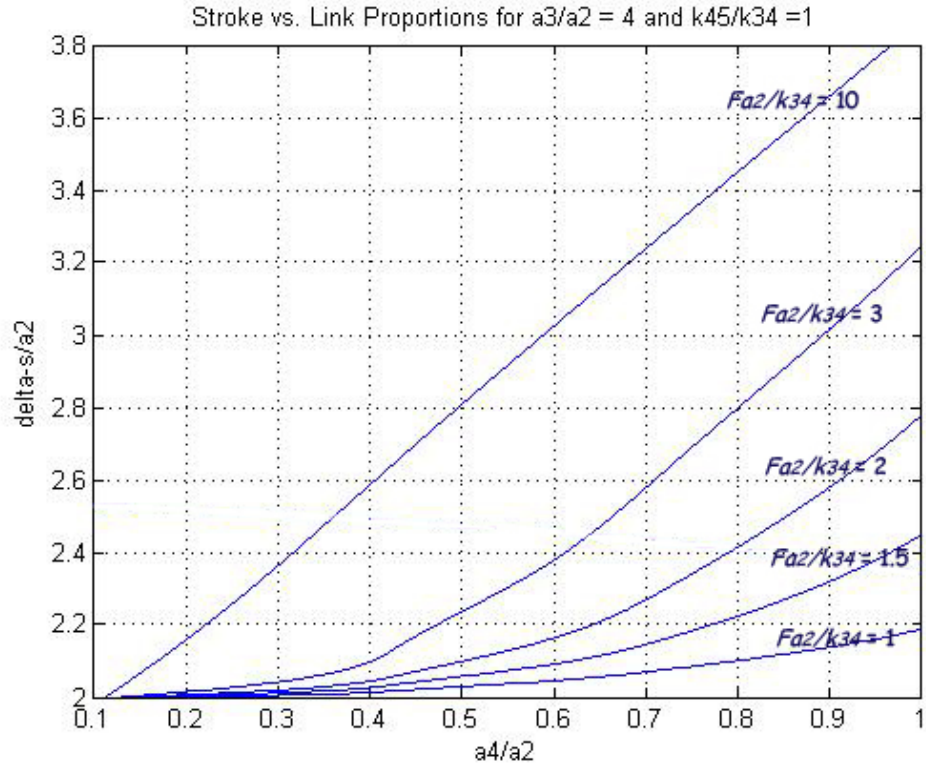


Figure 4.18b The Design Chart and the corresponding Spring Deflection of the Variable Stroke Mechanism for $k_{45}/k_{34} = 1$ and $a_3/a_2 = 4$

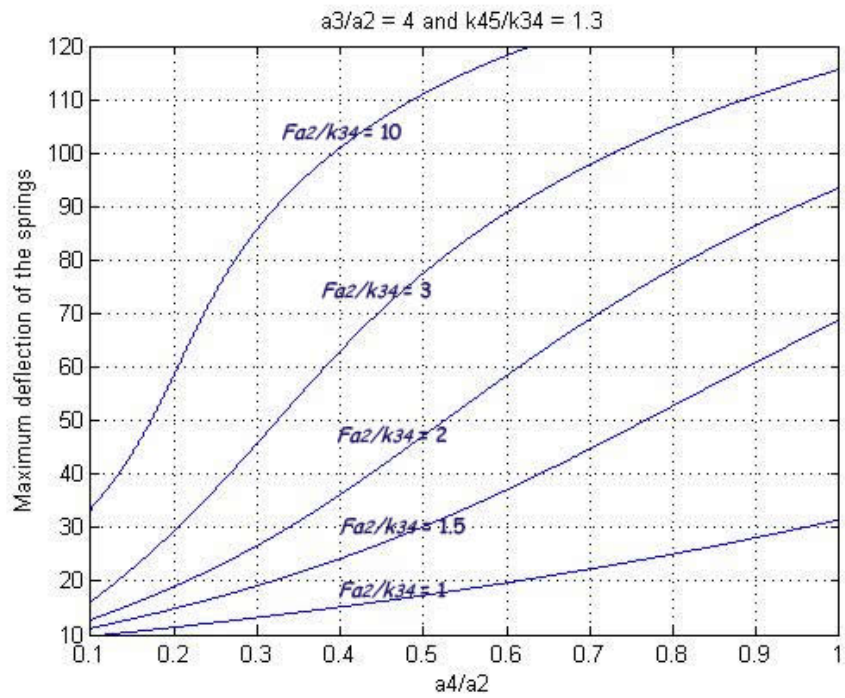
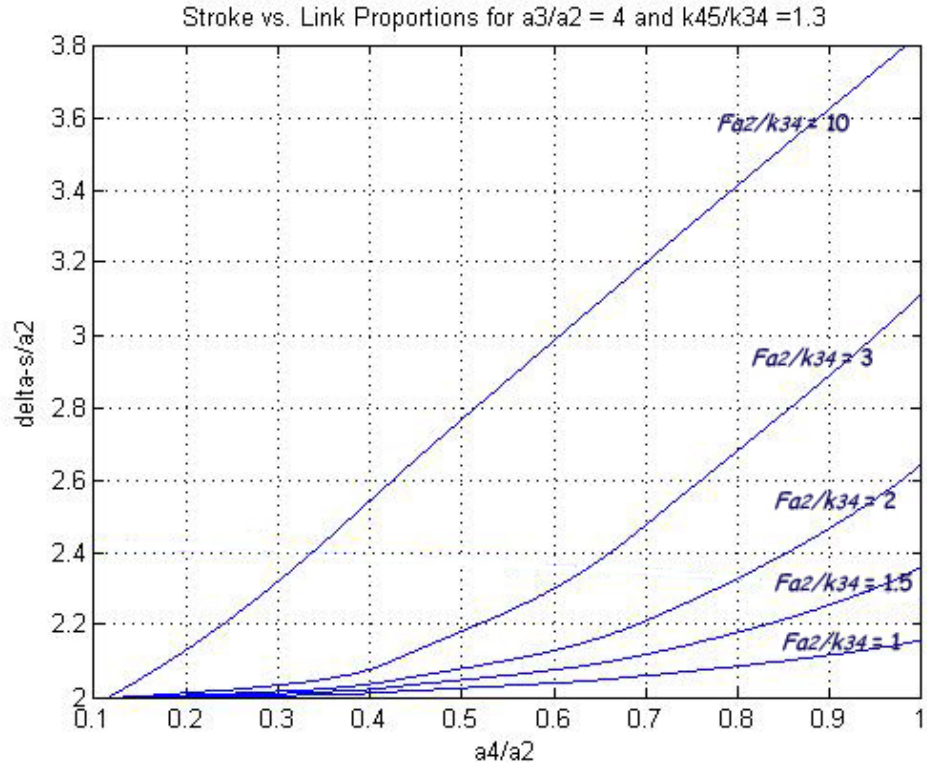


Figure 4.18c The Design Chart and the corresponding Spring Deflection of the Variable Stroke Mechanism for $k_{45}/k_{34} = 1.3$ and $a_3/a_2 = 4$

From many trials it is concluded (which are not shown here) that link 3 (a_3/a_2) does not have a major effect on the stroke of the mechanism. Also from the charts given in Figure 4.17 and 4.18, it is seen a_3/a_2 does not affect the results significantly.

For a required output-force and stroke there are infinite set of solutions. Designer is free to synthesize various mechanisms. In the next example, according to the charts above, a mechanism is synthesized.

4.11 Example

Design a variable stroke mechanism for maximum output-link force $F = 100\text{N}$ and an output stroke of 100mm. Assume variation of F_{15} as it is in Figure 4.16. Take $a_3/a_2 = 2.5$, $a_4/a_2 = 0.5$ and $k_{45}/k_{34} = 1$. The maximum allowable spring deflection is required to be 100° .

According to requirements, the design chart given in Figure 4.17 is suitable. Let Fa_2/k as 2. Then from 4.17b $\Delta s_{15}/a_2$ will be 2.1 and corresponding maximum spring deflection is 64° .

Since the stroke is required to be $\Delta s_{15} = 100\text{mm}$, $100/a_2 = 2.1$ then $a_2 = 47.62\text{mm}$. Since $a_3/a_2 = 2.5$ then a_3 will be 119.04mm. Also $a_4/a_2 = 0.5$ therefore $a_4 = 23.81\text{mm}$. Since $F = 100$ and $a_2 = 47.62\text{ mm}$ then $(Fa_2/k = 2)$ k is 2.381Nm/rad.

4.12 Example

For the mechanism designed in Example 4.11, determine new stroke if the maximum output-load is increased to 3/2 of its initial value.

For the second loading Fa_2/k will be 3. According to Figure 4.17b, for $a_3/a_2 = 5/2$, $a_4/a_2 = 0.5$, $Fa_2/k = 3$ $\Delta s_{15}/a_2$ is 2.25. Since $a_2 = 47.62\text{mm}$ Δs_{15} is 107.145mm. The corresponding maximum spring deflection is 94° .

CHAPTER V

FIVE-BAR MECHANISM

5.1 Introduction

Initially, for simplicity of the equations a two degree-of-freedom, five-link in-line slider-crank mechanism (Figure 4.1) is taken into the consideration in chapter IV. In this part a more complicated unconstrained two degree-of-freedom mechanism is considered. It is a five-bar mechanism as shown in Figure 5.1:

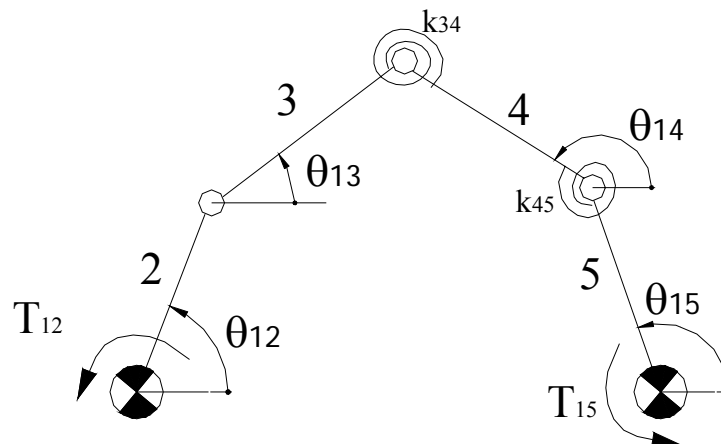


Figure 5.1 Five-Bar Variable Structure Mechanism

The two torsional springs (k_{34} , k_{45}) are mounted between links 3 and 4 and links 4 and 5. The input is at crank (link 2) and the output is at link 5. The link proportions are assumed to be selected such that the crank can make full-rotations and the output link oscillates. The output-load is assumed to be resistive to the motion of the output link of the mechanism. The direction of rotation of the crank is assumed to be counter clock-wise.

This mechanism is analyzed with the method of virtual work similar to the variable stroke mechanism. The analysis procedure is explained in detail in Section 5.2.

Unlike in the case of variable stroke mechanism, defining the output-link load according to the crank position is not possible for the five bar mechanism. The major problem in the analysis of the five-bar mechanism is the uncertainty of the position of direction change of the output-link prior to kinematic analysis. (This problem is clearly stated in Section 5.3) Therefore, a technique for approximate estimation of the dead centers of the unconstrained multi degree-of- freedom mechanisms is introduced by the author in Section 5.6.

Finally, a generalization procedure is introduced in Section 5.8 to obtain design charts relating the output torque and spring constants and output stroke of the mechanism. The design charts are given in Example 5.9.

5.2 Analysis of the Five-Bar Mechanism

In this part, the analysis of the mechanism using the method and the assumptions given in Section 3.2 is presented.

The virtual work of the active loads is (Figure 5.2):

$$\delta W_1 = T_{12} \delta \theta_{12}, \quad \delta W_2 = T_{15} \delta \theta_{15} \quad (5.1)$$

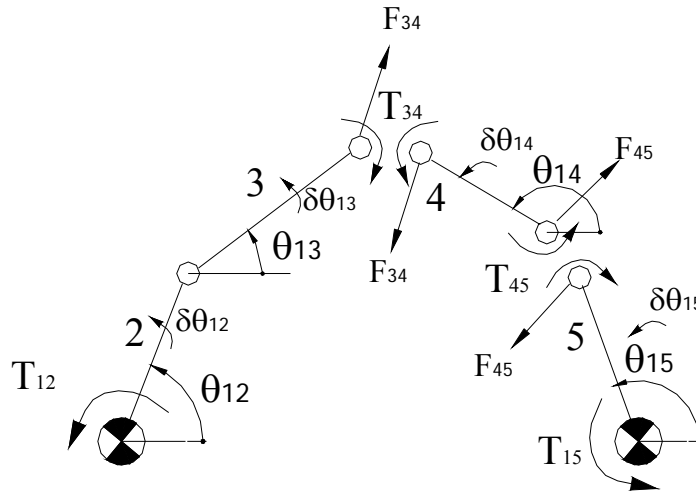


Figure 5.2 The Five-Bar Mechanism with the Spring Forces shown Active

The virtual works of the springs are (Figure 5.2);

$$\delta W_3 = -T_{34} \delta \theta_{13} + T_{34} \delta \theta_{14}, \quad \delta W_4 = T_{45} \delta \theta_{14} - T_{45} \delta \theta_{15} \quad (5.2)$$

where,

$$T_{34} = k_{34}(\theta_{13} - \theta_{14} + c_{34}), \quad T_{45} = k_{45}(\theta_{14} - \theta_{15} + c_{45}) \quad (5.3)$$

“ k_{ij} ” represents linear spring stiffness, “ c_{ij} ” is the spring initial position constant between i^{th} and j^{th} links . Also a_i represents length of the i^{th} link.

Then, the virtual work of all the active forces is

$$\delta W = \delta W_1 + \delta W_2 + \delta W_3 + \delta W_4 \quad (5.4)$$

Or,

$$\delta W = T_{12}\delta\theta_{12} + T_{15}\delta\theta_{15} + T_{s34}(-\delta\theta_{13} + \delta\theta_{14}) + T_{s45}(-\delta\theta_{15} + \delta\theta_{14}) \quad (5.5)$$

Since the five-bar mechanism is a two degree-of-freedom mechanism, the virtual work for a system with two degree-of-freedom can be expressed in generalized coordinates as;

$$\delta W = Q_1\delta q_1 + Q_2\delta q_2 \quad (5.6)$$

Where Q_i represents generalized forces and q_i represents virtual displacements.

Therefore, the four infinitesimal displacements in Equation 5.5 must be reduced to two virtual displacements.

The loop closure equations of the mechanism are

$$a_2 \cos \theta_{12} + a_3 \cos \theta_{13} - a_4 \cos \theta_{14} - a_5 \cos \theta_{15} = a_1 \quad (5.7)$$

$$a_2 \sin \theta_{12} + a_3 \sin \theta_{13} - a_4 \sin \theta_{14} - a_5 \sin \theta_{15} = 0 \quad (5.8)$$

By taking the differentials across of Equations 5.7 and 5.8 yields,

$$-a_2 \sin \theta_{12} \delta\theta_{12} - a_3 \sin \theta_{13} \delta\theta_{13} + a_4 \sin \theta_{14} \delta\theta_{14} + a_5 \sin \theta_{15} \delta\theta_{15} = 0 \quad (5.9)$$

$$a_2 \cos \theta_{12} \delta \theta_{12} + a_3 \cos \theta_{13} \delta \theta_{13} - a_4 \cos \theta_{14} \delta \theta_{14} - a_5 \cos \theta_{15} \delta \theta_{15} = 0 \quad (5.10)$$

From Equations 5.9 and 5.10, virtual displacements can be determined as;

$$\delta \theta_{13} = \frac{a_2 \sin(\theta_{14} - \theta_{12}) \delta \theta_{12} + a_5 \sin(\theta_{15} - \theta_{14}) \delta \theta_{15}}{a_3 \sin(\theta_{13} - \theta_{14})} \quad (5.11)$$

$$\delta \theta_{14} = \frac{a_2 \sin(\theta_{13} - \theta_{12}) \delta \theta_{12} + a_5 \sin(\theta_{15} - \theta_{13}) \delta \theta_{15}}{a_4 \sin(\theta_{13} - \theta_{14})}. \quad (5.12)$$

Substituting Equations 5.11 and 5.12 into Equation 5.5, yields the form below:

$$\delta W = \delta \theta_{12} \cdot Q_1 + \delta \theta_{15} \cdot Q_2 \quad (5.13)$$

The principle of virtual work tells that a necessary and sufficient condition for generalized equilibrium is that each of the generalized forces Q_i must vanish.

$$Q_1 = 0, \quad Q_2 = 0 \quad (5.14)$$

According to above procedure, after some manipulations, two equilibrium equations can be obtained as:

$$T_{12} + k_{34}(\theta_{13} - \theta_{14} + c_{34}) \frac{\left\{ \frac{a_2}{a_4} \sin(\theta_{12} - \theta_{13}) - \frac{a_2}{a_3} \sin(\theta_{12} - \theta_{14}) \right\}}{\sin(\theta_{14} - \theta_{13})} \quad (5.15)$$

$$- k_{45}(\theta_{14} - \theta_{15} + c_{45}) \frac{a_2 \sin(\theta_{12} - \theta_{13})}{a_4 \sin(\theta_{14} - \theta_{13})} = 0$$

$$\begin{aligned}
& T_{15} + k_{34}(\theta_{13} - \theta_{14} + c_{34}) \frac{\left(\frac{a_5}{a_4} \sin(\theta_{13} - \theta_{15}) - \frac{a_5}{a_3} \sin(\theta_{14} - \theta_{15}) \right)}{\sin(\theta_{14} - \theta_{13})} \\
& + k_{45}(\theta_{14} - \theta_{15} + c_{45}) \left\{ 1 - \frac{a_5 \sin(\theta_{13} - \theta_{15})}{a_4 \sin(\theta_{14} - \theta_{13})} \right\} = 0
\end{aligned} \tag{5.16}$$

Kinematic and force analysis of the mechanism can be performed by solving Equations 5.7, 5.8, 5.15, 5.16 simultaneously.

If four of the five position variables are known, T_{15} and T_{12} can be determined in closed-form. But generally this is not the required case.

If the output force (T_{15}) and the crank angle (θ_{12}) are known (this is the most common case), Equations 5.7, 5.8, 5.15, 5.16 become highly non-linear for the rest unknown parameters. These parameters are; θ_{13} , θ_{14} , stroke θ_{15} , input torque T_{12} .

Analytical solution of these non-linear equations may not be possible. Therefore, a numerical solution method can be performed.

These non-linear equations are solved numerically via Matlab (by using the “fsolve” function which finds a root (zero) of a system of nonlinear equations). All the equations of the mechanisms investigated in following examples are solved for full-rotation of crank with one degree of increment. Many trials show that feasible solutions of these non-linear equations require close initial guesses. For instance, a set of initial guess for zero degree of crank angle may not be appropriate for the same mechanism at 180^0 . Therefore, in order to find quick and good solution, the code used for solution is modified so that initial guesses are obtained from the previous cycle’s set of solutions.

5.3 Definition of the Output-Link's Torque Function with Differential Method

In this study, during the analyses of all the mechanisms, it is assumed that the output-load varies in between a maximum value in work stroke and one-fifth of its work-stroke value in return stroke. Also both forces are assumed to be resistive to the motion of the output-link. According to this output loading criteria, for the in-line variable-crank mechanism analyzed in the previous parts, defining the output-load function is easy. Because (as explained in Section 4.2 in detail) for the in-line variable stroke mechanism for resistive output loads, when $\theta_{12} = 0$ or $\theta_{12} = \pi$ the mechanism is “approximately” at the dead centers. Therefore, according the position of crank, the load at the output-link can be easily defined as required. But the case is different when five-bar mechanism is taken into consideration. Because, there is no direct relation between position of the crank and the dead centers of the mechanism as in the case of the variable stroke mechanism

Since kinematics of multi degree-of-freedom unconstrained mechanisms is unknown before the loads are applied; in general working range of output-link is also uncertain. Moreover, magnitude of the output load is a major parameter that directly affects the output-link's oscillation interval. Without knowing working zone of output-link before kinematic analysis, defining an “exact” output-link load function which changes its direction at the dead centers is impossible.

Since the equations of the motion of the five-bar mechanism are solved numerically, one of the simplest methods is to relate output-torque with difference of the output-link angle for each step of the numerical solution.

In the next example, the direction of the output-link is determined by taking differential of θ_{15} in each step. If direction of rotation of θ_{15} is negative, the mechanism is in work stroke or vice-versa (Figure 5.1). The output link torque (T_{15}) is defined as h_1 or $-h_1/5$ according to work or return stroke respectively.

5.4 Example

Perform the analysis of a five-bar mechanism with the following link lengths and spring constant by the method mention in Section 5.2: $a_1 = 2.5$ unit, $a_2 = 0.7$, $a_3 = 1.7$, $a_4 = 1.7$, $a_5 = 1.5$, $k_{34} = k_{45} = 5$ N.unit/rad. Take $h_1 = 0.5$. From the procedure mentioned in Section 5.5, initial spring constants can be taken as $c_{34} = 2.5$ and $c_{45} = -0.5$. The output-loading is as follows:

$$\text{For } i = 1, 2, \dots, 360 \quad (5.17)$$

$$\theta_{12}(i) = i \frac{\pi}{180} \quad (5.18)$$

$$\Delta\theta_{15}(i) = \Delta\theta_{15}(i) - \Delta\theta_{15}(i-1) \quad (5.19)$$

$$\text{If } \Delta\theta_{15}(i) < 0, \quad T_{15} = h_1 \quad (\text{work - stroke}) \quad (5.20)$$

$$\text{Else,} \quad T_{15} = \frac{-h_1}{5}, \quad (\text{reverse - stroke}) \quad (5.21)$$

According to the above loading, by solving Non-linear Equations 5.7, 5.8, 5.15, 5.16 numerically, θ_{13} , θ_{14} , θ_{15} and T_{12} can be determined. In Figure 5.3 θ_{13} , θ_{14} and θ_{15} vs. θ_{12} are shown:

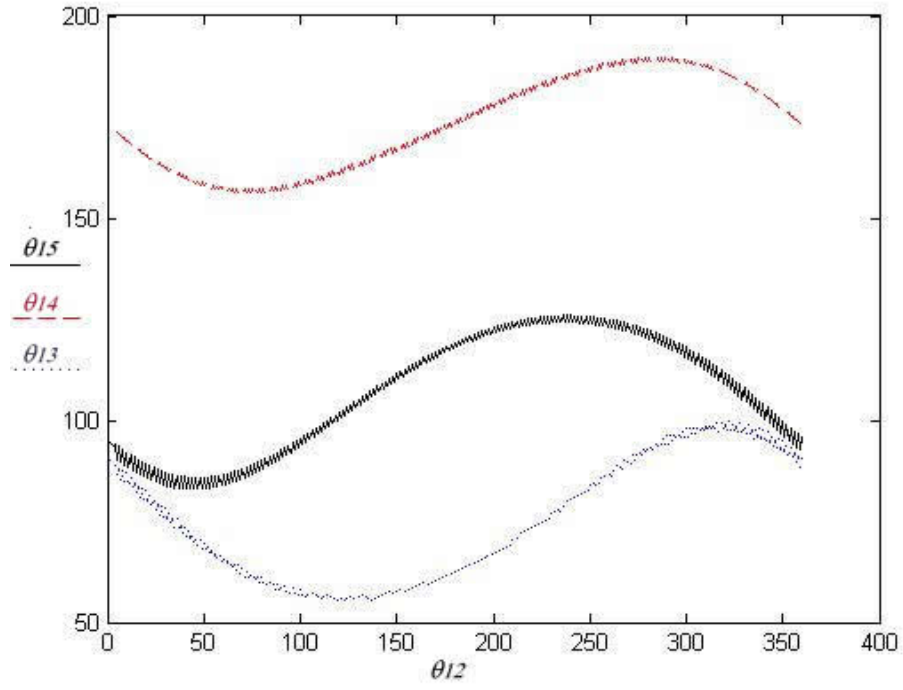


Figure 5.3 $\theta_{13}, \theta_{14}, \theta_{15}$ vs. θ_{12}

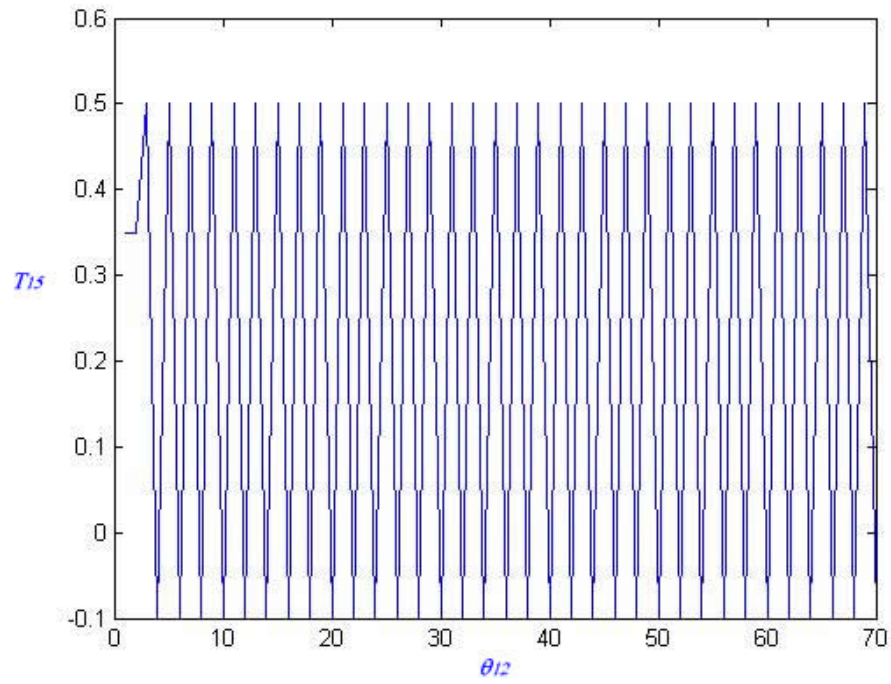


Figure 5.4 T_{15} vs. θ_{12}

From Figure 5.4 it is seen that, both sign and magnitude of the output-link torque fluctuates between 0.5 and -0.1 continuously. Therefore, motion of the links is hesitant for whole cycle (Figure 5.3).

In order to get rid of this characteristic, one may obtain a function that decreases magnitude of the output link torque around dead centers of the mechanism:

According to Equation 5.22 output torque can be related with increments of the output-link. Around dead centers of the mechanism, this equation minimizes the magnitude of the output-torque, since difference of an output-link angle of a mechanism decreases when the mechanism is at or close to its dead centers. Therefore, in theory smooth changes can be obtained at dead centers

$$T_{15i} \propto h_1 \cdot (\theta_{15i} - \theta_{15i-1}) \quad (5.22)$$

However, many trials show that, this torque definition also causes undesired oscillations of the output-link near dead centers of the mechanism. In the next example this phenomenon is shown. In the following example the same mechanism in Example 5.4 is analyzed with the output-loading defined as in Equation 5.22.

5.5 Example

Perform the analysis of five-bar mechanism with the following link lengths and spring constant, by the method mention in Section 5.2 $a_1 = 2.5$ unit, $a_2 = 0.7$, $a_3 = 1.7$, $a_4 = 1.7$, $a_5 = 1.5$, $k_{34} = k_{45} = 5$ N.unit/rad. Take $h_1 = 8$. From the procedure mentioned in Section 5.7, initial spring constants can be taken as $c_{34} = 2.5$ and $c_{45} = -0.5$. The output-loading is as follows (Equation 5.22 is taken into consideration):

$$\text{For } i = 1, 2, \dots, 360 \quad (5.23)$$

$$\theta_{12}(i) = i \frac{\pi}{180} \quad (5.24)$$

$$\Delta\theta_{15}(i) = \Delta\theta_{15}(i) - \Delta\theta_{15}(i-1) \quad (5.25)$$

$$\text{If } \Delta\theta_{15}(i) < 0, \quad T_{15} = -h_1 |\Delta\theta_{15}(i)| \quad (\text{work - stroke}) \quad (5.26)$$

$$\text{Else,} \quad T_{15} = \frac{h_1 |\Delta\theta_{15}(i)|}{5}, \quad (\text{reverse - stroke}) \quad (5.27)$$

By solving non-linear Equations 5.7, 5.8, 5.15, 5.16 numerically; θ_{13} , θ_{14} and θ_{15} and T_{12} can be determined. In Figure 5.5 θ_{13} , θ_{14} , θ_{15} vs. θ_{12} are shown:

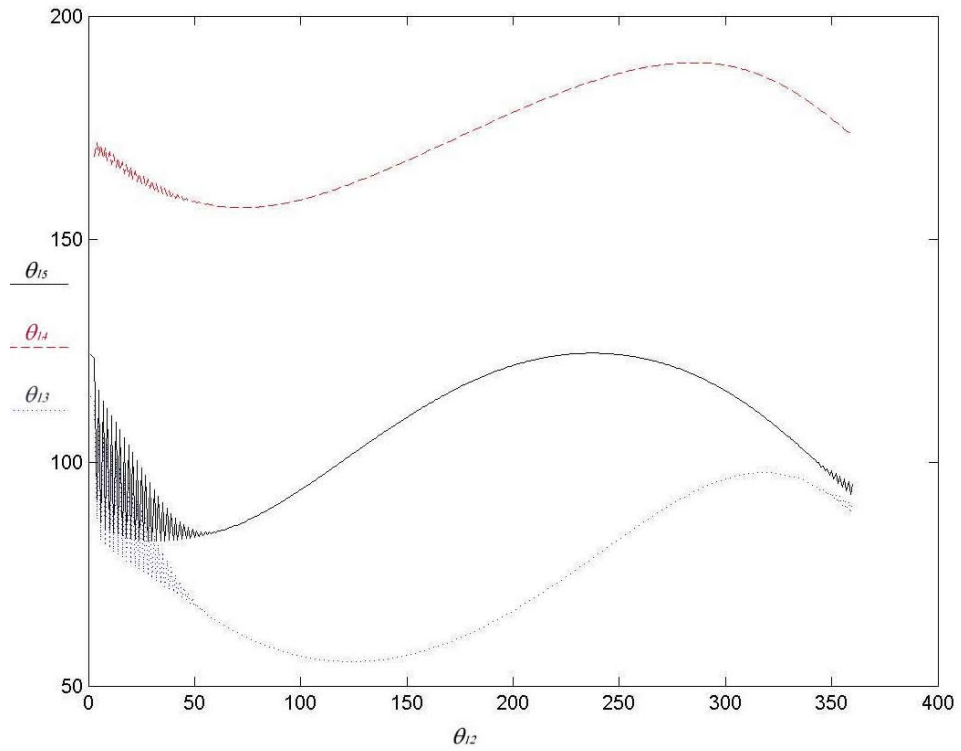


Figure 5.5 $\theta_{13}, \theta_{14}, \theta_{15}$ vs. θ_{12}

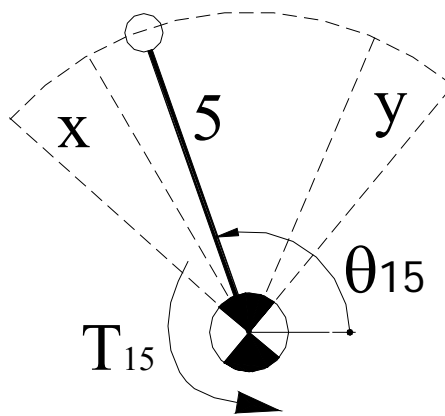


Figure 5.6 Oscillatory Regions for the Output-Link

In Figure 5.5 it is shown that, at the regions indicated (x, y) (Figure 5.6), the output-link starts to hesitate (Equation 5.22) Because, just after folded and extended positions of the mechanism, direction of rotation of the output-link changes.

Therefore, in the next step sign of the output torque (Equation 5.22) also changes. After one more step due to direction change of the torque (in most cases) the output-link moves back to a position further than its folded position (or extended) before the direction change. Then since direction of the motion of the output-link angle is changed again, the next step will be affected due to Equation 5.22. In order to obtain smooth torque variation at the output-link, the output-link angle increments are required to increase or decrease monotonically in between desired values.

Many trials showed that, unless having too small output-load (with respect to the stiffness of the springs), these undesired oscillations take place around the dead centers of the mechanism.

Using variable step sizes depending on position of the output-link or some complex algorithms did not yield a convenient solution to the output link torque for all mechanisms. Therefore, another, rather simple and convenient method is required to obtain smoothly increasing and decreasing torque at the output-link.

5.6 An Approximate Estimation Technique of Dead Centers of the Five-Bar Mechanism

As it is mentioned in Section 5.3, for unconstrained multi-degree of freedom mechanisms, dead center positions can not be determined before applying the loads. But, the author introduced an approximate estimation technique for dead centers for unconstrained five-bar mechanism without using to the difference of the output-link angle for each step of the numerical solution.

From many examples, it is observed that for resistive output-loads, the five-bar mechanism behaves like an imaginary four-bar mechanism formed with the imaginary coupler-link (dashed line), links 2 and 3 that are shown in Figure 5.7. This imaginary line (variable length) connects the input and output-link of the mechanism.

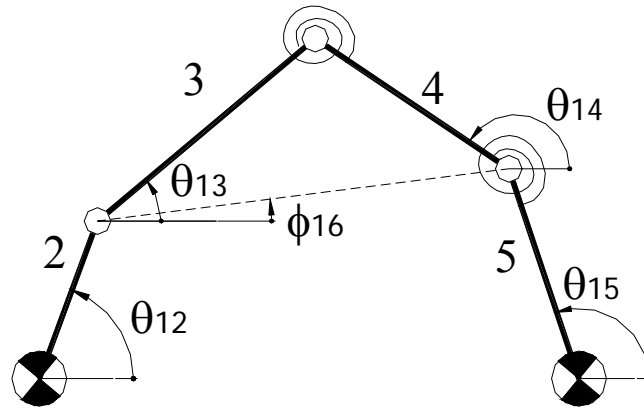


Figure 5.7 The Imaginary Coupler-Link for The Five-Bar Mechanism

Mathematically speaking, if the output load is resistive to the motion of the output-link or the output-load is zero, it is observed that;

$$\text{For } 0 \leq \theta_{12} \leq 2\pi \text{ and } \dot{\theta}_{12} > 0; \quad (5.28)$$

Approximately;

- If $0 < \theta_{12} - \phi_{16} < \pi$, then $\dot{\theta}_{15} > 0$, (5.29)

- If $\pi < \theta_{12} - \phi_{16} < 2\pi$, then $\dot{\theta}_{15} < 0$. (5.30)

Therefore, it can be concluded that if $\theta_{12} = \phi_{16}$, the mechanism is at or very close to its extended position and if $\theta_{12} = \phi_{16} + \pi$, the mechanism is at or very close to its folded position.

Since, a function satisfying below conditions is required; then, it is clear that a function is essential whose magnitude is approximately zero when $\theta_{12} - \phi_{16} = 0$ and π . Sine function is one of the appropriate solutions for the requirements above. Also it will have a peak when $\theta_{12} - \phi_{16} = \pi/2, 3\pi/2$. And also in between these values, sine function smoothly increases and decreases.

- Around the dead centers of the mechanism the output-link torque must be too small (nearly zero) to obtain a smooth change of direction of the load.
- In between the maximum and minimum values the change of the output-torque must be smooth.

One of the possible output-torque relations considering the imaginary coupler-link can be defined as:

$$\text{For } 0 \leq \theta_{12} \leq 2\pi; \quad (5.31)$$

$$\text{If } 0 \leq \theta_{12} - \phi_{16} < \pi, \quad T_{15} = \frac{-h_1}{5} \cdot |\sin(\theta_{12} - \phi_{16})|, \quad (\text{reverse - stroke}) \quad (5.32)$$

$$\text{Else,} \quad T_{15} = h_1 \cdot |\sin(\theta_{12} - \phi_{16})|, \quad (\text{work - stroke}) \quad (5.33)$$

where h_1 is maximum value of the output - torque.

In the next example, analysis of the five-bar mechanism investigated in previous examples is performed with this torque function (5.31-32-33).

5.7 Examples

5.7.1 Example

Perform the analysis of a five-bar mechanism with the following link lengths and spring constant, by the method mention in Section 5.2 $a_1 = 2.5$ unit, $a_2 = 0.7$, $a_3 = 1.7$, $a_4 = 1.7$, $a_5 = 1.5$, $k_{34} = k_{45} = 3$ N.unit/rad. Maximum torque (h_1 , Equation 5.31-32-33) during the work stroke is $h_1 = 1$ Nunit. From the procedure mentioned in Section 5.8, initial spring constants can be taken as $c_{34} = 2.5$ and $c_{45} = -0.5$

θ_{13} , θ_{14} , θ_{15} and T_{12} can be determined by solving Non-linear Equations 5.7, 5.8, 5.15, 5.16 numerically (By using the codes given in Appendices D and E); In Figure 5.8 θ_{13} , θ_{14} , θ_{15} vs. θ_{12} are shown:

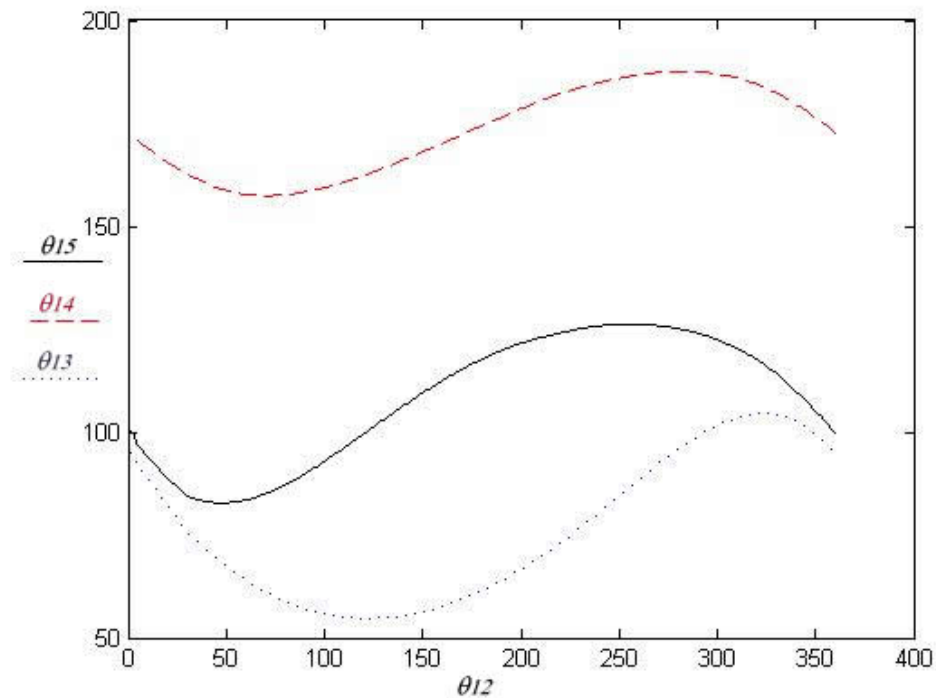


Figure 5.8 θ_{13} , θ_{14} , θ_{15} vs. θ_{12} for $k_{34} = k_{45} = 3$ N.unit/rad

5.7.2 Example

Perform the analysis of the five-bar in the Example 5.7.1 with same data except different initial spring constants; $k_{34} = k_{45} = 5 \text{ N.unit/rad}$

By solving Non-linear Equations 5.7, 5.8, 5.15, 5.16 numerically (By using the codes given in Appendices D and E); θ_{13} and θ_{14} and T_{12} can be determined. In Figure 5.9 θ_{13} , θ_{14} , θ_{15} and vs. θ_{12} are shown:

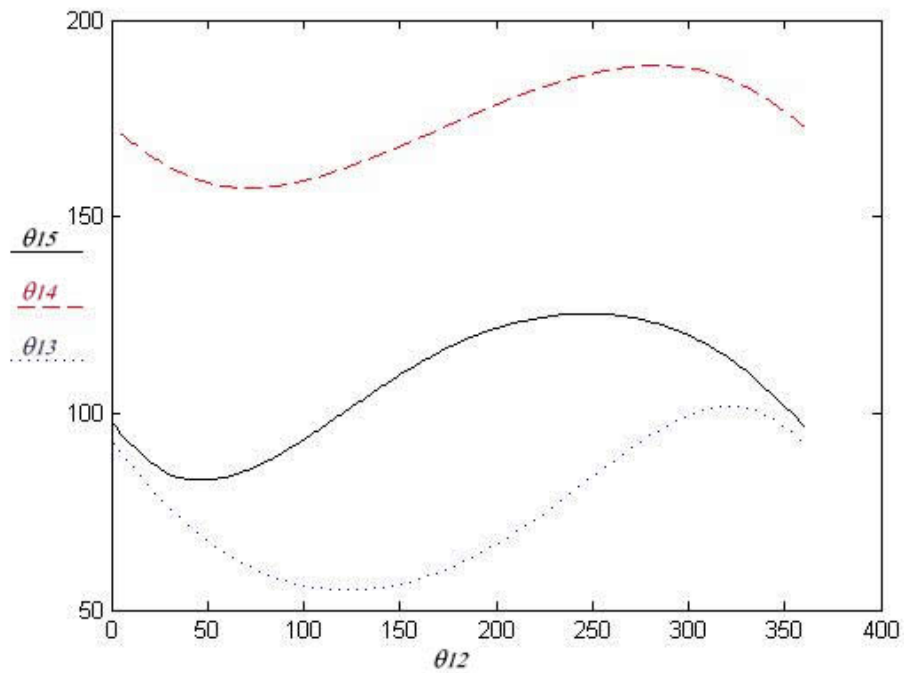


Figure 5.9a θ_{13} , θ_{14} , θ_{15} vs. θ_{12} $k_{34} = k_{45} = 5 \text{ N.unit/rad}$

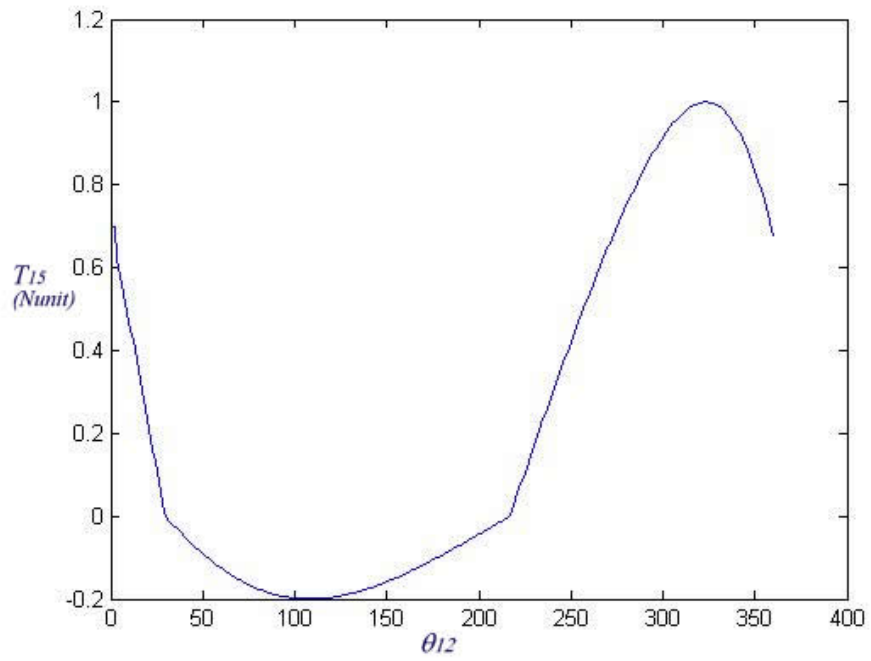


Figure 5.9b T_{15} vs. θ_{12} $k_{34} = k_{45} = 5$ N.unit/rad

5.7.3 Example

Perform the analysis of the five-bar in Example 5.7.1 with same data, except a different initial spring constants $c_{34} = 1.5$ and $c_{45} = -0.5$

By solving Non-linear Equations 5.7, 5.8, 5.15, 5.16 numerically (By using the codes given in Appendices D and E); θ_{13} , θ_{14} , θ_{15} and T_{12} can be determined. In Figure 5.10 θ_{13} , θ_{14} , θ_{15} vs. θ_{12} are shown:

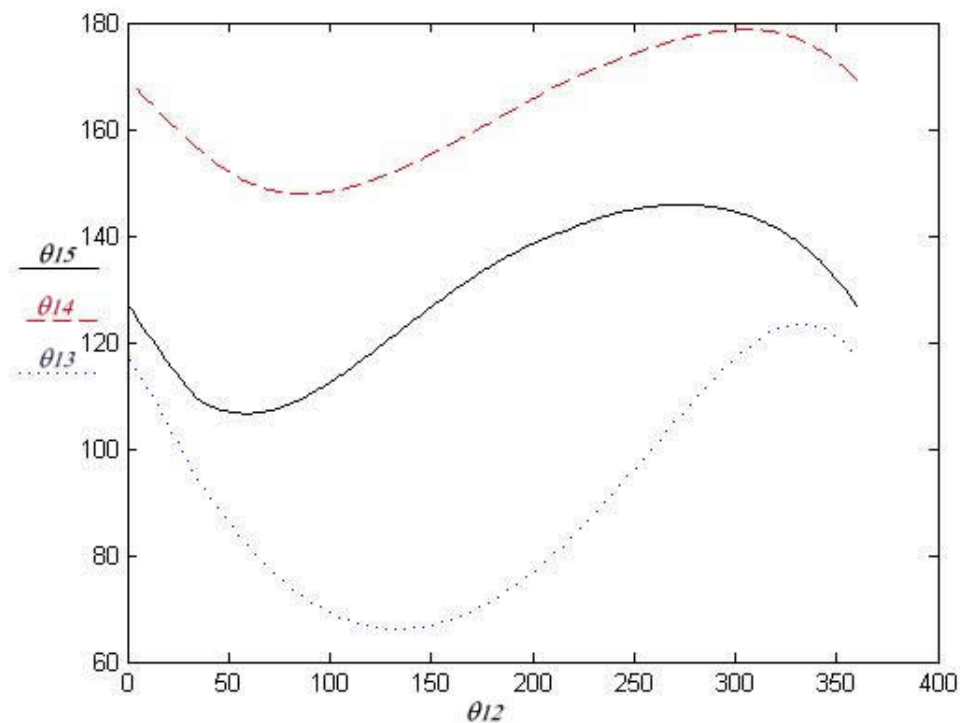


Figure 5.10 θ_{13} , θ_{14} , θ_{15} vs. θ_{12} for $c_{34} = 1.5$ and $c_{45} = -0.5$

Both these examples and many other examples (not shown) indicate that motion of the links is smooth for whole cycle with Equations 5.31-32-33. There are no sharp and sudden changes in motion of the links.

In Example 5.7.2, stiffness of the springs is increased 5/3 times. But from the plots it is seen that, kinematics of the mechanism is nearly the same in Examples 5.7.1 and

5.7.2. When the initial spring constant is changed, as in Example 5.7.3, kinematics of the mechanism is radically changed. These examples indicate that when the appropriate parameter is changed, the mechanism can be adaptable for different tasks. From Examples 5.7-1-2-3 it is seen that the motion of the links (Figures 5.8a, 5.9, 5.10) smoothly changes for the whole cycle according to the loading given in Equation 5.31-32-33. It is seen from Figure 5.9a that the dead centers of the mechanism occur at $\theta_{12} = 45^0$ and $\theta_{12} = 240^0$. From Figure 5.9b it is also seen that the output-link torque changes its direction when $\theta_{12} = 30^0$ and $\theta_{12} = 220^0$. From many examples, approximately this amount of error (up to 25^0) in torque function's direction change position is observed. Therefore, the method of approximate estimation of dead centers can be assumed feasible

5.7.4 Example

Display the mechanism for every 45° crank angle of a five bar mechanism for the following data: $a_1 = 1$ unit, $a_2 = 0.3$, $a_3 = 0.7$, $a_4 = 0.7$, $a_5 = 0.5$, $k_{34} = k_{45} = 3$ N.unit/rad. The maximum torque (h_1 , Eq. 5.31-32-33) during the work stroke is $h_1 = 1$ Nunit. From the procedure mentioned in Section 5.8, initial spring constants can be taken as $c_{34} = 2.5$ and $c_{45} = -0.5$

By solving Non-linear Equations 5.7, 5.8, 5.15, 5.16 numerically and using Matlab the animation can be performed. The animation of the structure for every 45° crank angles is shown in the following figures.

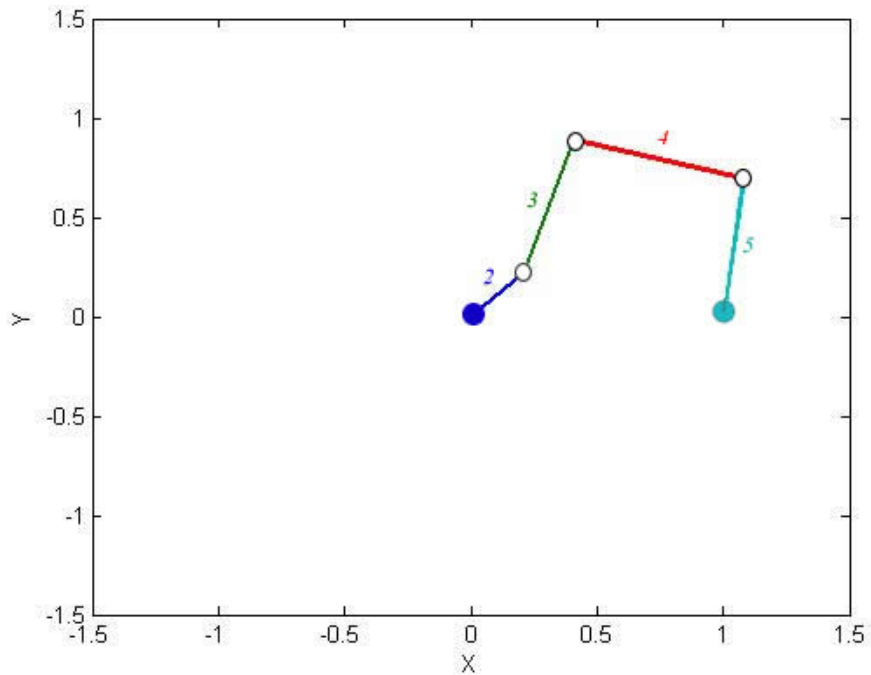


Figure 5.11a Sketch of a Five-Bar Mechanism

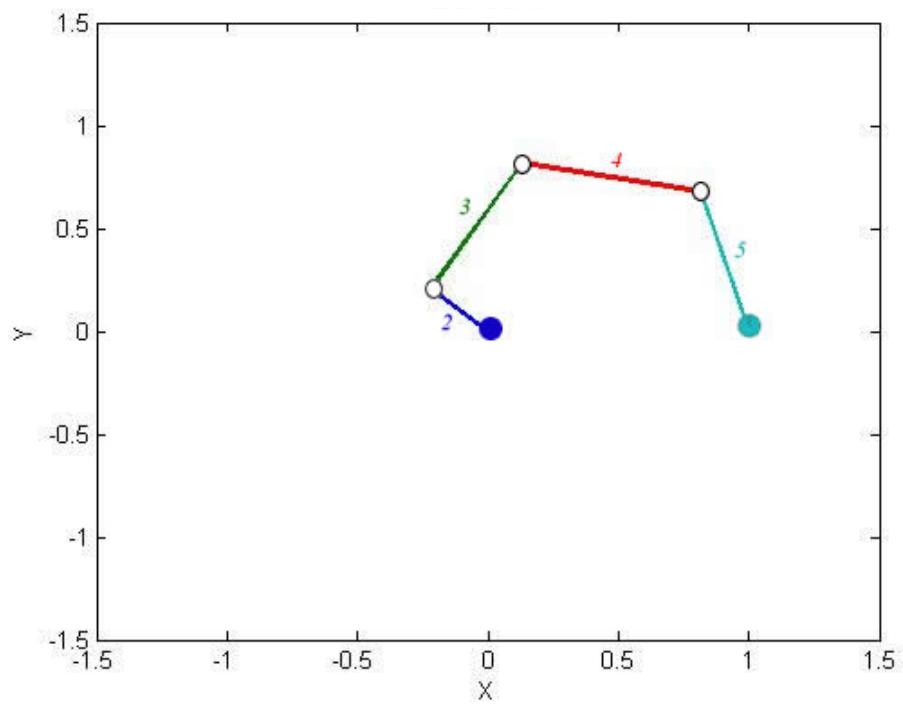
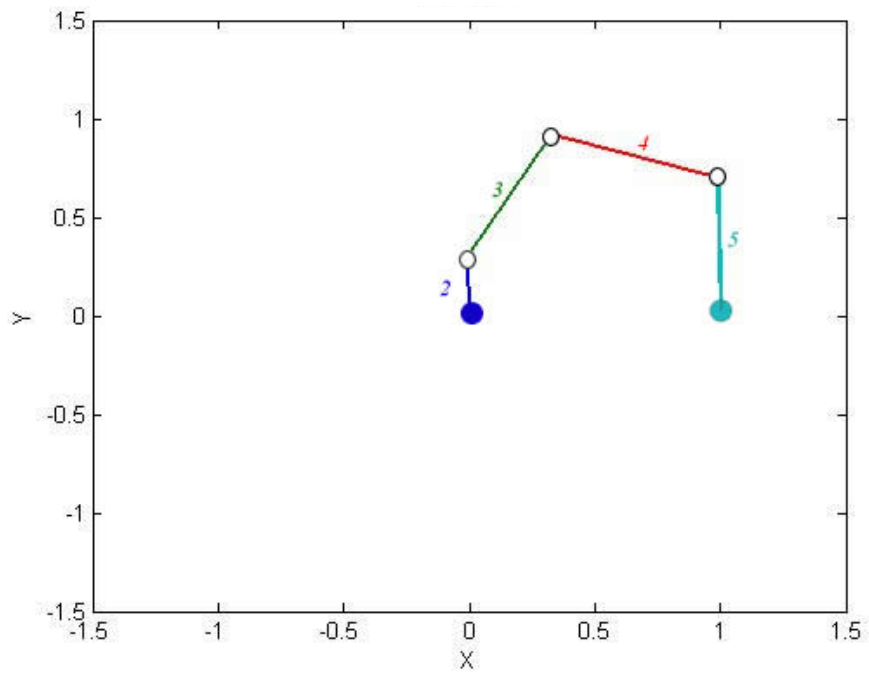


Figure 5.11b Sketch of a Five-Bar Mechanism

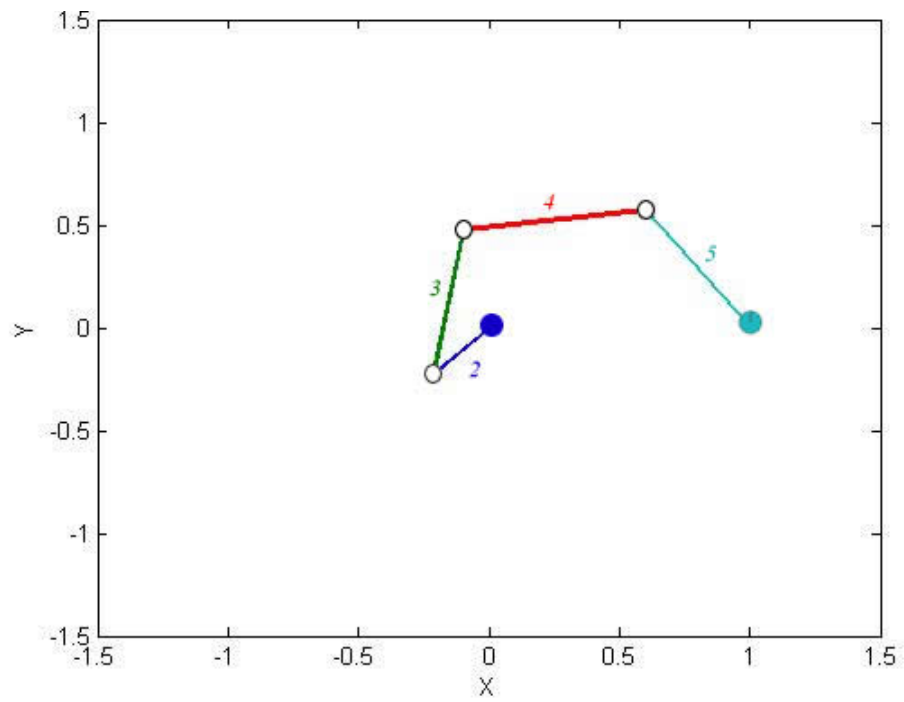
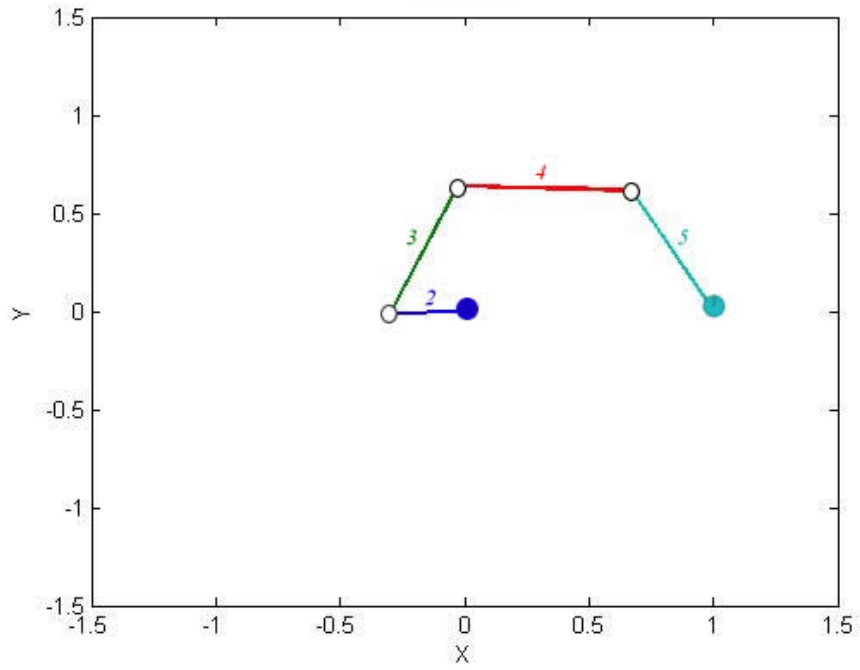


Figure 5.11c Sketch of a Five-Bar Mechanism

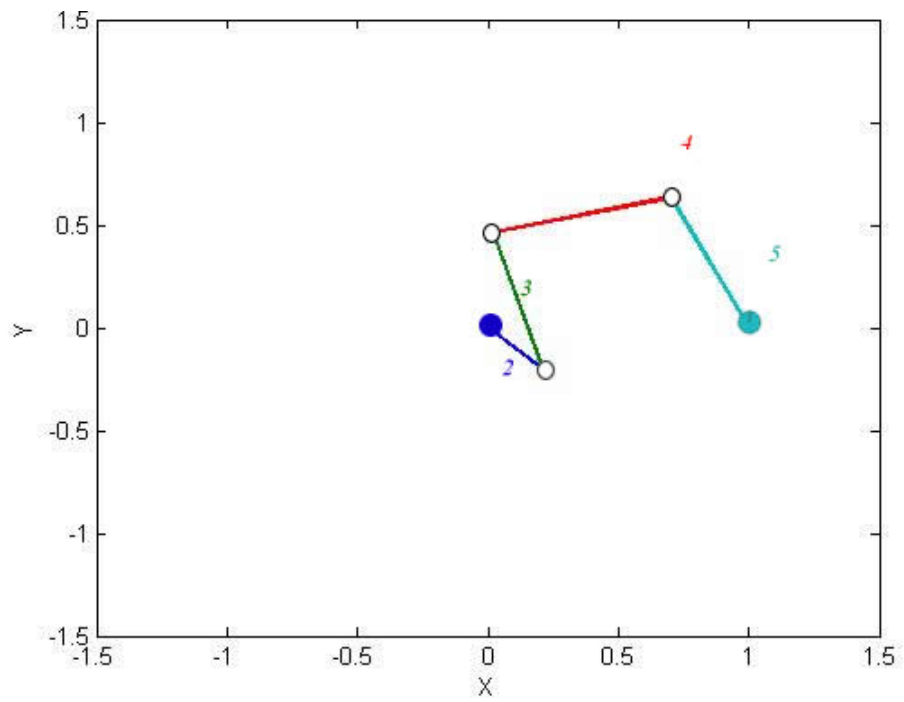
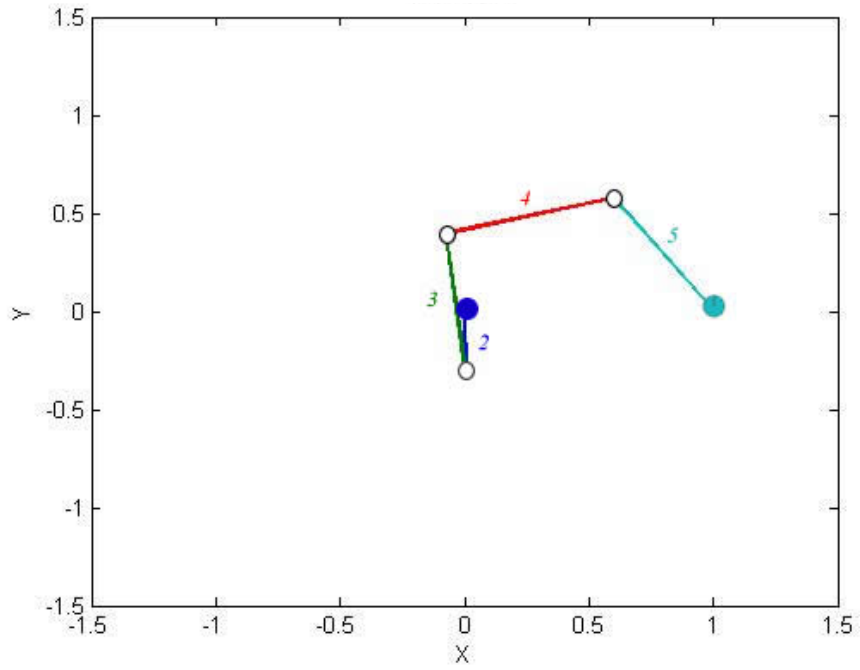


Figure 5.11d Sketch of a Five-Bar Mechanism

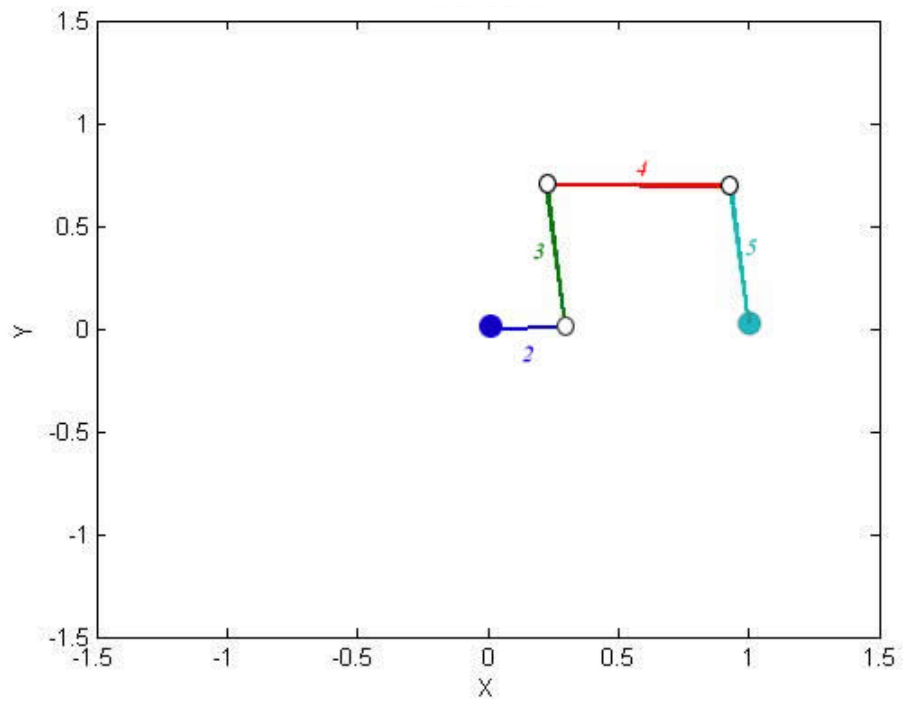


Figure 5.11e Sketch of a Five-Bar Mechanism

5.7.5 Example

Sketch input and output link torque of a five-bar mechanism with the following link lengths, by the method mention in Section 5.2 $a_1 = 2.5$ unit, $a_2 = 0.7$, $a_3 = 1.7$, $a_4 = 1.7$, $a_5 = 1.5$ for $k_{34} = k_{45} = 3$ N.unit/rad, 5 N.unit/rad and 3 N.unit/rad ($c_{34} = 1.5$ and $c_{45} = -0.5$) respectively. The maximum torque (h_1 , Eqs. 5.31-32-33) during the work stroke is $h_1 = 1$ Nunit. From the procedure mentioned in Section 5.7, initial spring constants can be taken as $c_{34} = 2.5$ and $c_{45} = -0.5$

By solving Non-linear Equations 5.7, 5.8, 5.15, 5.16 numerically (By using the codes given in Appendices D and E); the output and input torque can be determined for the required data. The results are shown in Figures 5.12-13-14 respectively.

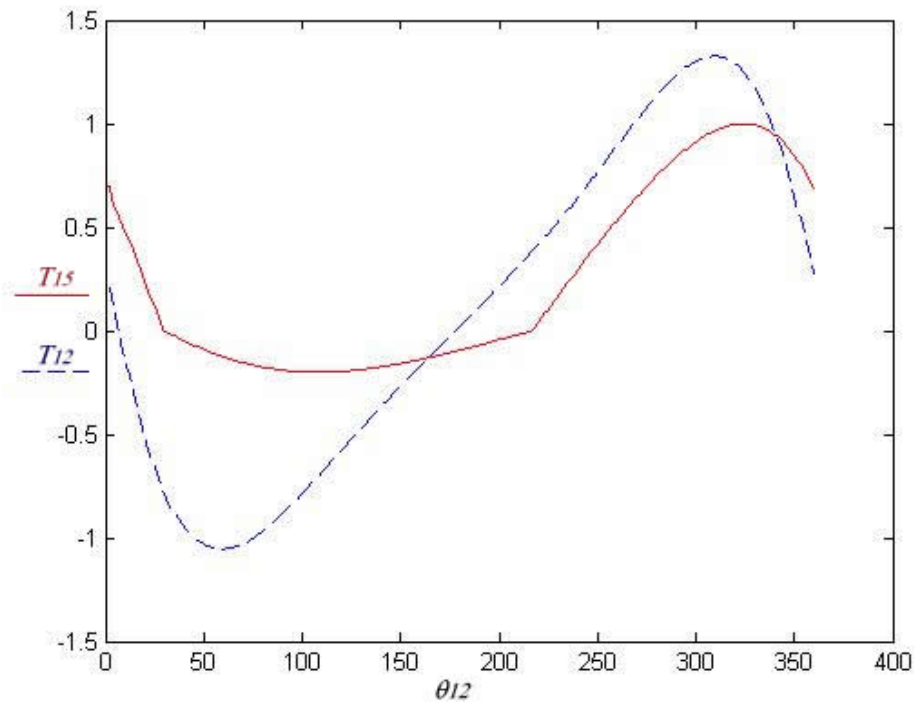


Figure 5.12 T_{12}, T_{15} vs. θ_{12} for $k_{34} = k_{45} = 3$ N.unit/rad

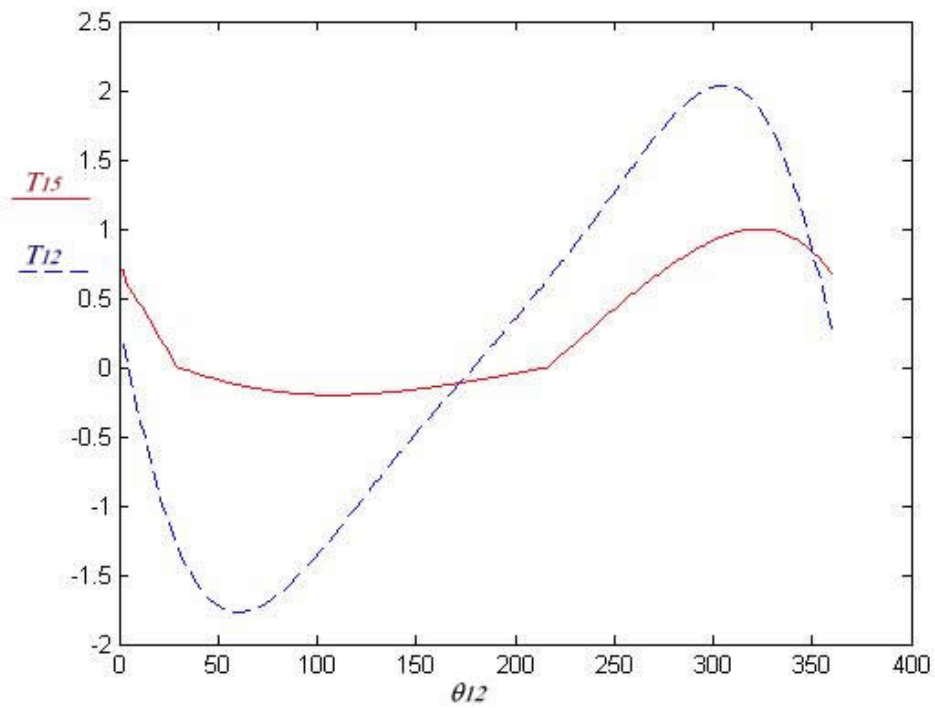


Figure 5.13 T_{12}, T_{15} vs. θ_{12} for $k_{34} = k_{45} = 5$ N.unit/rad

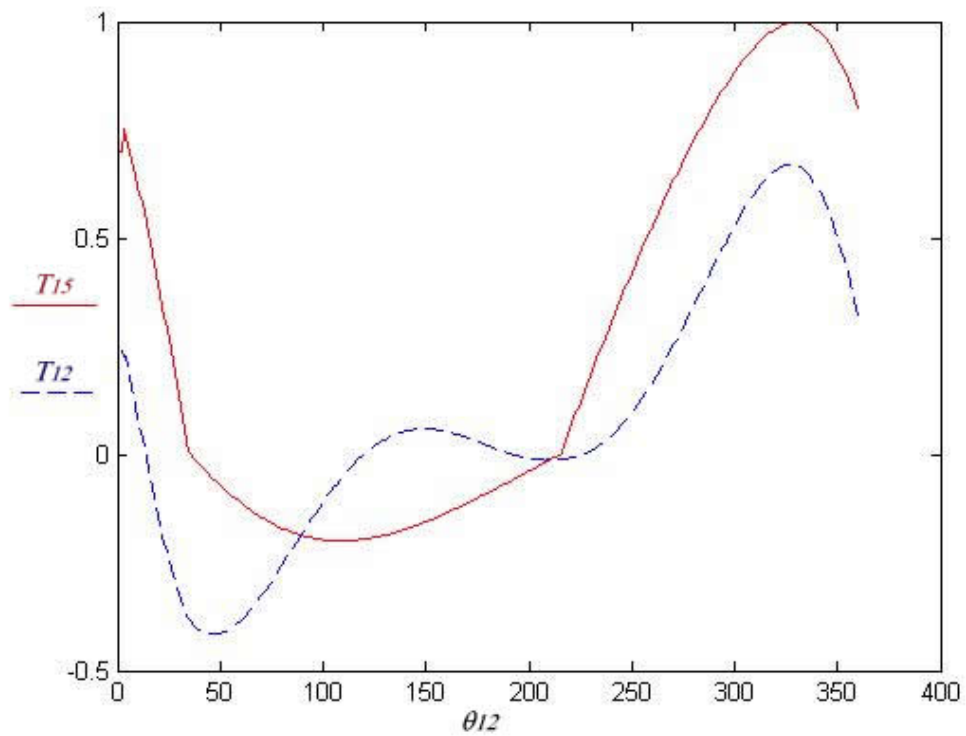


Figure 5.14 T_{12}, T_{15} vs. θ_{12} for $k_{34} = k_{45} = 3$ N.unit/rad and $c_{34} = 1.5$ and $c_{45} = -0.5$

From Figure 5.12 it is seen that, when k_{34} and k_{45} are equal to 3 N.unit/rad, magnitude of the output-link torque (T_{15}) is approximately 0.7 times of the input torque (T_{12}) during the work-stroke. But, when k_{34} and k_{45} are equal to 5 N.unit/rad, magnitude of the output-link torque is roughly half of the input torque during the work-stroke. From the Figure 5.8-9 it is seen that, kinematics of the mechanism is nearly the same. However, it is observed that spring constants have a major effect on magnitude of the input-torque (T_{12}). Energy storage of the mechanism may increase and decrease according to the stiffness of the spring. If appropriately optimized, this characteristic may become advantage for some cases.

5.8 Generalization of the Five-Bar Mechanism

Similar to the variable stroke mechanism, synthesis of the five-bar mechanism is uncertain. But at least, a chart relating the output force and spring constants and output stroke of the mechanism is essential.

In equations 5.7, 5.8, 5.15, 5.16 there are ten free design parameters ($a_1 a_2 a_3 a_4 a_5 a_4 k_{34} k_{45} c_{34} c_{45}$) for the structure. For every combination of these parameters a different output-stroke ($\Delta\theta_{15}$) may be obtained. Also output-torque " T_{15} " is a free parameter. Since this is an unconstrained mechanism, all these eleven parameters are functions of the kinematics of the mechanism. So a simple-two dimensional chart will be possible by fixing a lot of parameters. Therefore a three-dimensional chart will be more powerful for a design chart. Nevertheless, there are still too many parameters, so a simplification is required.

Firstly, all the related equations (5.7, 5.8, 5.15, 5.16) can be divided by a_1 . So, link proportions can be considered as $a_5/a_1 a_4/a_1, a_3/a_1$ and a_2/a_1 .

Successive trials showed that, the spring initial position constant " c_{ij} " does not have a major effect on the stroke of the mechanism. At this moment, this parameter can be kept constant with a suitable value. Therefore, appropriate values for c_{34} and c_{45} must be determined for a combination of parameters. An initial guess is required at this step. In Figure 5.15 one of the possible compliant five-bar mechanisms is shown. Assuming that link proportions of the mechanism shown in figure is roughly in averages that will be analyzed in next steps, estimation can be done according to this mechanism

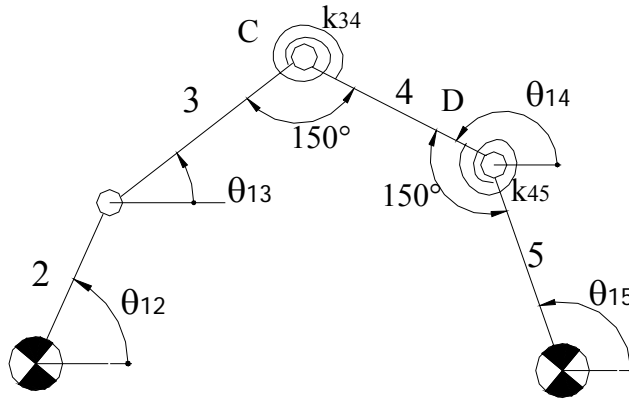


Figure 5.15 The Five-Bar Variable Structure Mechanism

At this position assuming that the two springs applies exactly no torque to the links, the spring initial position constants can be determined as follows:

Torque applied to 3rd and 4th links is:

$$T_{s34} = k_{34}(\theta_{13} - \theta_{14} + c_{34}) = 0 \quad (5.34)$$

From Figure 15 considering the angles at joint C:

$$\theta_{13} + \pi - \theta_{14} + 150^0 \frac{\pi}{180^0} = \pi \quad (5.35)$$

From Eq 5.34 and 5.35 c_{34} can be found as 2.618

Torque applied to 4th and 5th links is:

$$T_{s45} = k_{45}(\theta_{14} - \theta_{15} + c_{45}) = 0 \quad (5.36)$$

From Figure 5.15, considering the angles at joint D:

$$\pi - \theta_{15} + \theta_{14} + 150^\circ \frac{\pi}{180^\circ} = 2\pi \quad (5.37)$$

From Eq 5.36 and 5.37 c_{45} can be found as -0.523.

So one take $c_{34} = 2.5$ and $c_{45} = -0.5$. Several trials showed that this intuitive approach for the initial spring position constants is appropriate.

Next, torque and spring constants can be simplified; in equations 5.15, 5.16, it is seen that; input torque T_{12} and output torque T_{15} are linearly proportional with the spring constant k . Therefore, increasing both spring constant and output torque magnitude linearly yields exactly the same kinematics. Then spring constant and output torque can be considered as a single design parameter. Therefore dividing both of these equations by k , a more useful T_{15}/k ratio is introduced.

Referring to Section 5.6 output loading can be determined. From Equation 5.31-32-33 below equation can be derived for the general case. Let the maximum value of the output-force T_{15} , is T during the work stroke ($180^\circ < \theta_{12} < 360^\circ$) and one-fifth of this value during the return stroke ($T_{15} = -T/5$):

$$\text{For } 0 \leq \theta_{12} < 2\pi \text{ and } \dot{\theta}_{12} > 0; \quad (5.38)$$

$$\text{If } 0 \leq \theta_{12} - \phi_{16} < \pi, \quad T_{15} = \frac{-T}{5} \cdot |\sin(\theta_{12} - \phi_{16})|, \quad (\text{reverse - stroke}) \quad (5.39)$$

$$\text{Else,} \quad T_{15} = T \cdot |\sin(\theta_{12} - \phi_{16})|, \quad (\text{work - stroke}) \quad (5.40)$$

where T is the maximum value of the output - torque.

Rearranging the kinematic and force equations (5.8, 5.9, 5.15, 5.16) according to above procedure;

Dividing Equation 5.7 by a_1 , 5.41 can be obtained:

$$\frac{a_2}{a_1} \cos \theta_{12} + \frac{a_3}{a_1} \cos \theta_{13} - \frac{a_4}{a_1} \cos \theta_{14} - \frac{a_5}{a_1} \cos \theta_{15} = 1 \quad (5.41)$$

Dividing Equation 5.8 by a_1 , 5.42 can be obtained:

$$\frac{a_2}{a_1} \sin \theta_{12} + \frac{a_3}{a_1} \sin \theta_{13} - \frac{a_4}{a_1} \sin \theta_{14} - \frac{a_5}{a_1} \sin \theta_{15} = 0 \quad (5.42)$$

Dividing Equation 5.15 by k_{34} , 5.43 can be obtained:

$$\begin{aligned} & \frac{T_{12}}{k_{34}} + (\theta_{13} - \theta_{14} + c_{34}) \frac{\left\{ \frac{a_2/a_1}{a_4/a_1} \sin(\theta_{12} - \theta_{13}) - \frac{a_2/a_1}{a_3/a_1} \sin(\theta_{12} - \theta_{14}) \right\}}{\sin(\theta_{14} - \theta_{13})} \\ & - \frac{k_{45}}{k_{34}} (\theta_{14} - \theta_{15} + c_{45}) \frac{\frac{a_2}{a_1} \sin(\theta_{12} - \theta_{13})}{\frac{a_4}{a_1} \sin(\theta_{14} - \theta_{13})} = 0 \end{aligned} \quad (5.43)$$

Multiplying Equation 5.16 by, $1/k_{34}$, 5.44 can be obtained:

$$\begin{aligned} & \frac{T_{15}}{k_{34}} + (\theta_{13} - \theta_{14} + c_{34}) \frac{\left(\frac{a_5/a_1}{a_4/a_1} \sin(\theta_{13} - \theta_{15}) - \frac{a_5/a_1}{a_3/a_1} \sin(\theta_{14} - \theta_{15}) \right)}{\sin(\theta_{14} - \theta_{13})} \\ & + \frac{k_{45}}{k_{34}} (\theta_{14} - \theta_{15} + c_{45}) \left\{ 1 - \frac{a_5/a_1 \sin(\theta_{13} - \theta_{15})}{a_4/a_1 \sin(\theta_{14} - \theta_{13})} \right\} = 0 \end{aligned} \quad (5.44)$$

Now there are six free parameters: five design parameters (a_5/a_1 , a_4/a_1 , a_3/a_1 , a_2/a_1 and k_{45}/k_{34}) and a torque to spring ratio T/k_{34} . For all combination of these parameters, different output swing can be achieved. In order to generalize the approach, unit length can be taken into consideration. So, the spring constants becomes *Nunit/rad*.

Five design parameters and a torque-spring ratio make two-dimensional chart insufficient in this case. In Section 4.8 there were four parameters, therefore two-dimensional chart with keeping two parameters constant was sufficient to obtain a design chart. To use one more parameter in design charts three-dimensional charts must be taken into consideration. Generally three-dimensional charts are hard to read but in this case it is obligatory to use design three-dimensional charts.

On a three-dimensional chart, on one axis output swing angle can be shown, on the other two axes two of the five design parameters (a_5/a_1 , a_4/a_1 , a_3/a_1 , a_2/a_1 and k_{45}/k_{34}) can be shown. Then three design parameters must be kept constant for the same chart. Generally, variations of length of the input (crank) and output-link affects output-link swing more than coupler link(s). Therefore while preparing the charts; the rest two-axis can be used for crank and output-link

By using Matlab, for the constant $a_3/a_1 = a_4/a_1$ and k_{45}/k_{34} ratio, increasing a_2/a_1 and a_5/a_1 bit by bit for a set of T/k_{34} equations 5.41, 5.42, 5.43 5.44 can be solved numerically for whole crank rotation. After full-rotation of the crank, maximum and minimum value of the θ_{15} can be determined. Then, stroke of the mechanism can be determined. For the interval of the pre-determined design parameters, this procedure can be repeated. Interpolating the data a design chart can be obtained.

The data obtained from the result of the above is plotted with the function “grid data” in Matlab for the following examples. Grid data fits a surface of the form $z = f(x, y)$ to the data in the (usually) non-uniformly spaced vectors (x,y,z) . The surface always passes through the data points. Triangle-based cubic interpolation method is used. The grid-data command uses the method documented in [14] and [15].

5.9 Examples

5.9.1 Example

Determine three dimensional design charts to obtain output-link swing for each $k_{45}/k_{34} = \{0.7, 1, 1.3\}$. Take the rest of the variables as:

- $a_2/a_1 = \{0.2, 0.3, \dots, 0.5\}$
- $a_5/a_1 = \{0.6, 0.7, \dots, 1\}$
- $T/k_{34} = \{0.1, 1.2\}$

Where the fixed parameters are:

$$c_{34} = 2.5 \text{ and } c_{45} = -0.5, \quad a_3/a_1 = a_4/a_1 = 0.7.$$

Also check the maximum spring deflections from their corresponding un-deflected positions for each chart

By solving equations 5.41, 5.42, 5.43 5.44 numerically (using the codes given in Appendices D and F) and using “cubic spline interpolation” for the related data, the below charts are obtained.

The maximum spring deflection chart indicates the absolute value of the greater deflection of the two springs from their un-deflected position that occurs after the full-rotation of the crank.

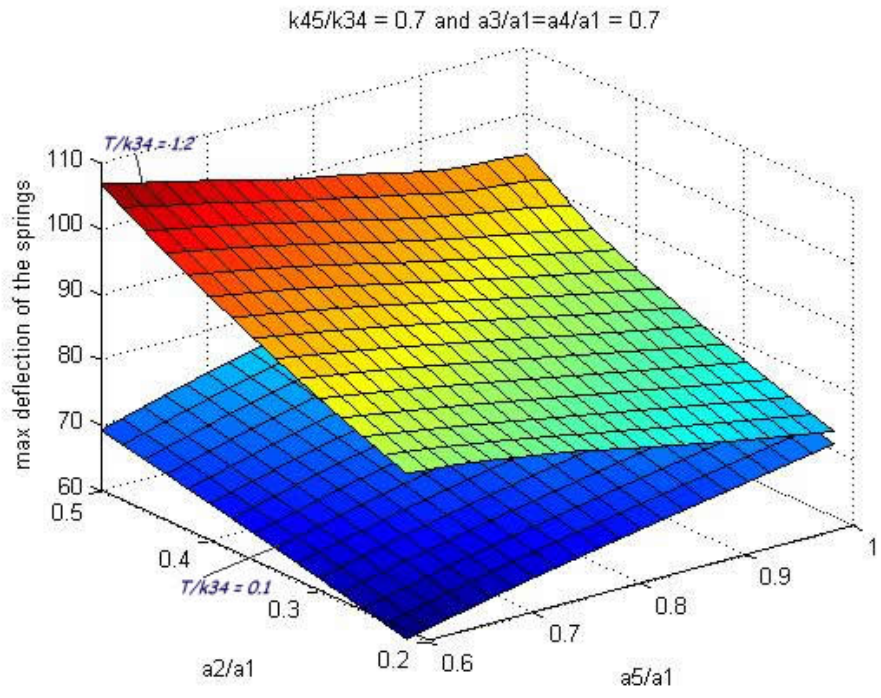
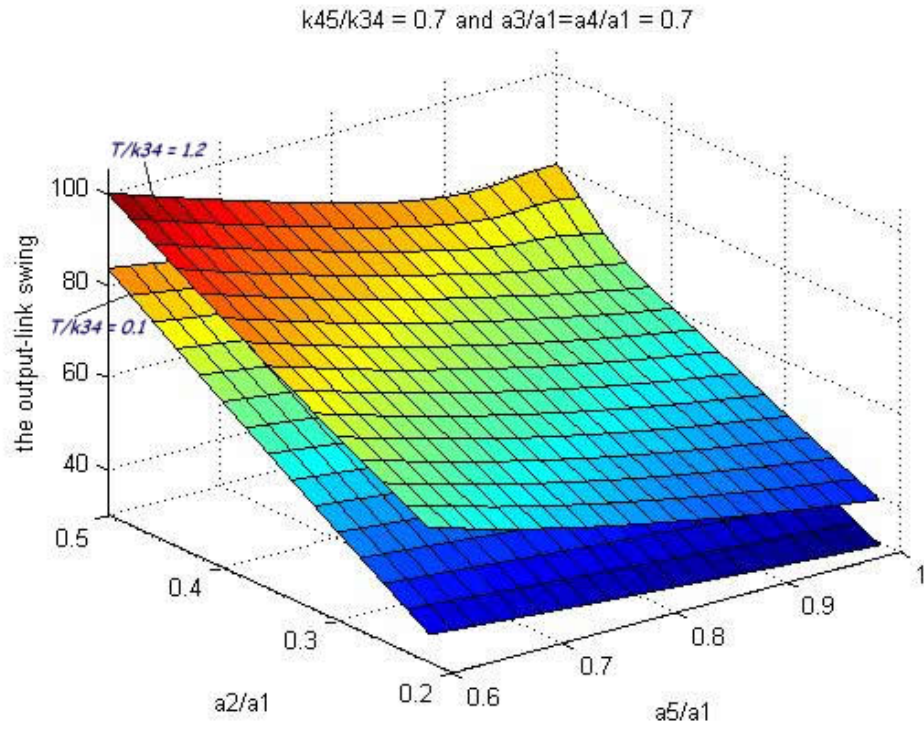


Figure 5.16a The Design Chart and the corresponding Spring Deflection of the Five-Bar Mechanism for $k_{45}/k_{34} = 0.7$ and $a_3/a_1 = a_4/a_1 = 0.7$

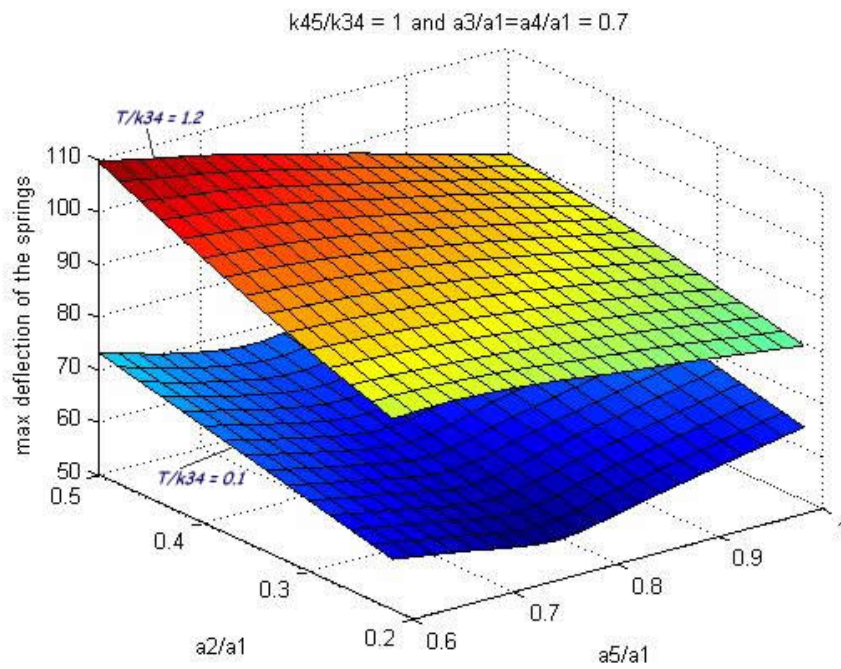
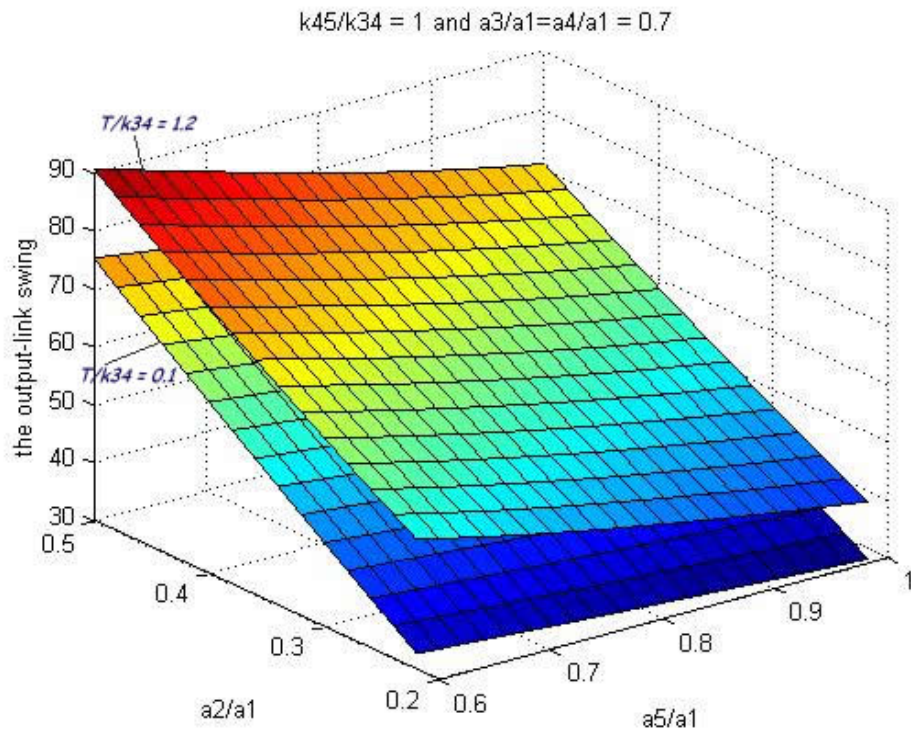


Figure 5.16b The Design Chart and the corresponding Spring Deflection of the Five-Bar Mechanism for $k_{45}/k_{34} = 1$ and $a_3/a_1 = a_4/a_1 = 0.7$

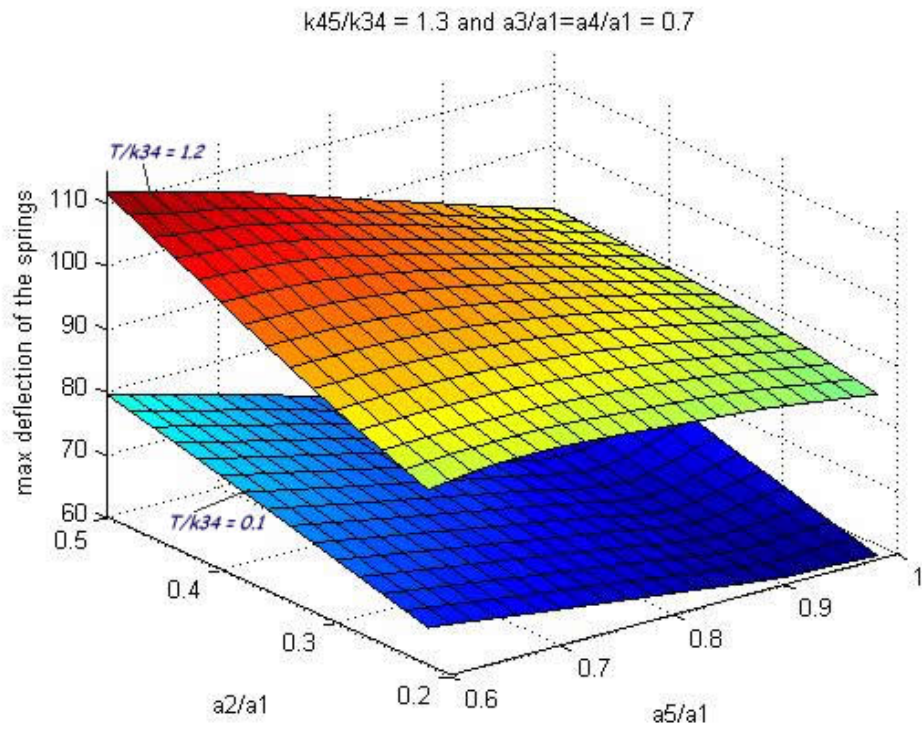
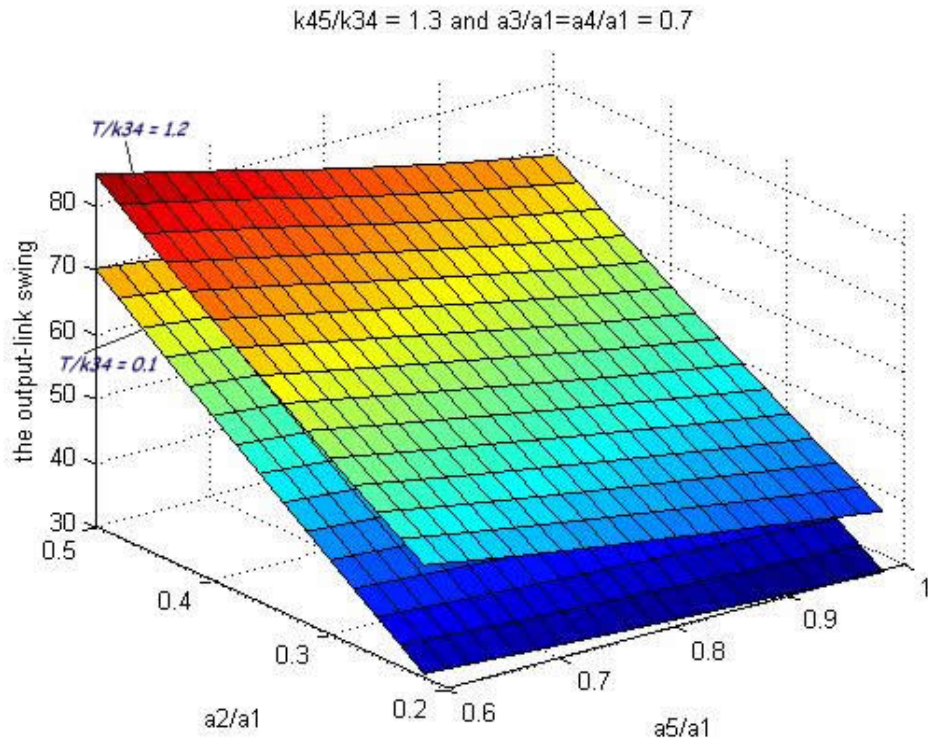


Figure 5.16c The Design Chart and the corresponding Spring Deflection of the Five-Bar Mechanism for $k_{45}/k_{34} = 1.3$ and $a_3/a_1 = a_4/a_1 = 0.7$

5.9.2 Example

Determine three dimensional design charts to obtain output-link swing for each $k_{45}/k_{34} = \{0.7, 1, 1.3\}$. Take the rest of the variables as:

- $a_2/a_1 = \{0.2, 0.3, \dots, 0.5\}$
- $a_5/a_1 = \{0.6, 0.7, \dots, 1\}$
- $T/k_{34} = \{0.1, 0.8\}$

Where the fixed parameters are:

$$c_{34} = 2.5 \text{ and } c_{45} = -0.5, \quad a_3/a_1 = a_4/a_1 = 1.2.$$

Also check the maximum spring deflections from their corresponding un-deflected positions for each chart.

By solving equations 5.41, 5.42, 5.43 5.44 numerically (using the codes given in Appendices D and F) and using “cubic spline interpolation” for the related data, the below charts are obtained.

The maximum spring deflection chart indicates the absolute value of the greater deflection of the two springs from their un-deflected position that occurs after the full-rotation of the crank.

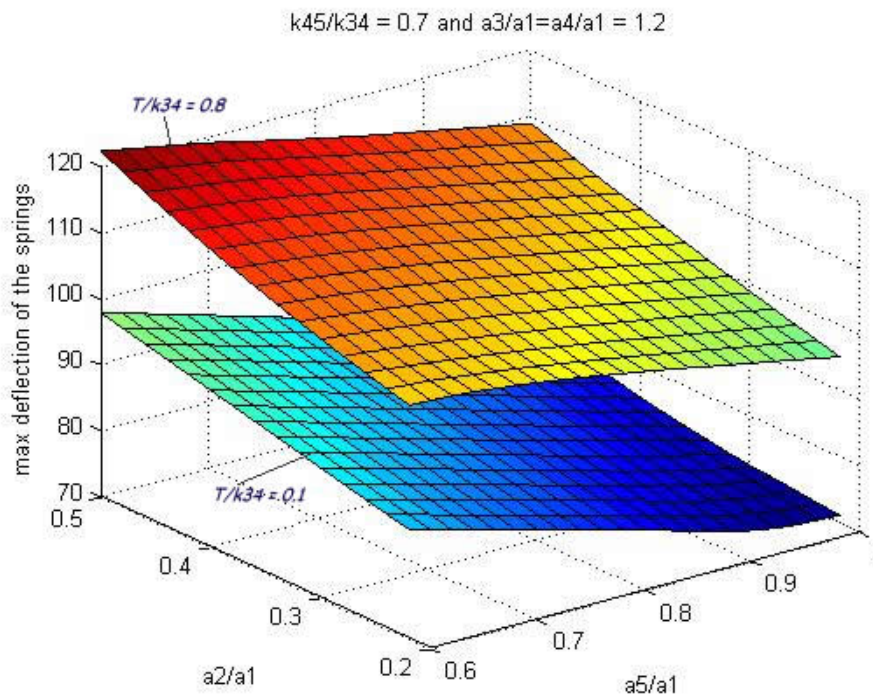
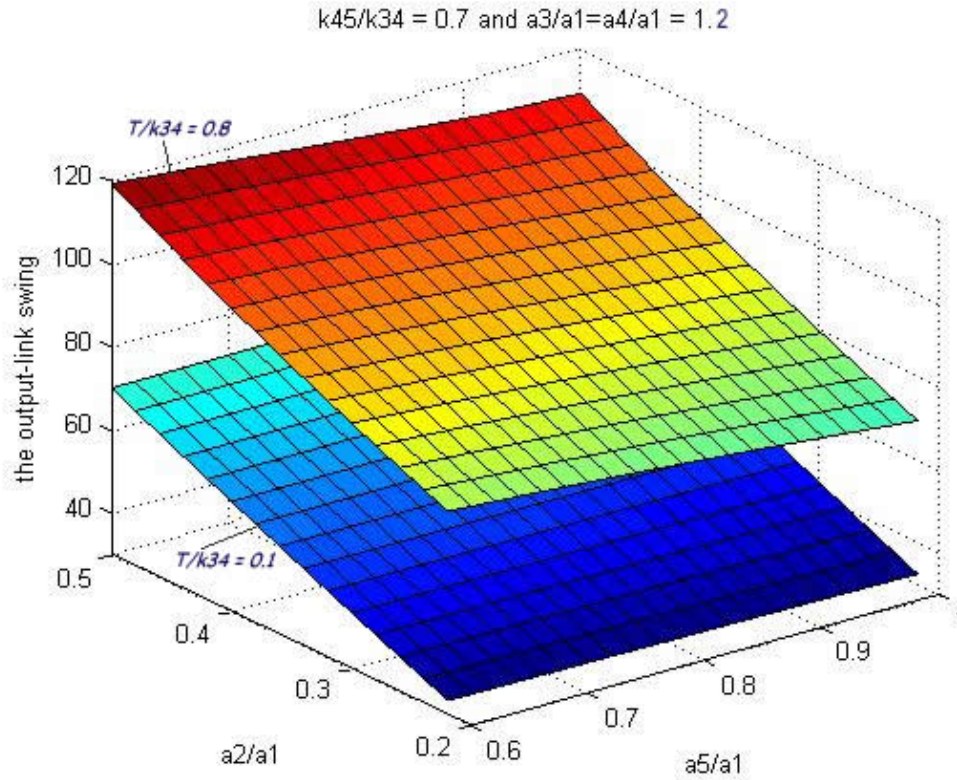


Figure 5.17a The Design Chart and the corresponding Spring Deflection of the Five-Bar Mechanism for $k_{45}/k_{34} = 0.7$ and $a_3/a_1 = a_4/a_1 = 1.2$

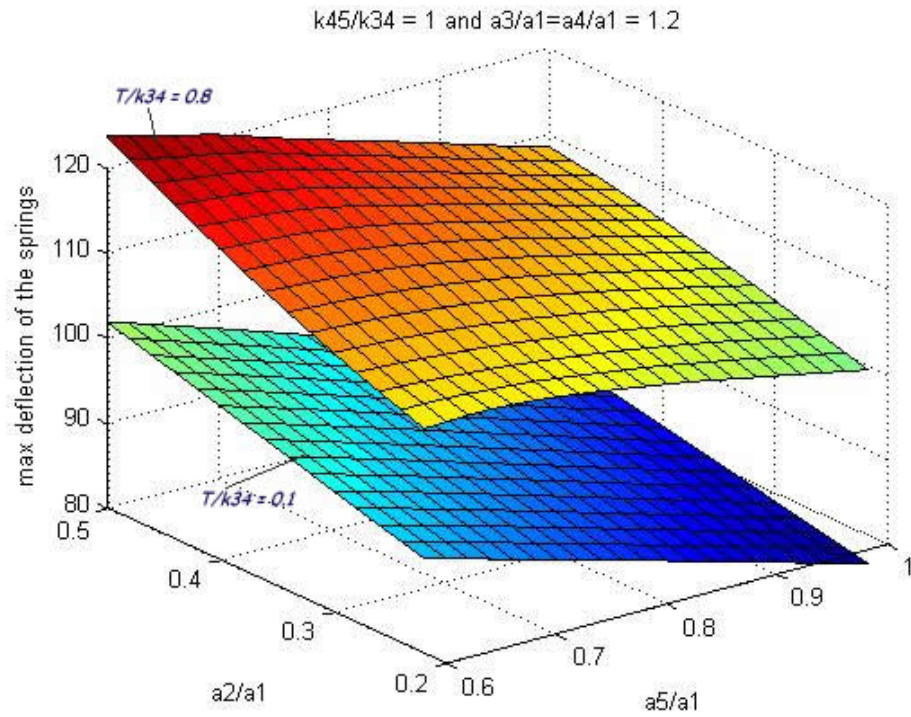
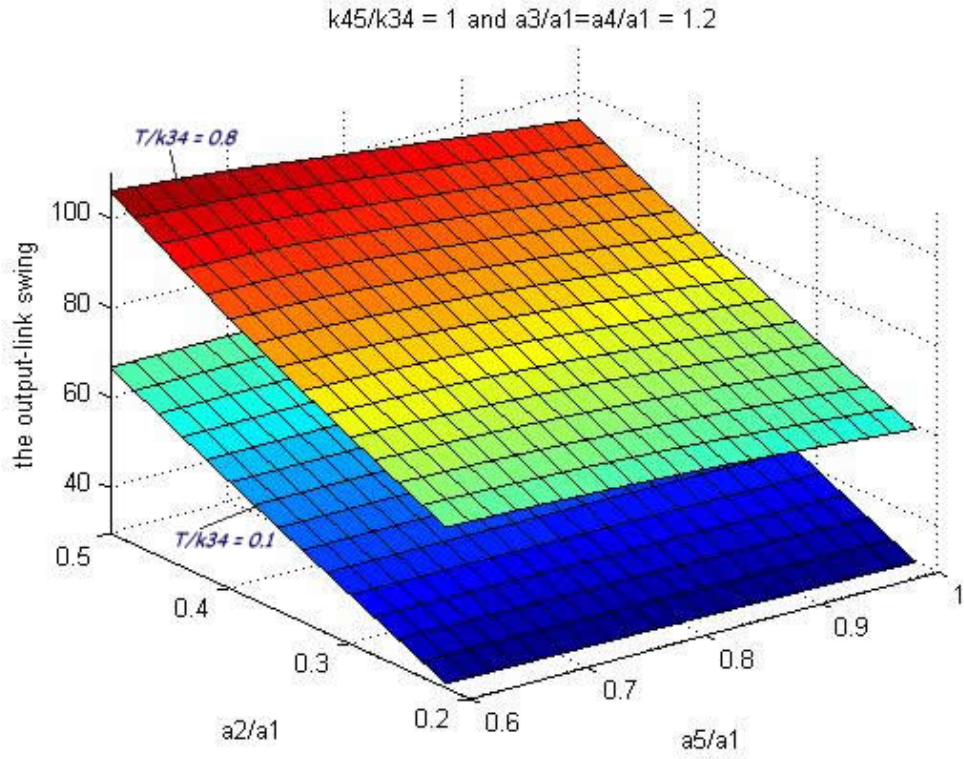


Figure 5.17b The Design Chart and the corresponding Spring Deflection of the Five-Bar Mechanism for $k_{45}/k_{34} = 1$ and $a_3/a_1 = a_4/a_1 = 1.2$

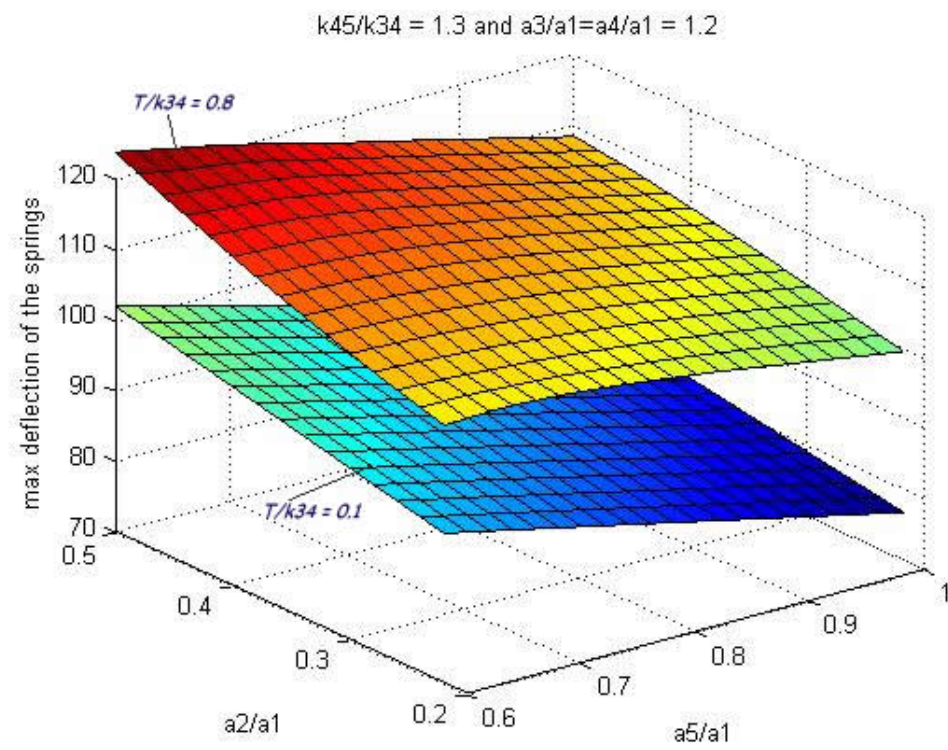
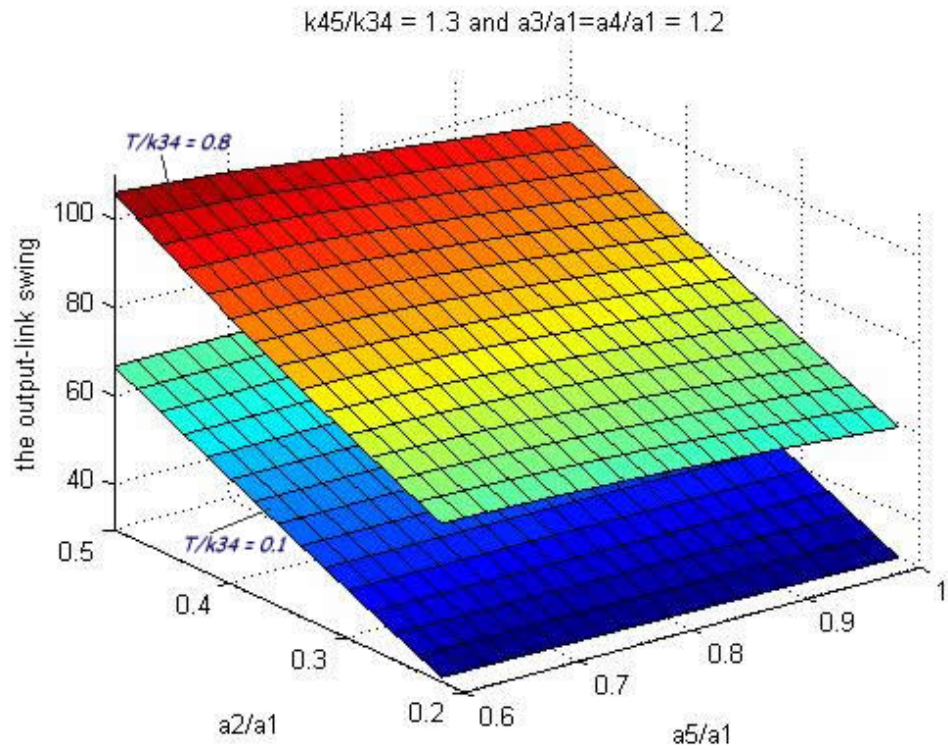


Figure 5.17c The Design Chart and the corresponding Spring Deflection of the Five-Bar Mechanism for $k_{45}/k_{34} = 1.3$ and $a_3/a_1 = a_4/a_1 = 1.2$

One can easily determine link proportions from the design charts shown in Figure 5.16, 5.17, 5.18 according to the required loading and output torque conditions.

Examples 5.9-1 and 2 also show that if five-bar mechanism is appropriately designed, it has flexibility according to the varying output torque. All these three examples show that when T/k_{34} ratio changes output-link swing also changes significantly.

CHAPTER VI

CONCLUSIONS and RECOMMENDATIONS

In this study, analysis and design procedures are developed for unconstrained multi degree-of-freedom partially compliant mechanisms. The approaches are shown with two different mechanisms. Initially, a five-link in-line slider-crank mechanism (variable stroke mechanism) is analyzed (Section 4.2). The kinematic and force analysis of the mechanism is performed simultaneously. Then, a two-dimensional design chart according to output-link oscillation using dimensionless parameters is produced. In the second part of the study, “five-bar mechanism” (Section 5.2) is investigated. Similar analysis and design approaches are used. Also an original method (Section 5.6) to estimate dead centers of the five-bar mechanism is developed.

After the study, it is concluded that the kinematic and force analysis of multi degree-of-freedom unconstrained mechanisms can be performed by using the method of virtual work (Section 3.2) and numerical solution methods (by using the codes given in appendices). The codes (Appendices) are modified so that initial guesses are obtained from the previous cycle's set of solutions to obtain accurate solutions quickly.

In this study, during the analyses of all the mechanisms, it is assumed that the output-load varies between a maximum value in the work stroke and one-fifth of its work-stroke value in return stroke. Also both the loads are assumed to be resistive to the motion of the output link. Since kinematics of multi degree-of-freedom unconstrained mechanisms is uncertain before the loads are applied, the working zone of the output-link is also uncertain. Before the kinematic analysis, without knowing working zone of the output-link defining an "exact" output-link load function which changes its direction at the dead centers is not possible. Therefore, a procedure is required to determine the output-link torque function. But the variable stroke mechanism is an exception to this case.

In the given examples it is observed that, for the in-line variable stroke mechanism (Figure 4.1) with resistive output loads, the mechanism is "approximately" at its dead centers when $\theta_{12} = 0$ or $\theta_{12} = \pi$. In other words, as in the case of the conventional in-line slider-crank mechanism the position of crank is the major parameter that defines working and return strokes. Then, the output-link load can be simply a function of the crank's position for the "inline" variable stroke mechanism. In fact, as it is shown in Examples 4.5-1-2-3 (Figures 4.6a, 4.9b, 4.11b), the direction changes of the output-link (dead centers) occur approximately around $\theta_{12} = 0$ or $\theta_{12} = \pi$ according to the loading given by Equation 4.23 (Note that these examples do not guarantee that the dead centers always occur when $\theta_{12} = 0$ or $\theta_{12} = \pi$ for all types of loadings)

However, the case is different when the five-bar mechanism is considered. Because, there is no direct relationship between the position of the crank and the dead centers

of the mechanism as in the case of the variable stroke mechanism. Since the equations of the motion of the five-bar mechanism are solved numerically, one of the simplest methods is to relate output-torque with difference of the output-link angle for each step of the numerical solution. However, many trials show that this approach (Section 5.3) causes the output-link to hesitate as it is shown in Examples 4.4 and 4.5. Therefore, using variable step sizes depending on position of the output-link or some complex algorithms did not yield a convenient solution for the output link torque for all mechanisms. Therefore, another, rather simple and convenient method is required to obtain a smoothly increasing and decreasing torque at the output-link.

According to this requirement, an original estimation technique (Section 5.6) for the dead centers of the unconstrained five-bar mechanism which does not use the difference of the output-link angle for each step of the numerical solution is introduced.

From the given examples, it is observed that for resistive output-loads the five-bar mechanism behaves like an imaginary four-bar mechanism formed with the imaginary coupler-link (dashed line), links 2 and 3 which are shown in Figure 5.7. Therefore, it is concluded that, according to this imaginary line, if $\theta_{12} = \phi_{16}$, the mechanism is at or very close to its extended position and if $\theta_{12} = \phi_{16} + \pi$, the mechanism is at or very close to its folded position. By using this approach an output-loading function (Equations 5.31-32-33) is formed. Also, it is observed that this torque function perfectly suits for various mechanism and loading conditions. Actually, from Examples 5.7-1-2-3 it is observed that the motion of the links (Figures 5.8a, 5.9, 5.10) smoothly changes for the whole cycle according to the loading given in Equations 5.31-32-33. In Example 5.7.2 after the analysis, from Figure 5.9a it is seen that the dead centers of the mechanism occur at $\theta_{12} = 45^{\circ}$ and $\theta_{12} = 240^{\circ}$. From Figure 5.9b it is also seen that the output-link torque changes its direction when $\theta_{12} = 30^{\circ}$ and $\theta_{12} = 220^{\circ}$. From many examples, approximately 0° to 25° amount of error in direction change position of torque function is observed.

Therefore, the method of approximate estimation of dead centers can be assumed feasible.

When the two different types of output-load functions for the variable stroke and the five-bar mechanism are compared, it can be clearly observed that with the one depending on the approximate dead center estimation technique the motion of the linkages around dead centers yields a smoother motion of the links. This comparison can be done from the position analyses of the output-links from Examples 5.7 and 4.5. Also the approach used to estimate dead centers of the five-bar may be useful for different types of unconstrained mechanisms.

It is also concluded that for some tasks, the input torque characteristics of both the variable stroke and five-bar mechanism may radically differ from rigid link mechanisms performing similar tasks. Examples 4.5.1-2-3 indicate that the input torque (Figure 4.7, 4.10, 4.10) of the mechanisms with different design parameters do not change significantly. However, when the five-bar mechanism is taken into consideration the situation is completely different. In Example 5.7.5, it is observed that the input torque (Figure 5.12-13-14) of the same five-bar mechanism with different spring constants and initial positions affects the input torque significantly for similar output-loadings. Therefore, it can be stated that in some cases, the spring parameters may significantly affect the kinematics and input torque loading of the mechanisms. Also, if a mechanism is properly optimized for a given task or, in other words, if the internal energy can be increased during the return stroke and released during the work stroke, an actuator with smaller torque capacity can be used to drive the mechanism.

The design charts obtained through the parametric analyses of the variable stroke and five-bar mechanisms indicate that, for such mechanisms, variations in the output-link torque affects output-link stroke. In Figures 4.17-18 and 5.6-17, variation of the output-link stroke with respect to output-link loads is clearly indicated. Therefore, these design charts indicate that, when appropriately designed, these mechanisms can be used for the tasks where variable oscillation according to the loading is required.

In the literature, it is stated that in order to simply analysis and design of compliant mechanisms “pseudo-rigid-body” modeling (Section 2.1) technique is also used for the compliant mechanism “without” small flexural pivots members.

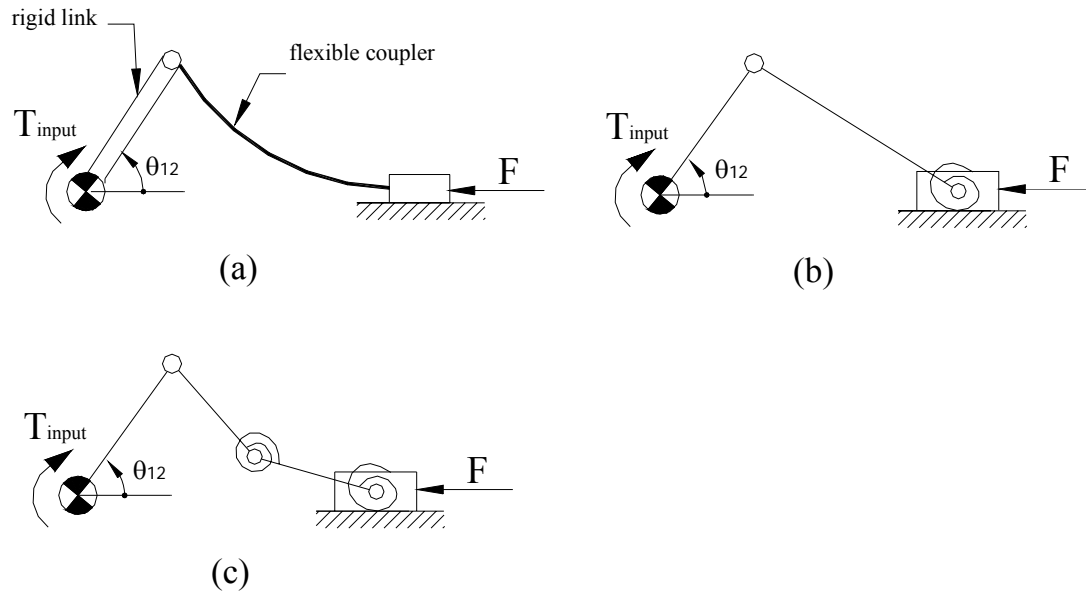


Figure 6.1 (a) Compliant Slider-Crank Mechanism in a Deflected Position, and its (b) single (c) two degree-of-freedom Pseudo-Rigid-Body Model

In Figure 6.1, a compliant slider-mechanism and its pseudo-rigid-body model is shown. This mechanism can be designed for a specified task by employing its pseudo-rigid-body model. After the design an equivalent flexible member [2] can be determined. However, with this approach, the kinematics of the real mechanism and its pseudo rigid-body-model may not be exactly the same. In other words, the pseudo-rigid-body modeling technique yields some error (depending on the size and stiffness properties of the linkage) in a design procedure.

However, if the number of the linkages in the pseudo-rigid-body model is increased, the error in the design procedure may be decreased. For example, if the five-link variable stroke mechanism (Figure 6.2c) (for which the analysis and design procedures are investigated in this study) is used for modeling the compliant slider-crank mechanism (Figure 6.1a), smaller error can be achieved after the design

procedure (Figure 6.2). Therefore, this dissertation can also be applied to modeling compliant mechanisms more accurately.

At the present time, for the tasks requiring flexibility, mechatronics system may become more advantageous than using complex structured. However, in some cases flexible mechanisms can be more advantageous than the mechatronics systems due to their lack of actuators, sensors and control system.

Since the analysis and design of the multi degree-of-freedom unconstrained mechanisms is a new subject, there are several properties that must be investigated. Movability of the mechanisms and determination of the transmission characteristics are important issues that must be studied.

With the optimization of the mechanisms, the major and minor parameters that affect the output-link stroke can be determined.

In this study unconstrained mechanisms are investigated according to a given output-link load. Similar mechanisms can be analyzed if the output load is applied from the coupler link(s).

The author believes that this study can be useful for the analysis and design of both unconstrained multi-degree-of-freedom mechanisms and compliant mechanisms.

REFERENCES

- [1] L.L. Howell, "Compliant Mechanisms", Wiley-Interscience Publications.
- [2] B.A. Salamon, "Mechanical Advantage Aspects in Compliant Mechanisms Design", M. S. Thesis, Purdue University, 1989.
- [3] L.L. Howell, A. Midha, "A Method for The Design of Compliant Mechanisms with Small-Length Flexural Pivots", Journal of Mechanical Design 116, p280-290, 1994.
- [4] L.L. Howell, A. Midha, "Parametric deflection approximations for end-loaded, large-deflection beams in compliant mechanisms", Journal of Mechanical Design 117, p156-165, 1998.
- [5] L.L. Howell, A. Midha, Tony W. Norton, "Limit positions of compliant mechanisms using the pseudo-rigid-body model concept" Mechanism and Machine Theory
Volume 35, Issue 1 , Pages 99-115, January 2000.
- [6] Trease, Moon, Kota "Design of Large-Displacement Joints" ASME Transactions, Journal of Mechanical Design, V127, p788-798, 2005.
- [7] T.Laliberte, C. Gosselin, "Simulation and Design of Underactuated Mechanical Hands", Mechanism Machine Theory 3 Vol. 33, No. 1/2, p39-57, 1998.
- [8] F. Freudenstein- E. Söylemez, "The Multiport Lever: A Mechanical Logic Element", J. Engng Ind., p. 353-359, May 1977.

- [9] E. Tanık – E. Söylemez, “Variable Structure Mechanisms Design”, The Ninth IFToMM International Symposium on Theory of Machines and Mechanisms, 2005.
- [10] L. Birglen, and C. M. Gosselin, “Kinetostatic Analysis of Underactuated Fingers”, IEEE Transactions on Robotics and automation, vol. 20, No. 2, April 2004.
- [11] A. Kireççi - L. C. Dulger - H. M. Gultekin, “Design of Hybrid Actuator”, 8th international Machine Design and Production Conference Proceedings, p. 65-74, September 1998.
- [12] B. Paul, “Kinematics and Dynamics of Planar Machinery”, Prentice Hall.
- [13]. Guerinot, Magleby, Howell, Todd "Compliant Joint Design Principles for High Compressive Load Situations" ASME Transactions, Journal of Mechanical Design, V127, 774-781, 2005.
- [14] National Science and Technology Research Center for Computation and Visualization of Geometric Structures (The Geometry Center), University of Minnesota. 1993.
- [15] Sandwell, David T., "Biharmonic Spline Interpolation of GEOS-3 and SEASAT Altimeter Data", Geophysical Research Letters, 2, 139-142,1987

APPENDIX-A

Function of the Variable Stroke Mechanism

```
function f=mdof_vs_a(x,k,F,a2,a3,a4,c1,c2)
k1=100;
k2=100;
teta2=k*pi/180;
teta3=x(1);
teta4=x(2);
s=x(3);
T=x(4);
f(1)=-k1.*(teta3-teta4+c1).*((a2.*sin(teta2-teta4))/(a3.*sin(teta4-teta3)))-
T+k1.*(teta3-teta4+c1).*((a2.*sin(teta2-teta3))/(a4.*sin(teta4-teta3)))+k2.*(-
teta4+c2).*((a2.*sin(teta2-teta3))/(a4.*sin(teta4-teta3)));
f(2)=k1.*(teta3-teta4+c1).*((cos(teta3))/(a4.*(sin(teta4-teta3))))-F-k1.*(teta3-
teta4+c1).*((cos(teta4))/(a3.*sin(teta4-teta3)))+k2.*(-
teta4+c2).*cos(teta3)/(a4.*sin(teta4-teta3));
f(3)=a2.*sin(teta2)+a3.*sin(teta3)-a4.*sin(teta4);
f(4)=a2.*cos(teta2)+a3.*cos(teta3)-a4.*cos(teta4)-s;
```

APPENDIX-B

Code for the Analysis of the Variable Stroke Mechanism

```
clear
a(1)=30*pi/180
a(2)=170*pi/180
a(3)=7
a(4)=5
c1=1.5;
c2=1.5;
F1=200;
for k=1:1:361;
    if k<=5
        F=-0.12*F1*k+0.4*F1;
    elseif k>5 & k<175
        F=-F1/5;
    elseif k>=175 & k<186
        F=0.12*F1*k-21.2*F1;
    elseif k>=186 & k<355
        F=F1;
    else
        F=-0.12*F1*k+43.6*F1;
    end
    a2=1;
    a3=3;
    a4=1;
    teta2(k)=k*pi/180;
    a=fsolve(@(x) mdof_vs_a(x,k,F,a2,a3,a4,c1,c2),[a(1),a(2),a(3),a(4)]);
    teta3(k)=a(1);
```

```
teta4(k)=a(2);  
s(k)=a(3);  
T(k)=a(4);  
end
```

APPENDIX-C

Code for the Design Chart of the Variable Stroke Mechanism

```
clear
clc
a(1)=30*pi/180;
a(2)=170*pi/180;
a(3)=7;
a(4)=20;
c1=pi-0.4;
c2=pi-0.4;
for l=1:6;
    F=[1 1.5 2 3 5 10];
    F1=F(l)
    for m=1:10;
        a4=m/10;
        for k=1:1:361;
            if k<=5;
                F=-0.12*F1*k+0.4*F1;
            elseif k>5 & k<175
                F=-F1/5;
            elseif k>=175 & k<186
                F=0.12*F1*k-21.2*F1;
            elseif k>=186 & k<355
                F=F1;
            else
                F=-0.12*F1*k+43.6*F1;
            end
        end
    end
end
a2=1;
```

```

a3=3.5;
teta2(k)=k*pi/180;
a=fsolve(@(x) mdof_vs_a(x,k,F,a2,a3,a4,c1,c2),[a(1),a(2),a(3),a(4)]);
teta3(k)=a(1);
teta4(k)=a(2);
s(k)=a(3);
T(k)=a(4);
end
smax(l,m)=max(s);
smin(l,m)=min(s);
deltas(l,m)=smax(l,m)-smin(l,m)
a4p(l,m)=m/10
end
x=2:0.001:3.8;
y=interp1(deltas(l,:),a4p(l,:),x,'spline');
plot(x,y)
hold on
grid on
axis([2 3.8 0.1 1])
title('Stroke vs. Link Proportions for  $a_3/a_2 = 7/2$ ')
end

```


APPENDIX-D

Function of the Five-Bar Mechanism

```
function f=five_bar(x,k,T5,a1,a2,a3,a4,a5,c1,c2)
k1=5;
k2=5;
teta2=k*pi/180;
teta3=x(1);
teta4=x(2);
teta5=x(3);
T2=x(4);
f(1)=a2.*sin(teta2)+a3.*sin(teta3)-a4.*sin(teta4)-a5.*sin(teta5);
f(2)=a2.*cos(teta2)+a3.*cos(teta3)-a4.*cos(teta4)-a5.*cos(teta5)-a1;
f(3)=T2+k1.*(teta3-teta4+c1).*((a2.*sin(teta2-teta3))/(a4.*sin(teta4-teta3))-
(a2.*sin(teta2-teta4))/(a3.*sin(teta4-teta3)))-k2.*(teta4-teta5+c2).*((a2.*sin(teta2-
teta3))/(a4.*sin(teta4-teta3)));
f(4)=T5+k1.*(teta3-teta4+c1).*((a5.*sin(teta3-teta5))/(a4.*sin(teta4-teta3))-
(a5.*sin(teta4-teta5))/(a3.*sin(teta4-teta3)))+k2.*(teta4-teta5+c2).*(1-(a5.*sin(teta3-
teta5))/(a4.*sin(teta4-teta3)));
```

APPENDIX-E

Code for the Analysis of the Five-Bar Mechanism

```
clear
a(1)=50*pi/180;
a(2)=150*pi/180;
a(3)=80*pi/180;
a(4)=0;
c1=2.5;
c2=-0.5;
h1=1;
T5=0.8.*h1;
ini=1;
for k=ini:1:360;
    a1=2.5;
    a2=0.7;
    a3=1.7;
    a4=1.7;
    a5=1.5;
    teta2(k)=k*pi/180;
    a=fsolve(@(x) five_bar(x,k,T5,a1,a2,a3,a4,a5,c1,c2),[a(1),a(2),a(3),a(4)]);
    teta3(k)=a(1);
    teta4(k)=a(2);
    teta5(k)=a(3);
    T2(k)=a(4);
    A=[0+0.*i a2.*exp(i.*(teta2(k)))];
    B=[a2.*exp(i.*(teta2(k))) a2.*exp(i.*(teta2(k)))+a3.*exp(i.*(teta3(k)))];
    C=[a2.*exp(i.*(teta2(k)))+a3.*exp(i.*(teta3(k)))
    a2.*exp(i.*(teta2(k)))+a3.*exp(i.*(teta3(k)))- a4.*exp(i.*(teta4(k)))];
```

```

D=[a2.*exp(i.*(teta2(k)))+a3.*exp(i.*(teta3(k)))-a4.*exp(i.*(teta4(k)))
a2.*exp(i.*(teta2(k)))+a3.*exp(i.*(teta3(k)))-a4.*exp(i.*(teta4(k)))-
a5.*exp(i.*(teta5(k)))];
teta6= angle(C(1,2)-A(1,2));
T5p(k)=T5;
xx=(teta2(k)-teta6);
if k<ini+2
    T5p(k)=T5;
else
    if (teta2(k)-teta6)>0 & (teta2(k)-teta6)<1.00.*pi
        T5p(k)=-h1/5.*abs(sin(teta2(k)-teta6));
    else
        T5p(k)=h1.*abs(sin(teta2(k)-teta6));
    end
end
end

```

APPENDIX-F

Code for the Design Chart of the Five-Bar Mechanism

```
clear
a(1)=50*pi/180;
a(2)=150*pi/180;
a(3)=80*pi/180;
a(4)=0;
c1=2.5;
c2=-0.5;
ini=1;
a1=1.0;
a3=1.5;
a4=1.5;
for l=1:2;
    h1=[0.1 1 1];
    T5=0.7.*h1(l);
    for m=1:6;
        a5=m/(12.5)+0.52;
        for p=1:6;
            a2=p/(16.6)+0.14;
            for k=ini:1:360;
                teta2(k)=k*pi/180;
                a=fsolve(@(x) five_bar(x,k,T5,a1,a2,a3,a4,a5,c1,c2),[a(1),a(2),a(3),a(4)]);
                teta3(k)=a(1);
                teta4(k)=a(2);
                teta5(k)=a(3);
                T2(k)=a(4);
                A=[0+0.*i a2.*exp(i.*(teta2(k)))];
                B=[a2.*exp(i.*(teta2(k))) a2.*exp(i.*(teta2(k)))+a3.*exp(i.*(teta3(k)))];
```

```

C=[a2.*exp(i.*(teta2(k)))+a3.*exp(i.*(teta3(k)))
a2.*exp(i.*(teta2(k)))+a3.*exp(i.*(teta3(k)))-a4.*exp(i.*(teta4(k)))]';
D=[a2.*exp(i.*(teta2(k)))+a3.*exp(i.*(teta3(k)))-a4.*exp(i.*(teta4(k)))
a2.*exp(i.*(teta2(k)))+a3.*exp(i.*(teta3(k)))-a4.*exp(i.*(teta4(k)))-
a5.*exp(i.*(teta5(k)))]';
teta6= angle(C(1,2)-A(1,2));
T5p(k)=T5;
xx=(teta2(k)-teta6);
if k<ini+2
    T5p(k)=T5;
else
    d1teta5 = (teta5(k)-teta5(k-1));
    if (teta2(k)-teta6)>0 & (teta2(k)-teta6)<1.00.*pi
        T5p(k)=-h1(l)/5.*abs(sin(teta2(k)-teta6));
    else
        T5p(k)=h1(l).*abs(sin(teta2(k)-teta6));
    end
end
T5=T5p(k)
end
teta5max(m,p)=max(teta5).*180/pi;
teta5min(m,p)=min(teta5).*180/pi;
deltateta5(m,p)=(teta5max(m,p)-teta5min(m,p))
a5p(m,p)=m/(12.5)+0.52;
a2p(m,p)=p/(16.6)+0.14;
end
end
[a5pI,a2pI]=meshgrid(0:0.02:1);
ZI=griddata(a5p(:,.),a2p(:,.),deltateta5(:,.),a5pI,a2pI,'cubic');
surf(a5pI,a2pI,ZI)
axis([0.6 1 0.2 0.5 30 130])
hold on
grid on
end

```

CURRICULUM VITAE

PERSONAL INFORMATION

Surname, Name: Tanık, Engin
Nationality: Turkish (TC)
Date and Place of Birth: 5 December 1975 , Ankara
Marital Status: Single
Phone: +90 532 421 84 77
email: engtanik@gmail.com

EDUCATION

Degree	Institution	Year of Graduation
MS	METU Mechanical Engineering	2001
BS	G.Ü Mechanical Engineering	1998

WORK EXPERIENCE

Year	Place	Enrollment
1999-2006	METU Department of Mechanical Engineering	Teaching Assistant
1996 July	Türk Traktör A.Ş	Intern Engineering Student
1995 July	Arıkazan A.Ş	Intern Engineering Student

FOREIGN LANGUAGES

Advanced English

PUBLICATIONS

Tanık E, Söylemez E. “Değişken yapılı Mekanizmalar”, UMTS 2001, 10.Ulusal Makina Teorisi Sempozyumu, Eylül 2001, Konya.

Tanık E., Söylemez E., "Variable Structure Mechanisms Design", The Ninth IFToMM International Symposium on Theory of Machines and Mechanisms, Bucharest, Romania, September 1-4, 2005.

Tanık E., Söylemez E. “Değişken Stoklu Yedi Uzunlu Bir Mekanizma Tasarımı”, MATİM, Cilt:8, Sayı:2, Kasım 2006.

HOBBIES

Science, Motorcycling, Psychology, Classical Music, R/C Helicopters